# A Novel Mitochondrial-localized Purple Acid Phosphatase from Soybean Encoding ROS Scavenging Function

By
LI, Wing Yen Francisca

A Thesis Submitted in Partial Fulfillment of the Requirements for the Degree of
Doctor of Philosophy
in Biology

The Chinese University of Hong Kong
December 2009

**Thesis Committee**

Professor JIANG Liwen (Chair)
Professor LAM Hon-Ming (Thesis Supervisor)
Professor SUN Sai-Ming, Samuel (Committee Member)
Professor ZHANG Jian Hua (External Examiner)

**Statement**

All the experimental work reported in this thesis was performed by the author, unless specially stated otherwise in the text.

LI Wing Yen Francisca

**Abstract**

Purple acid phosphatases (PAPs) represent a diverse group of acid phosphatases in animals and plants. While the mammalian PAPs were found to be related to Reactive Oxygen Species (ROS) evolution in important physiological functions, the roles of plant PAPs remain largely unknown.

Recently, we have isolated a novel PAP-like gene (*GmPAP3*) from soybean that is induced by NaCl and oxidative stresses. Subcellular localization prediction programs suggested that GmPAP3 may be a novel PAP that localized in mitochondria. Most other PAPs are extracellularly located and membrane localization of PAPs was only verified in a few cases.

Mitochondrion is one of the major sites for the production of reactive oxygen species (ROS). Abiotic stresses such as salinity and osmotic stress can cause oxidative damage to organelle membranes due to excess accumulation of ROS. The inducibility of *GmPAP3* gene expression by salinity and oxidative stresses and the putative mitochondrial localization of GmPAP3 prompt us to further investigate the possible physiological roles of *GmPAP3* under abiotic stress-induced oxidative stress.

My Ph.D. study has been focused on the detailed functional analysis of the *GmPAP3* gene. The objectives of my research include: (i) to verified the subcellular localization of GmPAP3; (ii) to investigate the physiological functions of *GmPAP3* under NaCl and osmotic stress in both cellular level and *in planta* level. and (iii) to examine the significance of mitochondrial localization of GmPAP3 in relationship to its protective roles.

By immumolabeling and electronmicroscopy, the subcellular localization of GmPAP3 has been proved to be mainly localized in mitochondria, a primary site for ROS production. Ectopic expression of *GmPAP3* in transgenic tobacco BY-2 cells

mimicked the protective effects exhibited by the antioxidant ascorbic acid by: (1) increase the percentage of cells with active mitochondria; (2) reduce the percentage of dead cells; and (3) lower the accumulation of ROS under NaCl and osmotic stress treatments. However, when ectopically express a truncated *GmPAP3* with the mitochondria transit peptide removed, such protective effect was not observed. This provides evidences on the significance of mitochondria localization to the physiological function of GmPAP3. In addition, when *GmPAP3* transgenic *Arabidopsis thaliana* seedlings were subjected to NaCl, osmotic stress, and oxidative stress treatments, the growth performance of the transgenic lines was significantly better than the wild type. To summarize, these studies has demonstrate that the mitochondrial localized GmPAP3 may play a role in stress tolerance by enhancing ROS scavenging.

# 摘要

紫色酸性磷酸酶(PAP)在動植物中廣泛存在。動物中的紫色酸性磷酸酶的生理功能已被證明與活性氧化物代謝有關，但植物中的紫色酸性磷酸酶的主要作用並不明確。本實驗室從大豆中分離出一個新的紫色酸性磷酸酶基因，並命名爲 *GmPAP3*。*GmPAP3* 基因表達受鹽脅迫和活性氧化物誘導，而在細胞定位預測軟件上被推斷爲定位在線粒體上。線粒體是細胞裡其中一個主要製造活性氧化物的細胞器，而在鹽或滲透脅迫下，在細胞器中累積的活性氧化物會增加。因此，我們推斷 GmPAP3 在生理功能上可能與在鹽或滲透脅迫下線粒體所增加的活性氧化物代謝有關。

爲了找出 GmPAP3 的功能和其與鹽脅迫的生理關係，這個研究計劃旨於：（一）確認 GmPAP3 的亞細胞定位；（二）研究 GmPAP3 的生理功能和其與鹽脅迫和活性氧化物代謝的關係；（三）研究 GmPAP3 的亞細胞定位對其生理功能的重要性。

在這個研究裡，我們以免疫標記和電子顯微鏡確認 GmPAP3 的定位在線粒體。爲了找出 GmPAP3 的生理功能和其與鹽脅迫、脫水脅迫和活性氧化物代謝的關係，我們對 *GmPAP3* 的轉基因烟草細胞系進行鹽脅迫或滲透脅迫的處理。，研究結果顯示表達 *GmPAP3* 的轉基因煙草細胞系，在鹽和滲透脅迫下，能: (1)保護線粒體的完整性; (2) 降底死亡細胞量; (3)降低細胞裡因脅迫而產生的活性氧化物。但在表達被移除線粒體轉運肽的 GmPAP3 的轉基因細胞系, 在鹽或滲透脅迫的處理下, 以上的保護效果都不復見。這證明了 GmPAP3 的亞細胞定位對其生理功能之重要性。此外，表達 *GmPAP3* 的轉基因擬南芥在鹽脅迫下長得比野生型擬南芥要好。總括而言，這些研究結果顯示出 GmPAP3 有著於鹽和脫水脅迫下減少線粒體活性氧化物產生的功能，在細胞於脅迫下的防禦扮演著重要的角色。

**Acknowledgements**

First of all, I would like to express my deepest gratitude to my supervisor, Prof. H. M. Lam, for giving me the chance to work in the field of plant molecular biology under his supervision. His patient guidance, tolerance and trust has guide me all the way through this few years of studies, which is full of ups and downs.

I would like to express my heartfelt thanks to my thesis committee, Prof. S.S.M. Sun and Prof. Liwen Jiang, and external examiner, Prof. J.H. Zhang for their patience of reviewing my thesis and their valuable comments. .

My gratitude also goes to Prof H.Liao, who involve in the early studies of *GmPAP3* under salt stress and phosphorus deficiency; and Prof. G. H. Shao for her early works on the characterization of salt tolerance and salt sensitive soybeans.

My deepest thanks to the following people who have been with me in the past years: Miss Iris Tong for her technical assistance and her superb management of the lab that keep our work going smoothly; Mr Freddie Kwok for his superb technical assistance in the confocal microscopy and electronmicroscopy; Mr Nicolas Koo, Ms. T.H. Phang and Ms. F.L.Wong, they are supportive teammates and is always helpful; Miss M.Y. Cheung, for her valuable comments and her "carrots and sticks"; and all my labmates in Prof. H.M. Lam's Lab for their supports, friendship and patience, making the daily work much more interesting even in the most frustrating moment.

Last but not least, I would like to express my gratitude to my family, especially my mother, for her love and care during all these years of studies; and my friends who have been sending in encouraging words every day.

This work was supported by the Hong Kong RGC Earmarked Grant CUHK4434/04M and the Hong Kong UGC AoE Plant & Agricultural Biotechnology Project AoE-B-07/09 (to H.-M.L.)

| | |
|---|---|
| ABA | Abscisic acid |
| APX | Ascorbate peroxidases |
| AOX | Alternative oxidase |
| ASC | Ascorbate |
| ASC-GSH cycle | Ascorbate-Glutathione cycle |
| ATP | Adenosine triphosphate |
| C:I | Chloroform:isoamylalcohol |
| $CaCl_2$ | Calcium chloride |
| CAT | Catalase |
| CSPD | Disodium 3-(4-methoxyspiro{1,2-dioxyetane-3,2'-(5'-chloro) tricycle [3.3.1.1$^{3,7}$]decan}-4-yl)phenyl phosphate |
| C-terminal | Carboxyl terminal |
| Cu | Copper |
| CUHK | The Chinese University of Hong Kong |
| DEPC | Diethyl pyrophosphate |
| DHA | Dehydroascorbate |
| DIG | Digoxigenin |
| DNA | Deoxyribonucleic acids |
| dNTPs | Deoxyribonucleoside triphosphate |
| EDTA | Ethylenediamine-tetraacetic acid |
| EGTA | Ethylene glycol tetraacetic acid |
| Fe | Iron |
| $Fe^{2+}$ | Iron (II) ion |
| $Fe^{3+}$ | Iron (III) ion |
| g | Gram |
| *GmPAP3* | Full length GmPAP3 |
| *GmPAP3** | Truncated GmPAP3 |
| GPX | Glutathione peroxidases |
| GSH | Glutathione (reduced form) |
| GSSG | Glutathione (oxidized form) |
| GST | Glutathione-S-transferases |
| GR | Glutathione reductase |
| $H^+$ | proton |
| $H_2$DCFDA | 2'-7'-dichlorodihydrofluorescein diacetate |
| $H_2O$ | Water molecule |

| | |
|---|---|
| $H_2O_2$ | Hydrogen peroxide |
| LB | Luria Broth |
| M | Molar |
| MDHA | monodehydroxyascorbate |
| MDHAR | Monodehydroxyascorbate reductase |
| mg | Milligram |
| Mg | Magnesium |
| $Mg^{2+}$ | Magnesium ion |
| $MgCl_2$ | Magnesium chloride |
| ml | Milliliter |
| mM | millimolar |
| Mn | Manganese |
| $Mn^{2+}$ | Manganese ion |
| MOPS | 3-[N-Morpholino]propanesulfonic acid |
| mRNA | Messenger RNA |
| MS | Murashige & Shoog |
| N | Nitrogen |
| $Na^+$ | Sodium ion |
| NaCl | Sodium Chloride |
| NADP | Nicotinamide adenine dinucleotide phosphate |
| NADPH | Reduced Nicotinamide adenine dinucleotide phosphate |
| NaOAc | Sodium acetate |
| NaOH | Sodium hydroxide |
| ng | nanogram |
| nm | nanometer |
| N-terminal | Amino terminal |
| $^1O_2$ | Singlet oxygen |
| $O_2^{\cdot -}$ | Superoxide anion |
| $OH^{\cdot}$ | Hydroxyl radical |
| PAP | Purple acid phosphatases |
| PBS | Phosphate buffer saline |
| P:C:I | Phenol:chloroform:isoamylalcohol (25:24:1) |
| PCR | Polymerase chain reaction |
| Rh123 | Rhodamine 123 |
| RNA | Ribonucleic acid |
| ROS | Reactive oxygen species |
| SDS | Sodium dodecyl sulphate |
| SOD | Superoxide dismutase |

| | |
|---|---|
| ssDNA | Single-stranded DNA |
| TBS | Tris Buffered Saline |
| TBST | Tris Buffered Saline with Tween 20 |
| Tris base | Tris(hydroxymethyl)aminomethane |
| Tris-HCL | Tris(hydroxymethyl)aminomethane hydrochloric acid |
| U | Unit |
| UV | Ultraviolet |
| V | Volt |
| Zn | Zinc |
| $Zn^{2+}$ | Zinc ion |
| µl | microliter |
| µM | micromolar |

## Table of Contents

List of figures:

List of Tables:

# Chapter 1 General Introduction

## 1.1 Reactive oxygen species and abiotic stresses

### 1.1.1 Abiotic stress will cause enhanced ROS production in plants

Plant responds to a variety of abiotic stresses, including salinity, osmotic, heat and cold stresses with an increase of Reactive oxygen species (ROS) production (Mittler, 2002; Mahalingam & Fedoroff, 2003; Fedoroff, 2006; Miller *et al.*, 2008). The accumulation of ROS, such as $^1O_2$, $O_2^{\cdot-}$, $H_2O_2$ and $HO^{\cdot}$, during abiotic stresses was long thought to be a consequence of disturbed cellular redox homeostasis, a by-product of stress metabolism as well as an overall unwelcome by-product of aerobic metabolism (Suzuki & Mittler, 2006; Miller *et al.*, 2008). In the below sections, the origin of ROS, and the production of ROS under abiotic stresses will be discussed.

### 1.1.2 Reactive Oxygen Species, its origin and production

Oxygen is unarguably one of the most important elements on earth as it is required to support all forms of aerobic life. While ground state $O_2$ is rather "safe" and unreactive, its reactive derivatives could be harmful to all life forms. Yet the evolution of aerobic metabolic processes such as respiration

and photosynthesis unavoidably lead to the production of reactive oxygen species (ROS) in mitochondria, chloroplasts, and peroxisomes, making oxygen a best friend, or worst enemy (Ref: Foyer 1994).

In plants ROS are continuously produced as by-products of various metabolic pathways localized in different cellular compartments (Foyer *et al.*, 1994). Undesirably high level of ROS could cause many adverse effects to the plant cell, including inhibition of sensitive enzymes, chlorophyll degradation, lipid peroxidation (Yu, 1994), indiscriminate attack of macromolecules including DNA (Kasai *et al.*, 1986), and may eventually lead to cell death (Fath *et al.*, 2001). When the formation of reactive oxygen species become damaging, the cells are said to be under oxidative stress.

Reactive oxygen species are formed during certain redox reactions and during incomplete reduction of oxygen or oxidation of water by the mitochondria or chloroplast electron transfer chains. The different species of oxygen radicals and their sources were summarized in Table 1.

There are several processes which can leads to the production of ROS in normal physiological condition. One is the physical activation of ground state $O_2$ by transfer of excitation energy from a photoactivated pigment such as an excited cholorophyll molecule to $O_2$, producing a singlet oxygen. i.e.:

$Chlorophyll^{*} + O_2 \rightarrow chlorophyll + {}^1O_2$

$^1O_2$ subsequently stimulates production of other ROS such as hydrogen peroxide ($H_2O_2$), superoxide anion ($O_2^{\cdot -}$), and hydroxyl ($HO^{\cdot}$) radicals. These reactive molecules, especially $HO^{\cdot}$, are highly destructive to lipids, nucleic acids, and proteins.

Other processes which will cause ROS production involve chemical activation of $O_2$, i.e.:

$O_2 + e^- \rightarrow O_2^{\cdot -}$

$O_2^{\cdot -} + e^- + 2H^+ \rightarrow H_2O_2$

$H_2O_2 + e^- + H^+ \rightarrow HO^{\cdot} + H_2O$

In this process, all three intermediates of the univalent reduction i.e. superoxide ($O_2^{\cdot -}$), hydrogen peroxide ($H_2O_2$), and hydroxyl radical ($HO^{\cdot}$) are all chemically reactive and biologically toxic.

**Table 1.** Formation and characteristics of major reactive oxygen species.

| Compound | Shorthand notation(s) | Source | Characteristics |
|---|---|---|---|
| Singlet oxygen | $^1O_2$ | Photosystem II $e^-$ transfer reactions (chloroplasts), UV irradiation, photoinhibition | Highly diffusible and capable of reacting with organic molecules. |
| Superoxide | $O_2^{\cdot -}$ | Mitochondria e- transfer reactions, Mehler reaction in chloroplasts (reduction of $O_2$ by iron-sulphur center Fx of Photosystem I), glyoxysomal photorespiration, peroxisomes activity, plasma membrane oxidation of paraquat, nitrogen fixation, reactions of $O_3$ and $OH^-$ in apoplastic space. | Capable of both oxidation and reduction, it may react to produce several other reactive species, and may undergo spontaneous or enzymatic dismutation to $H_2O_2$. |
| Hydrogen peroxide | $H_2O_2$ | Photorespiration, β-oxidation, proton-induced decomposition of $O_2^{\cdot -}$ | It is not a free radical, but participates as oxidant or reductant in many cellular reactions. $H_2O_2$ is highly diffusible through membranes and aqueous compartments, and it may directly inactivate sensitive enzyme at a low concentration. |
| Hydroxyl radical | $OH^{\cdot}$ | Decomposition of $O_3$ in presence of protons in apoplastic space | The most powerful oxidizing species in biological systems, it will react non-specifically with any biological molecule |

(Modified from (Buchanan *et al.*, 2000))

In addition, transition metals such as iron and copper (M), which frequently have unpaired electrons, are very good catalysts of oxygen reduction, following the reaction:

$$M^n + O_2 \rightarrow M^{n+1} + O_2^{\cdot -}$$

In aqueous neutral pH solutions, $O_2^{\cdot -}$ can generate $H_2O_2$, which can subsequently decompose to produce $OH^{\cdot}$ by the Haber-Weiss reaction which involves iron or copper (M) following the reactions:

$$M^{n+1} + O_2^{\cdot -} \rightarrow M^n + O_2$$

$$M^n + H_2O_2 \rightarrow M^{n+1} + OH^- + OH^{\cdot}$$

When iron is the transition metal in the Haber-Weiss reaction, it is called the Fenton reaction. Fenton chemistry occurs in vivo, but organisms carefully control it by limiting the availability of both $Fe^{2+}$ and $H_2O_2$ (Halliwell and Gutteridge, 1990, 2006). In biological systems, Ferric/Ferrous complexes may act as protectors against $O_2^{\cdot -}$ damage. Protection can be achieved through disproportionation of $O_2^{\cdot -}$ catalyzed by several metal ligands (L-M) according to a mechanism analogous to a superoxide dismutase reaction (Fridovich, 1995).

$$L\text{-}M^{n+1} + O_2^{\cdot -} \rightarrow L\text{-}M^n + O_2$$

$$L\text{-}M^n + O_2^{\cdot -} + 2H^+ \rightarrow L\text{-}M^{n+1} + H_2O_2$$

### 1.1.3 Major sites of ROS production

Organelles with a highly oxidizing metabolic activity or with an intense rate of electron flow, such as chloroplast and mitochondria, or microbodies, are major source of ROS production in plant cells (Miller *et al.*, 2008). Fig. 1 Summarize the sources of ROS in plant cells. In the below sections, chloroplast and mitochondria as major sites of ROS production will be discussed.

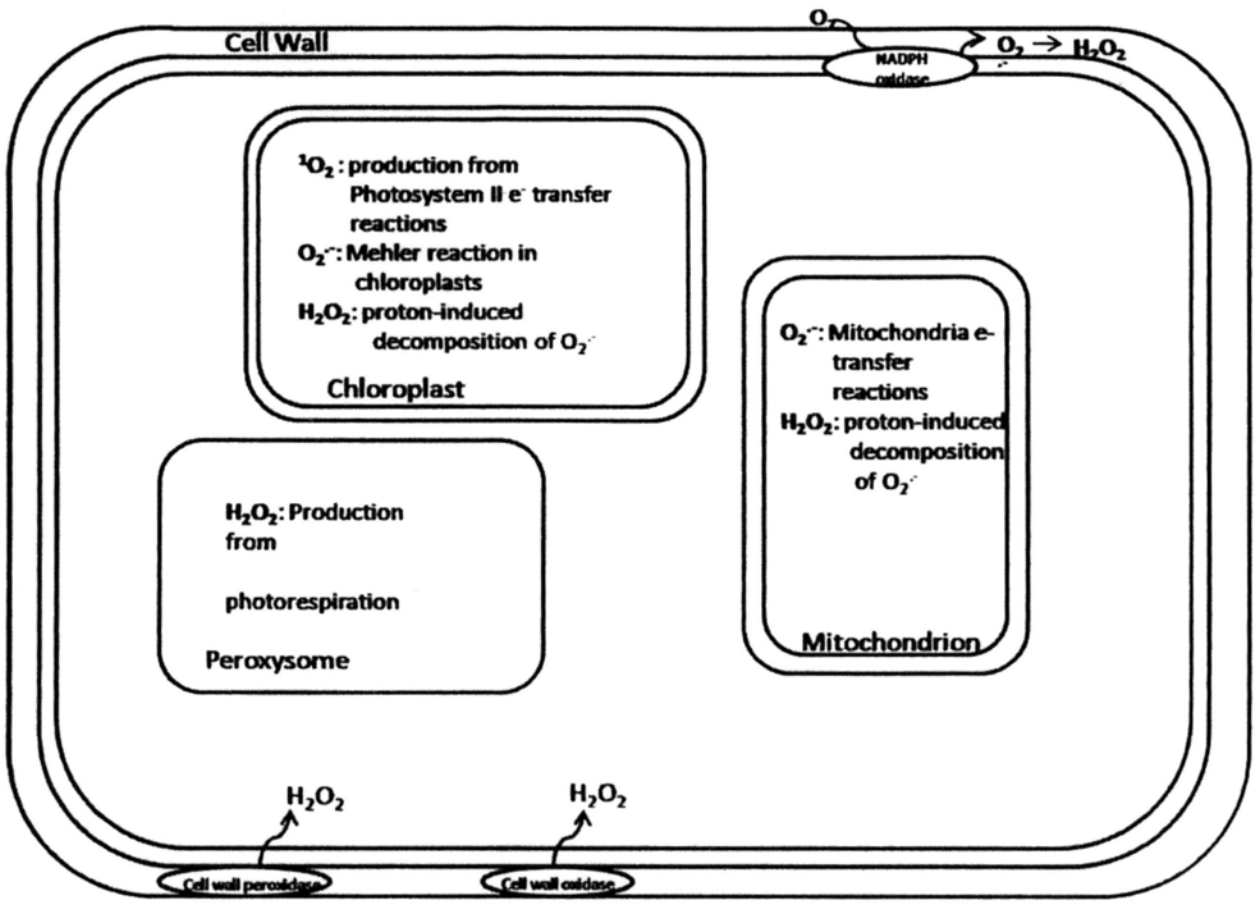


**Fig. 1.** Sources of ROS in plant cells. [Modified from (Bhattacharjee, 2005)]

1.1.3.1 Chloroplast

In photosynthetic tissues, chloroplasts are the major source of reactive oxygen species formation (Bhattacharjee, 2005). There are several sources of ROS in the chloroplast, leading to the production of all of the above mentioned ROS (Asada, 1994; Foyer & Harbinson, 1994). The reaction centers of PSI and PSII in chloroplast thylakoids are the major generation site of reactive oxygen species (Asada, 2006). PSI may donate electrons to $O_2$ in the Mehler reaction to generate $O_2^{\cdot-}$ when the pool of NADP is mostly reduced. Also, photoexcited Chlorophyll molecules can interact directly with $O_2$ to generate the very reactive singlet oxygen (Foyer *et al.*, 1994). Photoproduction of superoxide by PSII has also been reported (Ananyev *et al.*, 1994).

1.1.3.2 Mitochondria

Plant mitochondria differ significantly from their animal counterparts, with specific electron transport chain (ETC) components and functions in processes such as photorespiration (Noctor *et al.*, 2007). Mitochondria consume oxygen during respiratory electron transport. The electron transport chain in plant mitochondria contains complexes I-IV, as well as five enzymes not present in mammalian mitochondria: an alternative oxidase (AOX) and four NAD(P)H dehydrogenases

(Moller, 1997; Moller & Rasmusson, 1998). When oxygen interacts with the complex IV and AOX, 2 terminal oxidases in plant mitochondria, four electrons are transferred and the product is water (Siedow & Umbach, 1995). However, if oxygen interacts with reduced components of the electron transport chain, such as Complex I and Complex III, ROS formation will be resulted (Moller, 2001).

The situation of oxidative stress in plant mitochondria is less clear (Moller, 2001), since earlier studies on oxidative stress in plants mainly focus on the effect of ROS on photosynthetic system, as chloroplast is believed to be the major target of ROS. Recently, though, it has become apparent that alterations in mitochondrial ROS production or electron transport chain can have far reaching consequences for the cell (Noctor *et al.*, 2007; Schwarzländer *et al.*, 2009). It was suggested that mitochondria are the main target for oxidative damage under osmotic stress (Bartoli *et al.*, 2004). In fact, in the plant cell, mitochondria represent a major source of ROS production and consequent oxidative damage, as indicated by proteomic studies (Sweetlove *et al.*, 2002; Bartoli *et al.*, 2004; Taylor *et al.*, 2004).

### 1.1.4 ROS accumulation induced by Salt and osmotic stress in plants

A secondary effect of salt and osmotic stress is the increase of reactive oxygen species (ROS), which include singlet oxygen, superoxide anion radicals, hydroxyl radicals, and hydrogen peroxide (Smirnoff, 1998; Bartels, 2001; Apel & Hirt, 2004; Banu *et al.*, 2008). The production of ROS during these stresses results from pathways such as photorespiration, from the photosynthetic apparatus and from mitochondrial respiration. In the following section, we will focus our discussion on how oxidative stress induced when plants were under salt stress and dehydration stress.

#### 1.1.4.1 Oxidative stress is induced when plants are under salt stress

ROS are produced as by-products of normal metabolism in plant cells. Under normal conditions, the several lines of oxidative defense system are enough to keep the production and removal of ROS in equilibrium. When under stressing conditions such as salt stress, many important metabolic processes are being disturbed, thus upsetting the equilibrium between the formation and the scavenging of highly reactive oxygen species, so that an oxidative stress may result (Hernandez *et al.*, 1993; Hernandez *et al.*, 1995;

Gossett *et al.*, 1996; Gomez *et al.*, 1999; Rubio *et al.*, 2009). Though little is known about the underlining mechanism of how salinity induce oxidative stress, it was suggested that salt stress could affect the NADH-induced production of $O_2^-$ in the mitochondria (Hernandez *et al.*, 1993). It was found that under salt-treatment, both the NADH- and succinate-dependent generation of $O_2^-$ were induced, and the $O_2^-$ generation in salt-sensitive pea plants rose 2-3 times in mitochondria (Hernandez *et al.*, 1993). It is also suggest that an impair ROS scavenging system may occur under salt stress (Hernandez *et al.*, 1993; Gomez *et al.*, 1999; Mittova *et al.*, 2003). In mitochondria of NaCl-sensitive pea plants, salinity brought about a significant decrease of ROS scavenging enzymes MnSOD and Cu/ZnSOD I activities (Hernandez *et al.*, 1993). In a NaCl-sensitive cultivar of tomato, there is an increase in $H_2O_2$ content and lipid peroxidation, which accompanied by decreased activity of antioxidant and ROS scavenging enzymes such as Ascorbate, SOD and MDHAR activity in the mitochondria; and decreased level of reduced ascorbate and glutathione in the peroxisomes (Mittova *et al.*, 2003; Mittova *et al.*, 2004). A recent study on Arabidopsis also showed that changes in superoxide dismutase (SOD) transcripts abundance accurately reflected the severity of the salt stress (Attia *et al.*, 2008). All in all, these studies indicate

the importance of ROS scavenging in salt stress tolerance.

1.1.4.2 Oxidative stress is induced when plants are under osmotic stress

During osmotic stress, it is now a text book knowledge that an abscisic acid (ABA) signal causes stomatal closure. The important consequences are that there is a drastic decrease in intercellular $CO_2$, yet the photosynthetic capacity remain high, resulting in over-reduction of components within the electron transport chain, and thus electrons being transferred to oxygen at PSI or via the Mehler reaction. This generates reactive oxygen species (ROS), such as superoxide, hydrogen peroxide ($H_2O_2$) and the hydroxyl radical, if the plant is not efficient in scavenging these molecules (Chaves & Oliveira, 2004). The rate of $O_2^{\cdot}$ formation increases under water dehydration could lead to lipid peroxidation, fatty acid saturation, and ultimately membrane damage (Moran *et al.*, 1994). The content of oxidatively damaged proteins increase in the thylakoids of droughted leaves, and these damages could be partly recovered by increase of ascorbate content (Tambussi *et al.*, 2000). The ROS scavenging enzyme Ascorbate peroxidase (APX) were found to be essential for osmotic stress tolerance. The importance of APX in stress tolerance was demonstrated in APX-antisense transgenic tobacco, which is highly susceptible to oxidative injury (Orva & Ellis, 1997). Overproduction of Arabidopsis cytosolic APX in

the chloroplast of tobacco is able to protect the plant from osmotic stress and oxidative stress (Badawi *et al.*, 2004). All of these evidences suggest that oxidative stress is being induced when plants are under osmotic stress. A most dramatic example which demonstrates how important of ROS scavenging is to osmotic stress tolerance is the studies of the resurrection plant *Myrothamnus flabellifolia* (Kranner *et al.*, 2002). This woody shrub can survive severe desiccation of its vegetative organs, and able to recover rapidly upon rehydration. Upon desiccation, redox shifts of the antioxidants glutathione and ascorbate towards their oxidized form were observed. Rewatering of the plant induced formation of ascorbate and glutathione, simultaneous reduction of their oxidized forms, and rapid production of other antioxidants such as α-tocopherol and of various carotenoids. This study has demonstrated the importance of ROS scavenging system in drought tolerance and aid plants' survival under osmotic stress.

## 1.2 Regulation of intracellular ROS content in plant cells

ROS is constantly produced in all cellular compartments as a by-product of normal cellular metabolism and that cell survival will depend upon adequate protection. Since ROS are produced in different cellular compartments and exist in different species with vary diffusibility, solubility and propensity to react with various biological molecules, plant cells have evolved multiple lines of defenses including both scavenging enzymes and non-enzymatic antioxidants.

### 1.2.1 Enzymatic defense of ROS

These involve multiple enzymes that work together to convert the reactive ROS into stable substance such as $H_2O$. This sophisticated enzymatic system in plants include superoxide dismutase (SOD), ascorbate peroxidase (APX), glutathione peroxidase (GPX), and catalase (CAT). SODs act as the first line of defense against ROS, dismutating superoxide to $H_2O_2$. While APX, GPX and CAT subsequently detoxify $H_2O_2$ and they also participates in the regeneration of the antioxidant ascorbate and glutathione.

1.2.1.1 Superoxide dismutase (SOD)

Superoxide dismutases (SOD) are metalloenzymes first discovered by McCord and Fridovich (1969) that convert $O_2^{\cdot -}$ to $H_2O_2$ in all aerobic organisms in the following reaction:

$$2O_2^{\cdot -} + 2H^+ \xrightarrow{SOD} O_2 + H_2O_2$$

Because superoxide is the first product of univalent reduction of oxygen and also the first species to form in many biological systems, SOD is considered as the primary defense against oxygen radicals (Bannister *et al.*, 1987). The dismutation is catalyzed by the metal ion (Cu, manganese, or iron) at the active site. Depends on the metal ion in the active site, SODs are classified as different classes, and these different SODs present in different subcellular compartments.

1.2.1.2 Ascorbate peroxidase, Glutathione reductase and the Ascorbate-Glutathione cycle

The product of SOD, hydrogen peroxide, requires further detoxification. This is achieved by several enzymes and non-enzymatic substrate working together and may be differ among the various cellular compartments. In plant, the Ascorbate-Glutathione cycle (ASC-GSH cycle), or so called "Halliwell-Asada pathway" has been the most established ROS detoxification pathway.

Fig. 2 below shows the detail of the Ascorbate-Glutathione. The first step of the cycle is the reduction of $H_2O_2$ to water by APX. This requires the consumption of Ascorbate present in the chloroplast and it will be oxidized to monodehydroxyascorbate (MDHA).

$$2\ \text{Ascorbate} + H_2O_2 \xrightarrow{\text{APX}} 2\ \text{MDHA} + 2H_2O$$

MDHA may give rise to dehydroxyascorbate (DHA). Both MDHA and DHA must be reduced to regenerate the Ascorbate pool, which can be achieved by several reactions:

(1) non-enzymatic reduction by ferredoxin:

$$\text{MDHA} + Fd_{red} \longrightarrow \text{ascorbate} + Fd_{ox}$$

(2) reduction of MDHA by MDHA reductase (MDHAR) in the stroma, using NADPH:

$$2\ \text{MDHA} + \text{NADPH} \xrightarrow{\text{MDAR}} 2\ \text{Ascorbate} + NADP^+$$

(3) reduction of DHA to ascorbate by DHA reductase (DHAR) with glutathione (GSH) as the reducing substrate

$$DHA + 2\,GSH \xrightarrow{GSH} Ascorbate + GSSG$$

The last step of the cycle was regeneration of Glutathione by the Glutathione reductase (GR) with NADPH as electron donor.

$$GSSG + NADPH \xrightarrow{GR} 2\,GSH + NADP^{+}$$

Some studies have demonstrated that ASC-GSH cycle occurs in the mitochondria as well as in peroxisomes. Jimenez *et al.* (1997) (Jimenez *et al.*, 1997)have been succeed in purify some of the key enzymes in the Ascorbate-Glutathione cycle in pea plants, including the APX and MDHAR, which is membrane bound, and the GR and DHAR in the matrix fraction. Chew *et al.* (2003) (Chew *et al.*, 2003)have demonstrated that in Arabidopsis, there is a dual-targeting of APX, MDHAR and GR to mitochondria and chloroplasts, and the mitochondrial targeting specific DHAR. The transcript levels for these genes were induced by oxidative stresses imposed on chloroplasts and/or mitochondria. These studies provide evidences on the existence of ASC-GSH cycle at in plant mitochondria.

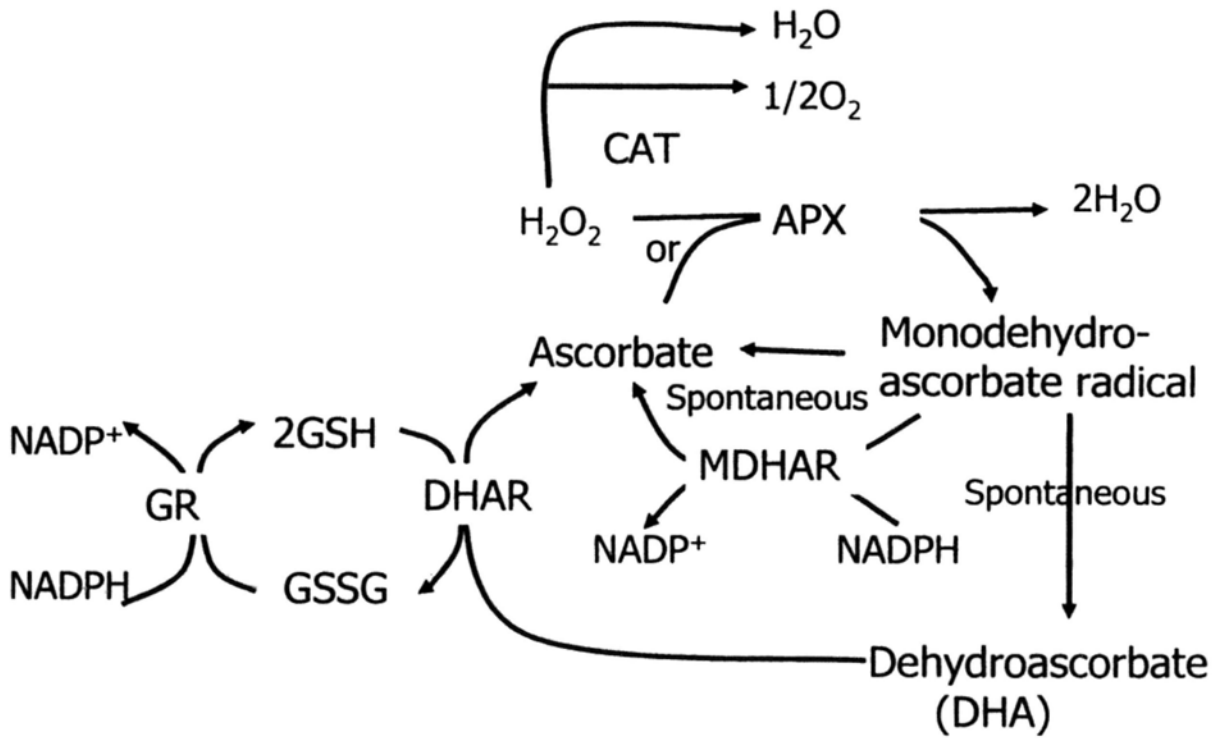


**Fig. 2**. The Ascorbate-Glutathione cycle.

The ascorbate-glutathione cycle is one of the major antioxidant defense systems in plant cells. First, Superoxide radicals are eliminated by superoxide dismutase in a reaction that yields hydrogen peroxide, $H_2O_2$. Hydrogen peroxide is consumed through its conversion to oxygen and water by catalase (CAT) or to water alone through the oxidation of ascorbate. Ascorbate is regenerated by way of two mechanisms. The enzymatic reduction of monodehydroascorbate takes place in the plastids. Alternatively, monodehydroascorbate that is spontaneously dismutated to dehydroascorbate can react with glutathione (GSH) to produce ascorbate and oxidized glutathione (GSSG) in a reaction catalyzed by dehydroascorbate reductase (DHAR). GSSG is reduced by glutathione reductase (GR), requiring the consumption of NADPH. (Modified from Foyer & Halliwell, 1976; Buchanan *et al.*, 2000; Perl-Treves & Perl, 2002)

1.2.1.3 Catalase

Catalases (CATs) efficiently scavenge $H_2O_2$ and do not require a reducing substrate to perform the task:

$$2\ H_2O_2 \xrightarrow{CAT} 2H_2O + O_2$$

In plants, catalase is localized in peroxisomes, to scavenge the $H_2O_2$ produced by the glycolate oxidase in the C2 photorespiratory cycle. In chloroplasts, no catalase was found yet (Asada, 1994), but a mitochondrial isozyme was identified in maize (Scandalios *et al.*, 1980).

1.2.1.4 Alternative oxidase (AOX)

In addition to the cytochrome respiratory pathway found in all eukaryotes, plants have a second, alternative pathway that diverges from the main respiratory chain at ubiquinone (Vanlerberghe *et al.*, 1997). This alternative pathway is comprised of a single protein the alternative oxidase (AOX) (Elthon & Mclntosh, 1987), which is thought to exist in the inner mitochondrial membrane as a homodimer. It is proved that AOX could lowers mitochondrial reactive oxygen production in plant cells (Maxwell *et al.*, 1999). Though how the AOX could achieve such function is still unknown, the most plausible explanation for why AOX may lower ROS levels is

that a second oxidase downstream of the ubiquinone pool maintains upstream electron-transport components in a more oxidized state, thereby lowering ROS generation by overreduced electrons carriers (Maxwell *et al.*, 1999).

### 1.2.2 Non-enzymatic antioxidant

Ascorbate and Glutathione are important antioxidants which participate in the Ascorbate-Glutathione cycle. In Plant cells, the most important reducing substrate for $H_2O_2$ detoxification is ascorbate (Noctor & Foyer, 1998). Ascorbate is a major primary antioxidant, reacting not only with $H_2O_2$ but also with $O_2^{\cdot-}$, $OH^{\cdot}$, $^1O_2$, and lipid hydroperoxides (Nijs & Kelley, 1991; Yu, 1994). Ascorbate is also a powerful secondary antioxidant, reducing the oxidized form of α-tocopherol, an important antioxidant in nonaqueous phase (Padh, 1990). GSH, the reduced form of Glutathione, is important as an antioxidant and redox buffer (Foyer & Halliwell, 1976; Law *et al.*, 1983), and is responsible for the regeneration of not only ascorbate, but also tocopherol and carotenoids (Perl-Treves & Perl, 2002).

Another well-known non-enzymatic antioxidants is α-tocopherol. It is the major isomer of vitamin E, and is a phenolic antioxidant present in both plants and animals. Being a lipid-soluble molecule, it is very important as a chain terminator of free-radical reactions that cause lipid peroxidation (Burton & Ingold, 1982).

### 1.2.3 Cellular compartmentalization and coordination of ROS scavenging pathways

Organelles with a highly oxidizing metabolic activity or with an intense rate of electron flow, such as mitochondria and chloroplast, are major sources of ROS production in plant cells (Miller *et al.*, 2008). Thus these organelles are the front line of defense for excessive ROS accumulation (Mittler *et al.*, 2004). To prevent damages to essential cellular components, most ROS molecules are scavenged at the site of production such as mitochondria (Smirnoff, 1998; Bartoli *et al.*, 2004; Noctor *et al.*, 2007) and chloroplast (Foyer & Harbinson, 1994; Hernandez *et al.*, 1995; Bartels & Sunkar, 2005.). It is very important to have the ROS scavengers localized in the right place in order to have them working to cope with the excessively accumulate ROS. Table 2 below shortlisted the subcellular localization of several antioxidants and ROS scavenging enzymes.

**Table 2**. Subcellualr localization of selected ROS scavenging enzymes and Antioxidants.

| ROS Scavenging enzyme | | Subcellular localization |
|---|---|---|
| Ascorbate peroxidase (APX) | | Cytosol, plastids, mitochondria, peroxisome |
| Catalase (CAT) | | Glyoxysome, peroxisome |
| Dehydroascorbate reductase (DHAR) | | Cytosol, plastid, mitochondrion |
| Glutathione reductase (GR) | | Cytosol, mitochondrion, plastid stroma |
| Monodehydroascorbate reductase (MDHAR) | | Plastid, mitochondrion |
| Alternative oxidase (AOX) | | Mitochondrion |
| Superoxide dismutase (grouped by metal cofactor) | Cu/ZnSOD | Cytosol, peroxisome, plastid |
| | MnSOD | Mitochondrion |
| | FeSOD | Plastid |
| | | |
| Antioxidants | | Subcellular localization |
| Ascorbate | | Apoplast, cytosol, plastid, vacuole |
| Reduced Glutathione (GSH) | | Cytosol, mitochondrion, plastid |
| α-tocopherol | | Cell membranes (including membranes of plastid) |

[Modified from (Buchanan *et al.*, 2000; Mittler *et al.*, 2004)]

## 1.3 Purple acid phosphatase and its relationship with ROS in plants

### 1.3.1 General introduction on plants purple acid phosphatase (PAP)

Purple acid phosphatases (PAPs) are one of the largest groups of plant phosphatases which occur also in microorganisms and animals (Schenk *et al.*, 2000; Vogel *et al.*, 2001). All PAPs contain a binuclear metal site. The pink/purple color of their concentrated water solution is the result of a charge-transfer transition between "chromophoric" ferric ion and the tyrosine residue. The second "non-chromophoric" metal ion, occupying the binuclear site, is iron in mammalian PAPs, and zinc or manganese in plant enzymes (Vogel *et al.*, 2001). In plant there are 2 major groups of PAPs, one is those structurally closer to mammalian purple acid phosphatases, monomeric proteins with a molecular mass around 35 kDa (small plant PAPs), and another composed of homodimeric proteins with a polypeptide of about 55 kDa (large plant PAPs) (Schenk *et al.*, 2000). No matter small plant PAPs or large plant PAPs or mammalian PAPs, they all contain the 5 PAP metal-binding motifs and the 7 invariable residues (Table 3).

Table 3. The 5 conserve domains and 7 invariable residues in PAPs

| Source of PAPs | PAP conserved domains | | | | |
|---|---|---|---|---|---|
| | * | * * | * | * | * * |
| GmAY151271 | GDLG | GDLSY | GNHE | VLMH | GHVH |
| IbAJ006224 | GDLG | GDLSY | GNHE | VLMH | GHVH |
| LlAJ458941 | GDLG | GDLSY | GNHE | VLMH | GHVH |
| PvAF236109 | GDWG | GDNFY | GNHD | VIGH | GHDH |
| SsP09889 | GDWG | GDNFY | GNHD | VAGH | GHDH |

The first 2 letters of each protein label represent the abbreviated species name, followed by GenBank accession number. Gm: Glycine max; Ib: Ipomoea batatas; Ll: Lupinus luteus; Pv: Phaseolus vulgaris; Ss: Sus scrofa. Asterisks indicate the 7 invariable residues in the 5 metal-binding domains. (Modified from Schenk *et al.*, 2000; Olczak *et al.*, 2003).

### 1.3.2 The physiological role of PAPs

In mammals, a role of PAPs is ascribed to iron transport (Buhi *et al.*, 1982), bone resorption (Hayman *et al.*, 1996), antigen presentation and some redox reactions (Hayman *et al.*, 2000; Vogel *et al.*, 2001). However, the plant PAPs are rather unspecific, hydrolyzing a broad spectrum of phosphate esters and their functions is

unknown, although some of the functions are proposed (Olczak *et al.*, 2003). Some of the PAPs transcripts are regulated by phosphate level in the medium and soil suggests an important role for these enzymes in phosphate acquisition (Duff *et al.*, 1994). The activities and gene expression of most plant PAPs were frequently found to be phosphorus (P) regulated (induced under P starvation) (Cashikar *et al.*, 1997; del Pozo *et al.*, 1999; Li *et al.*, 2002), consistent with their roles in P metabolism. However, a systematic study of the *PAP* gene family in *Arabidopsis thaliana* showed that some of the gene members are irresponsive to P status (Li *et al.*, 2002).

### 1.3.3 Purple acid phosphatase that found to be involved in ROS metabolism in plant

In mammalian PAPs, the presence of a Fe(III)-Fe(II) di-iron binuclear center has been shown to endow theses proteins ROS scavenging as well as ROS-producing activities through Fenton's type reaction (Hayman & Cox, 1994; Kaija *et al.*, 2002).

While mammalian PAPs are found to be taking a role of ROS-generator and participate in pathogen defense (Klabunde *et al.*, 1995; Kaija *et al.*, 2002), the plant PAPs may have a very different role. A ROS scavenging role of a plant PAP from kidney bean (KBPAP) was proposed based on the observation that in the presence of Ascorbate, the Fe(III) of KBPAP could be reduced to Fe(II), which has such a low

redox potential that it immediately reduce oxygen to water to form Fe(III), thereby reduce the concentrations of free radicals (Klabunde *et al.*, 1995). There are several plant purple acid phosphatases are shown to display both Acid phosphatase as well as peroxidase activity. Including AtPAP17 and AtPAP26 in Arabidopsis (del Pozo *et al.*, 1999; Veljanovski *et al.*, 2006); and LeIAP in tomato (Bozzo *et al.*, 2002; Bozzo *et al.*, 2004). However, their possible roles in ROS metabolism are only implicated.

### 1.4 Previous studies on *GmPAP3*

By using Suppression subtractive hybridization techniques (SSH), Phang (2002) in Dr. H.M. Lam's lab have identified several salt-inducible gene candidates from soybean. The full length coding regions of selective fragments were obtained by 5' and 3'-RACE. One of the candidate gene is *GmPAP3* (GenBank accession no. AY151271), which was found to be strongly induced by NaCl stress in both leaves and roots of all the five cultivated and five wild soybean varieties tested. Liao *et al.* (2003) has continued the studies on *GmPAP3*. DNA sequence analysis and Phylogenetic analysis indicate that *GmPAP3* belongs to the class of Plant PAPs and PAP-like proteins and the invariable consensus metal binding residues were all conserved in GmPAP3. One of the most interesting characteristics of *GmPAP3* is that, unlike all the other plant PAPs, analysis of the putative protein sorting signals and subcellular localizations suggest the presence of a putative mitochondrion targeting transit peptide at the N-terminal of GmPAP3.

Sequence analysis reveals that GmPAP3 belongs to the class of plant PAPs, we hypothesize that the *GmPAP3*, just like many other PAPs, could be induced by phosphate starvation. However, unlike the 2 other soybean PAPs being tested, no P starvation induced gene expression was observed, while a strong induction of *GmPAP3* was observed in both leaves and roots under salt treatment.

Since GmPAP3 is predicted to be mitochondrial localized, we further tested if *GmPAP3* gene expression would also be induced by oxidative stress that is tightly related to the function of mitochondria under abiotic stresses. The herbicide (PQ) was used to mimic the effect of oxidative stress. Among the 3 soybean PAP genes tested, only *GmPAP3* was induced by PQ treatments. In this work we reported the discovery of *GmPAP3*, a novel purple acid phosphatase like gene in soybean, which not response to phosphate starvation but strongly induced under salt and oxidative treatments. Yet its physiological role under these stresses and its relationship to the adaptation of stress tolerance remains unknown.

I have continued to study this novel purple acid phosphatase with 2 main objectives: (i) to investigate the relationship of *GmPAP3* with abiotic stresses; (ii) to verified the subcellular localization of GmPAP3. Since NaCl will also lead to "physiological drought", we tested the effect of osmotic stress on the *GmPAP3* gene expression by treating soybean plants with PEG. The expression of *GmPAP3* under NaCl, PEG, and PQ treatments was studied (Fig. 3). All stresses led to an increase in the steady-state mRNA levels of *GmPAP3*, indicating that the *GmPAP3* gene expression is co-regulated by salinity, osmotic, and oxidative stresses. To verified the subcellular localization of GmPAP3, transgenic tobacco BY-2 cells expressing the GmPAP3-T7 gene construct was made. Using Immunolabeling and confocal

microscopy, the majority of GmPAP3-T7 fusion proteins (> 60 %) were found to be localized in mitochondria (Fig. 4, Table 4).

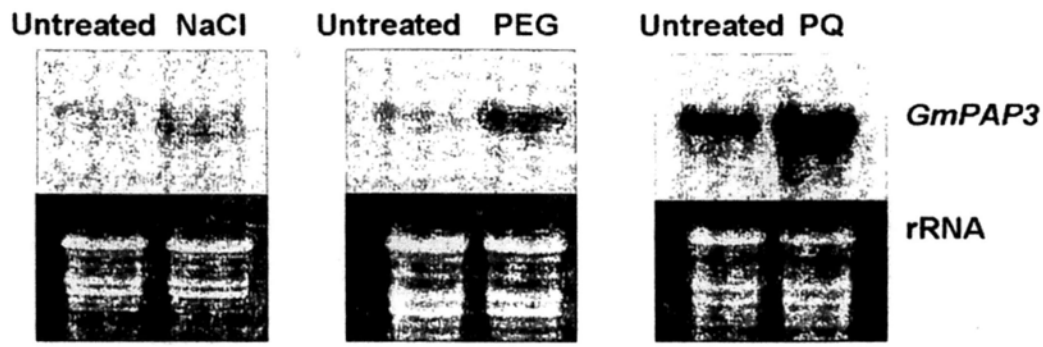


Fig.3. Northern blot analysis of *GmPAP3* under salinity, osmotic, and oxidative stresses. NaCl: 125 mM NaCl; PEG: 5 % PEG; PQ: 10 mM Paraquat. Ethidium bromide staining of rRNA was used as the reference for total RNA quantitation. Ten μg of total RNA was loaded onto each lane.

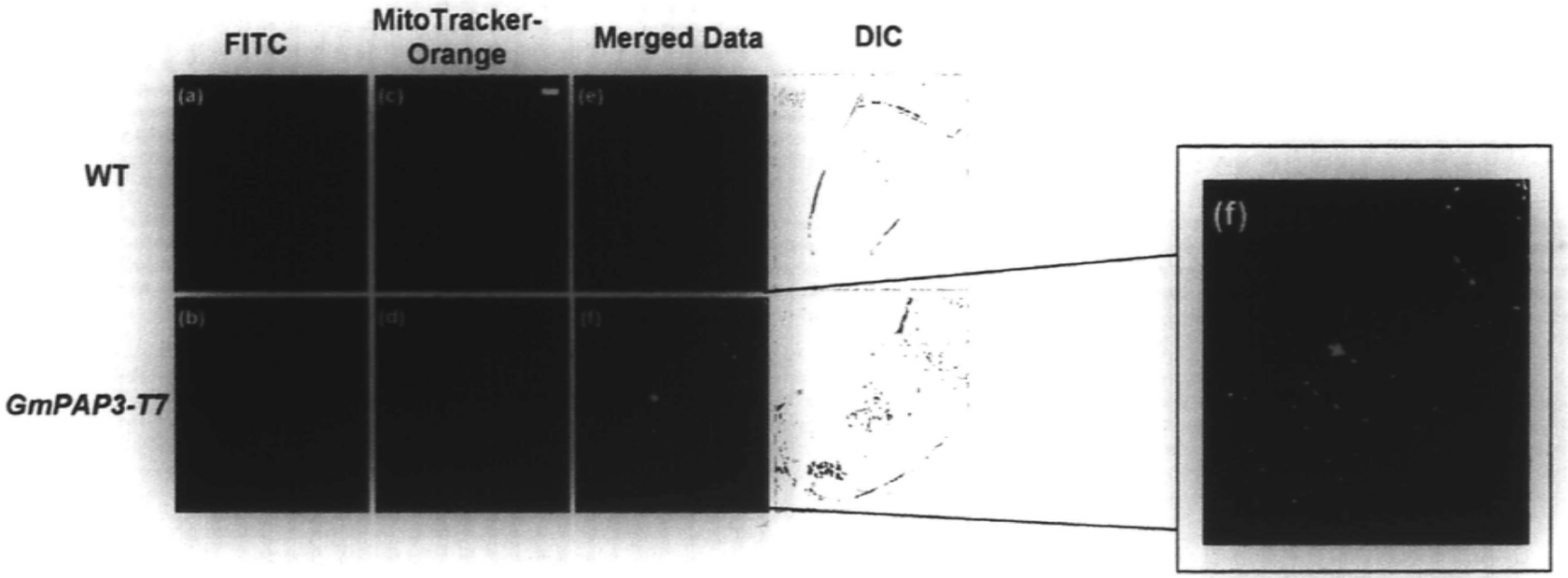


**Fig. 4.** Confocal microscopic studies of the subcellular localization of GmPAP3. A transgenic BY-2 cell line (1535-2) expressing the GmPAP3-T7 fusion protein was used. The T7 tag was tracked by the T7 antibody and then labeled with the FITC-conjugated secondary antibody (**a**, **b**). MitoTracker® Orange was used as a marker to locate mitochondria (**c**, **d**) .The signal of FITC (pseudocolored in green) and MitoTracker® Orange (pseudocolored in magenta) were visualized by confocal scanning microscopy, and the structures of the corresponding transgenic BY-2 cells were observed using differential interference contrast (DIC) (**g**, **h**) and the merged images were also shown (**e**, **f**). One typical spot with overlapping signals was indicated by an arrow. Scale bar = 10 μm. Quantitative analysis was shown in Table 4.

**Table 4.** Estimation of the percentage of mitochondrial localized GmPAP3 proteins

| *GmPAP3-T7* transgenic cell lines | % colocalization | number of cells analyzed |
|---|---|---|
| 1535-1 | 66 ± 6 % | 29 |
| 1535-2 | 65 ± 4 % | 31 |
| 1535-3 | 67 ± 5 % | 27 |

Experimental details were given in Fig. 4. Quantification for the extent of colocalization between the signals of FITC and MitoTracker® Orange was performed from one direction only (i.e. asking how much of the FITC signals colocalized with the MitoTracker® Orange signals, but not the other way round). Three independent cell lines were studied. The percentage of colocalization was expressed as the mean ± standard deviation (SD) for the number of cells analyzed.

## 1.5 Hypothesis and significance of this project

Abiotic stresses such as salt and osmotic stresses can disturb important metabolic processes, thus upset the equilibrium between the formation and the scavenging of reactive oxygen species (ROS), and resulting in excessive accumulation of ROS (Apel & Hirt, 2004; Chaves & Oliveira, 2004; Mittova *et al.*, 2004; Miller *et al.*, 2008). The inducibility of the *GmPAP3* gene expression by salinity, osmotic, and oxidative stresses and the suspected mitochondrial localization of GmPAP3 lead to the hypothesize that the physiological role of GmPAP3 might be related to abiotic stress, possibly through its involvement in reactive oxygen species forming and/or scavenging.

The objectives of this research are:

1) To verified the subcellular localization of GmPAP3.
2) To investigate the physiological functions of the *GmPAP3* gene in relationship to NaCl, osmotic , and oxidative stresses in both cell level and in *in planta* level.
3) To examine the significance of mitochondrial localization of GmPAP3 in relationship to its protective roles.

# Chapter 2 Materials and Methods

## 2.1 Materials

### 2.1.1 Plants, bacterial strains and vectors

The *Escherichia coli* strains DH5α and the plasmid pBluescript KSII(+) were used as the host and vector, respectively, for gene cloning unless stated otherwise. For co-cultivation transformation of *Nicotiana tabacum* Bright-yellow 2 (tobacco BY-2) cell lines, the *Agrobacterium tumefaciens* strain LBA 4404 containing Ti-plasmid (pAL4404) was employed as the bacterial host for the target gene. GmPAP3 (both with and without mitochondria transit peptide) were cloned into the plant expression vector V7/W104. In this study, some transgenic tobacco BY-2 cells and Arabidopsis lines constructed in my M.Phil study as well as some cell lines constructed in my Ph.D study were employed A list of plant hosts, bacterial strains, plasmid vectors and transgenic lines used in the research was shown in Table 5.

**Table 5**. Plants, bacterial strains and vectors used.

| **Bacteria/ Plasmid** | **Description** | **References** |
|---|---|---|
| *Agrobacterium tumefaciens*, LBA4404/ pAL4404 | For tobacco BY-2 cells transformation | (Hoekema *et al.*, 1983) |
| *Escherichia coli* DH5α | For regular gene cloning | Lab stock |
| | | |
| **Plant hosts** | **Description** | **References** |
| Columbia-0 | *A. thaliana* ecotype for transformation | Lab stock |
| Tobacco BY-2 cell lines | Tobacco wild type cells lines for transformation | A generous gift from Prof. Liwen Jiang |
| | | |
| **Plasmid vectors** | **Description** | **References** |
| pBluescript II KS (+) | Plasmid for subcloning of target gene | Strategene, La Jolla, CA, U.S.A. |
| V7/W104 plant expression vectors | Vectors for plant transformation of target genes | (Brears *et al.*, 1993b) |
| | | |
| **Transgenic lines** | **Description** | **References** |
| *GmPAP3* transgenic tobacco BY-2 cell lines 20 and 29 | These cell lines were constructed in my M.Phil study and were employed in functional analysis of GmPAP3 in this study. | (Li *et al.*, 2008) |

| | | |
|---|---|---|
| *GmPAP3* transgenic Arabidopsis thaliana line F42 and C25 | These cell lines were constructed in my M.Phil study and were employed in functional analysis of GmPAP3 in this study. | (Li *et al.*, 2008) |
| *GmPAP3* (truncated) transgenic cell lines 43 and 76 | These cell lines harbored the truncated GmPAP3 and were constructed in my Ph.D study and were used for study of significance of mitochondrial localization of GmPAP3. | This work |
| *GmPAP3* (full length) transgenic cell lines 1 and 8 | These cell lines harbored the full length GmPAP3 and were constructed in my Ph.D study together with the truncated GmPAP3 transgenic cell lines 43 and 76. They were used for study of significance of mitochondrial localization of GmPAP3. | This work |

### 2.1.2 Chemicals and Regents

Regular chemicals were purchased from Sigma-Aldrich Co. (Saint Louis, MO, U.S.A.). Organic solvents were from Merck & Co., Inc. (New Jersey, U.S.A.). Bacterial growth media were from Difco (Sparks, MD, U.S.A.) and Murashige & Shoog (MS) salt mixture was from Sigma-Aldrich (Saint Louis, MO, U.S.A). Phenolic compound, phytohormones and antibiotics used in bacteria and plant cultures were purchased from Aldrich Chem. (Saint Louis, MO, U.S.A.), Amresco Inc. (Solon, OH, U.S.A.) and Sigma-Aldrich Co. (Saint Louis, MO, U.S.A.). Metro-mix-200 soil for plant growth was from Hummert International Horticultural Supplier (Earth City, MO, U.S.A.). Chemicals for gel electrophoresis were from Bio-Rad Laboratories (Hercules, CA, U.S.A.). Restriction enzymes were from New England Biolabs. Inc. (Beverly, MA, U.S.A.) and Promega Biosciences (San Luis Obispo, CA, U.S.A.). Other enzymes for molecular biology experiments and reagents for DNA and RNA manipulation and detection were from Roche Diagnostic limited (Basel, Switzerland) (Appendix I), Clontech (San Jose, CA, USA) and Promega (San Luis Obispo, CA, U.S.A.). Positively charged nylon membrane for Northern blot were from Roche Diagnostic limited (Basel, Switzerland). Bio-MAX X-ray film was from Eastman Kodak (Rochester, NY, U.S.A.). Rhodamine 123 and MitoTracker-orange CMTMros, which act as probes for mitochondrial; and

H2DCFDA, which act as probe for $H_2O_2$, were from Molecular probes (Eugene, OR, USA). Chemicals for Electronmicroscopy were from Electron microscopy sciences (Hartfield, PA, U.S.A.). Detailed information on chemical used was listed in Appendix II.

### 2.1.3 Commercial kits

The following reagent kits were used in this research (Table 6) (For details, please see Appendix III).

**Table 6.** Commercial kits used.

| Kits | Experiments | Company |
|---|---|---|
| ABI prism dRhodamine terminator cycle sequencing ready reaction kit | DNA sequencing | Applied Biosystems (Foster City, CA, U.S.A.) |
| DIG detection system (CSPD, ready-to-use and Anti digoxigenin-AP, Fab fragments) | Southern and Northern blot analyses | Roche Diagnostic limited (Basel, Switzerland) |
| DIG DNA labeling kit | Generation of DIG-labelled DNA probes | Roche Diagnostic limited (Basel, Switzerland) |
| Lowicry HM20 Embedding kit | Electron microscopy samples preparation | Electron microscopy sciences (Hartfield, PA, U.S.A.) |
| PeroXOquant Quantitative peroxide assay kit | Lipid peroxides detection | PIERCE (Rockford, IL, U.S.A.) |
| Wizard plus minipreps DNA purification kit | Target genes subcloning | Promega Biosciences (San Luis Obispo, CA, U.S.A.) |
| Aurora$^{TM}$ Western Blot Chemiluminescent Detection | Western blot detection | System, ICN, Solon, OH, USA |

### 2.1.4 Primers and Adaptors

All primers were bought from Integrated DNA Technologies, Inc (Coralville IA, U.S.A.), Invitrogen (Carlsbad CA, U.S.A.). A full list of their sequences was shown Table 7.

**Table 7.** Primers and adaptors used.

| **Primer name** | **Sequence (5' to 3')** | **Use for** |
|---|---|---|
| HMOL 622 | TCCAACCACGTCTTCAAAGC | 35S promoter sequencing primer |
| T3 primer | AATTAACCCTCACTAAAGGG | Sequencing |
| T7 primer | GTAATACGACTCACTATAGGGC | Sequencing |
| HMOL 1556 | TTA ATA CAC GTG CGC ACC AAC | Cloning and sequencing of *GmPAP3* |
| HMOL 1557 | CAT TTT CAT CCT TTT CAA AAC GCC | Cloning and sequencing of GmPAP3 |
| HMOL 2050 | TTA ACC CAT TTG CTG TCC | PCR screening and sequencing of GmPAP3 |
| HMOL 2332 | GGA GGG TGA AAG CAT GCG | Cloning and sequencing of GmPAP3 |
| HMOL 6656 | AGA TCT AGA ATG TGG TTG GCT TCC TTT CG | Cloning and sequencing of GmPAP3 (from base 1), with XbaI site |
| HMOL 6657 | AGA TCT AGA ATG CTG CTG GCC ATG TTG | Cloning and sequencing of GmPAP3 (from base 106), with XbaI site |
| HMOL 6658 | CTT AAG CTT TTA CAT GCT GGC AAC TTC ATC | Cloning and sequencing of GmPAP3 (reverse primer, from base 1539) with HindIII site |

### 2.1.5 Antibodies

Primary antibody (polyclonal) targeting the GmPAP3 protein was obtained from a commercial service (Invitrogen, Custom Antibody) by injecting a synthetic peptide ('N'-SFVLHNQYWGHNRR-'C') into rabbits. Unpurified serum was used in western blot analysis and immunolabeling. Anti-rabbit (for GmPAP3 antibody) secondary antibody conjugated to an alkaline phosphatase (Sigma, St.Louis, MO, U.S.A.) was used to recognize the primary antibodies for western blot. ImmunoGold goat anti-rabbit secondary antibody (EMS, Hartfield, PA, U.S.A.) were used to recognize the primary antibodies in Immunobeling and Electromicroscopy.

### 2.1.6 Equipments and facilities used

All equipments and facilities were provided by Department of Biology, CUHK. An inventory is shown Appendix IV.

### 2.1.7 Buffer, solution, gel and medium

Unless otherwise stated, buffer, solution and medium were prepared according to the formulation listed in Appendix V.

### 2.1.8 Software

Sequence analysis was done by BlastN, BlastX and PSI-Blast programs provided in the webcite of National Center for Biotechnology information. (http://www.ncbi.nlm.nih.gov)

The images collected in confocal microscopy studies were processed with Adobe Photoshop CS and analyzed with ImageJ (program developed at the National Institutes of Health and available at http://rsb.nih.gov/nih-image/).

## 2.2 Methods

### 2.2.1 Molecular Techniques

2.2.1.1 Bacterial cultures for recombinant DNA and plant transformation

Bacterial strains (*E. coli* and *A. tumefaciens*) were inoculated from glycerol stocks (stored at -70°C) into LB broth (*E. coli*) or YEP broth (*A. tumefaciens*) and shake at 200 rpm (Orbital shaker, Lab. line 4628-1), 37°C, for overnight (*E. coli*) or at 250 rpm, 28°C, for two days (*A. tumefaciens*).

Antibiotics were added when appropriate to the growth media in final concentrations of 100mg/ L, 50mg/ L, 50mg/ L, 25mg/ L, 100mg/ L for ampicillin, kanamycin, rifampcin, gentamycin and streptomycin, respectively.

2.2.1.2 Recombinant DNA techniques

Restriction of DNA was normally done with 2 units of restriction enzyme per microgram of DNA in the presence of 1g/L Bovine serum albumin (BSA) in 1X restriction buffer (as recommended in the company product notes) and incubated at 37°C for 3 hours to 16 hours. Ligation of DNA fragments and vectors with compatible ends were performed with 1mM dATP and 3 units T4 DNA ligase (NEB)

in 1X T4 DNA ligase buffer (as recommended in the company product notes) and the reaction mixes were incubated at 16°C overnight. For blunt end ligation, the ligation was performed with 0.5mM dATPs and 3 units of T4 DNA Ligase (NEB) at 22°C overnight.

DNA purification was carried out using classical purification method. DNA samples were extracted with phenol: chloroform: isoamylalcohol (PCI) (25:24:1) once and chloroform: isoamylalcohol (CI) (24:1) for twice. Ethanol precipitation of nucleic acid was done by adding 2 Volume of absolute ethanol and 1/10 of Volume 3M Na Acetate pH 5.2 and kept at -20°C overnight. After centrifugation at 10 000g for 15 minutes and discarding the supernatant, the pellet was washed with 70% Ethanol and air-dried. Finally, the pellet was resuspended in sterilized deionized water and proceed to further process.

2.2.1.3 Preparation and transformation of DH5α, and *Agrobacterium* competent cells

(i) Preparation of $CaCl_2$-competent DH5α competent cells

DH5α cells was first inoculated into 5 ml LB medium and shook at 200 rpm (Orbital shaker, Lab. line 4628-1), 37°C overnight to make a starter culture. Four millilitres starter culture was then added to 400 ml LB medium and allowed to grow

to until optimal density at 600nm (O.D. 600) reached 0.4. The culture was chilled on ice for 10 minutes and centrifuged at 1600g for 7 minutes at 4°C. After discarding the supernatant, the cell pellet was resuspended in 80ml ice-cold 60mM $CaCl_2$ solution. The cell culture was then centrifuged at 1100g for 5 minutes at 4°C. Supernatant was discarded again and cell pellet was resuspended with 80ml ice-cold 60mM $CaCl_2$ solution. The suspension was allowed to stand on ice for 30 minutes. It was then centrifuged at 1100g for 5 minutes at 4°C. The pellet was finally resuspended with 8ml ice-cold $CaCl_2$ solution after discarding the supernatant. Aliquots of 0.1 ml were transferred into prechilled, sterile 1.5ml microcentrifugation tubes and stored at -70°C until ready to use [modified from (Sambrook & Russell, 2001)].

(ii) Transformation of DH5α competent cells

The plasmid DNA was transformed into DH5α competent cells via heat shock calcium chloride mediated transformation. The plasmid DNA was added to an aliquot of 0.1 ml pre-chilled competent cells. The mixture was allowed to sit in ice for 10 minutes, followed by a heat shock at 42°C was carried out for 2 minutes. Cells were immediately rescued by adding 0.5 ml LB broth and incubated at 37°C for 1 hour with shaking at 200 rpm (Orbital shaker, Lab. line 4628-1). The recovered cells

were spread on LB agar plate with appropriate antibiotic for selection and incubated at 37°C overnight.

(iii) Preparation of Electro-competent *Agrobacterium tumefaciens* cells

LBA4404/ pAL4404 was inoculated into 10ml YEP broth supplemented with antibiotics when appropriate and shook at 250 rpm (Orbital shaker, Lab. line 4628-1), 28°C, overnight to prepare a starter culture. Eight millilitres of dense culture was then inoculated into 400ml YEP medium which supplemented with appropriate antibiotics, and was allowed to grow until O.D.600 was around 0.5 to 1.0. The culture was harvested by chilling on ice for 15 minutes and centrifuged at 4000g for 15 minutes at 4°C. After discarding the supernatant, the cell pellet was resuspended with 400ml ice cold sterile deionized water. The suspension was centrifuged at 4000g for 15 minutes at 4°C again. The pellet was then resuspended with 200ml ice cold sterile deionized water after the removal of supernatant. The concentrated suspension was spun at 4000g for 15 minutes at 4°C. After discarding the supernatant, the cell pellet was resuspended with 4ml 10% glycerol (filter sterile with 0.2μm filter). The 4ml glycerol suspension was again centrifuged at 4000g for 15 minutes at 4°C. Finally, the cell pellet was resuspended in 0.4ml ice cold 10% sterile glycerol after the removal of the

supernatant. Forty microliters aliquots were aspirated into prechilled, sterile 1.5ml microcentrifugation tubes and stored at -70°C until ready to use (Dower *et al.*, 1992).

(iv) Transformation of electro-competent *Agrobacterium* cell

An aliquot of 40µl of electro-competent *Agrobacterium* strain was thawed on ice and mixed with 10ng of recombinant plasmid in a pre-chilled electroporation cuvette (Bio-Rad, Cat no. 165-2086). The mixture was further incubated on ice for 30 minutes. After drying the cuvette with tissue paper to remove moisture on the surface, the cuvette containing sample mixture was inserted into the gene pulser apparatus (BioRad GenePulser, Model No. 165-2076). Electroporation was performed at: 25 µF, 2.5 kV and 600 ohms. After discharge, 1ml SOC medium was immediately added to rescue the cells. The culture was then transferred to 1.5 ml microcentrifugation tubes and incubated at 28°C for 2 hours with shaking at 200 rpm (Orbital shaker, Lab. line 4628-1). The recovered culture was then spread on YEP agar plate supplemented with appropriate antibiotics (GV3101/pMP90: 50 mg/ L rifampicin, 25 mg/ L gentamycin; LBA4404/ pAL4404: 100mg/ L streptomycin; *Agrobacterium* containing W104 vector: 50 mg/ L kanamycin) and allowed to grow at 28°C for 2-3 days.

2.2.1.4 Gel electrophoresis

(i) DNA gel electrophoresis

Agarose gel was prepared by heat-dissolving 10mg/ ml agarose powder in 1X TAE using a microwave. After cooling down to below 70°C, 1μl 1mg/ ml ethidium bromide was added before pouring onto a gel caster. DNA samples in 1X bromophenol blue loading dye were normally loaded onto 1% agarose gels. The gel electrophoresis was run in 1X TAE buffer at 80 V for 30 minutes to 3 hours.

(ii) RNA denaturing gel electrophoresis

One percent denaturing gel was prepared by heat-dissolving 1g agarose gel powder in 87 ml DEPC-treated deionized water using a microwave. Ten milliliters 10X MOPS buffer and 3 ml formaldehyde (37%, pH≥4.0) were added after the temperature was cooled to below 70°C. The denaturing gel solution was then mixed and poured in a clean gel tray. 10 microgram aliquots of RNA sample was added in a final volume of 35μl solution containing 3.5 μl 10X MOPS, 17.5 μl 37% formamide, 6.13 μl formaldehyde, 1μl 1mg/ ml ethidium bromide and 1 μl 6X bromophenol blue loading dye. The sample mixture was denatured at 55°C for 20 minutes and then put immediately onto ice. The denatured RNA samples were loaded onto the denaturing agarose gel and gel electrophoresis was run in 1X MOPS buffer at 80 V for 2 hours.

2.2.1.5 DNA and RNA extractions

(i) DNA extraction from plant tissue

The classical CTAB extraction method modified from Doyle & Doyle, 1987 was used for extraction of genomic DNA. Approximately 1g plant tissue was first frozen and ground in liquid nitrogen before homogenized with 5ml 2X CTAB extraction buffer. The extract was then incubated at 60°C for 30 minutes before centrifuged at 3000g at room temperature for 10 minutes. Aqueous layer was transferred to a new tube and extracted with phenol: chloroform: isoamylalcohol (PCI) (25:24:1) once and chloroform: isoamylalcohol (CI) (24:1) for twice. Ethanol precipitation of nucleic acid was done by adding 2V of Isopropanol and kept at -20°C overnight. After centrifugation at 10 000g for 15 minutes and discarding the supernatant, the pellet was washed with CTAB washing buffer and air-dried. Finally, the pellet was resuspended in sterilized deionized water supplemented with 1μg/ ml RNaseA and incubated at 37°C for 1 hour to remove RNA (Doyle & Doyle, 1987).

(ii) Plasmid DNA extraction from bacterial cells

Plasmid DNA was isolated using the Wizard plus minipreps DNA purification kit (Promega). The procedures were according to the commercial manuals except

the volume of cell culture used. For high copy number plasmids, such as pBluescript, 5ml cell culture was used as starting material per reaction. However, for low copy number plasmids, such as V7/W104, 20ml cell culture was used instead.

(iii)RNA extraction from plant tissues

Plant RNA extraction protocol was modified from a standard protocol (Ausubel *et al.*, 1995). Approximately 5g plant tissue for RNA extraction was harvested and immediately frozen and ground in liquid nitrogen before homogenized in 25ml extraction buffer. The aqueous portion of the sample was then extracted twice with PCI followed by two rounds of CI extraction. One-tenth volume of 3M sodium acetate (pH 5.2) and 2 volumes of absolute ethanol were added to the resulting aqueous layer and the sample was stored at -20°C overnight to precipitate the nucleic acids. After centrifugation at 8000rpm for 20 minutes (Roter F34-6-38: Centrifuge 5810R, Eppendorf), supernatant was discarded and the nucleic acid pellet was resuspended with 1 ml 3M sodium acetate, pH 5.6 and the suspension was transferred to a 1.5ml microcentrifuge tube. After centrifugation at 13000 rpm for 30 minutes, mRNA and rRNA were precipitated and tRNA and DNA remained in the supernatant. After repeating the 3M sodium acetate pH5.6 extraction one more time (using 0.5ml this time), the pellet was then resuspended in 0.4ml 0.3M sodium acetate pH5.6 and the

RNA was precipitated by adding 1ml 100% ethanol and kept at -20°C overnight. After centrifugation at 13, 000 rpm (Refrigerated centrifuge 5810R, Eppendorf 03463) for 30 minutes and removal of supernatant, the RNA pellet was air-dried before resuspended in DEPC-treated deionized water.

2.2.1.6 Protein extractions

(i) Soluble protein extraction

In order to obtain membrane and soluble protein fractions from plant tissue, leaves were grinded with homogenizing buffer, followed by centrifugation at 2000rpm for 10min, supernatant is the soluble fraction, while the pellet was further centrifuged at 10000 rfc for 60 min. Supernatant was combined with the soluble fraction previously obtained and supplemented with 1% SDS. Membrane fraction was obtained by resuspending the pellet with homogenizing buffer supplemented with 2% SDS. Both the membrane and soluble protein fractions were boiled at 100°C for 10 min (modified from (Jiang & Rogers, 1998)).

(ii) Mitochondrial enriched protein fraction extraction

Mitochondria-enriched protein fraction was extracted by differential centrifugation as described (Douce *et al.*, 1987) with slight modifications. Plant material was gently homogenized in 2 volumes of ice-cold extraction buffer (0.25 M Sucrose, 5 mM EDTA, 1 mM EGTA, 1 mM dithioerythritol, 0.1 % BSA, 0.6 % PVPP in 10 mM HEPES-Tris, pH 7.4). The homogenate was filtered and squeezed through Miracloth and the mitochondria were immediately separated from the cytoplasmic fraction by centrifugation at 10000 g for 10 min. The resulting crude mitochondrial pellet was resuspended in medium I (0.25 M Sucrose, 5 mM EDTA, 1 mM EGTA, 0.1 % BSA in 10 mM HEPES-Tris, pH 7.4) and centrifuged at 600 g for 5 min to remove nuclei and heavy cell debris. This washing procedure was repeated twice. Washed mitochondria were resuspended in medium II (0.25 M Sucrose, 30 μM EGTA in 10 mM HEPES-Tris, pH 7.4) and stored on ice.

2.2.1.7 Generation of single-stranded DIG-labeled PCR probes

As both *GmPAP3* (both full length and truncated) were cloned into pBluescript II KS (+) vector, T7 promoter and T3 promoter primers were used for synthesizing the PCR probes. Round one PCR was performed by mixing 1 pg of recombinant

plasmid with 5μl of 10X reaction buffer (with $Mg^{2+}$, Roche), 1μl of 25mM $MgCl_2$, 1μl of 2mM dNTPs mix, 2.55μl of 1μM T7 primer and 2.55μl of 1μM T3 primer and 1U of *Taq* DNA polymerase (Roche). The final volume was made up to 50μl by milli-Q $H_2O$. The reaction was subjected to the following PCR profile (Table 8). The concentration of PCR product was determined by running 5μl of the product in 1% agarose gel.

Table 8. PCR profile for DIG-labeled DNA probe synthesis.

| Number of cycles | Length of time | Temperature |
|---|---|---|
| 1 cycle | 2 minutes | 94°C |
| 55 cycle | 20 seconds | 94°C |
| | 30 seconds | 53°C |
| | 1 minutes | 72°C |
| 1 cycle | 10 minutes | 72°C |

Round 2 PCR is a biased PCR. That is using one primer, to synthesis an anti-sensed, single-stranded PCR probes with the incorporation of DIG-labeled conjugates. About 100ng of Round 1 PCR product was mixed with 10μl of 10X reaction buffer (with $Mg^{2+}$, Roche), 2μl of 25mM $MgCl_2$, 2μl of DIG-labeled dNTPs (Roche), 2μl of 5μM T7 primer and 2U of *Taq* DNA polymerase (Roche). The final volume was made up to 100μl by Milli-Q $H_2O$. The reaction was subjected to PCR profile listed

in Table 8 again. 1μl PCR product was used to test the concentration of DIG-labeled probes.

2.2.1.8 Testing the concentration of DIG-labeled probes

1μl of probe and DNA/RNA DIG-labeled control (Roche) were diluted serially for 5, 50 and 500 folds. One μl of each dilution was doted on a positive charged nylon membrane (Roche) followed by UV crosslinking. The membrane was rinsed in 1X maleic acid buffer, pH7.5 (0.1M maleic acid, 0.15M NaCl) for 2 minutes, soaked in 1% blocking solution (1% w/v blocking reagent in 1X maleic acid) for 5 minutes twice and washed with 1X detection buffer, pH9.5 (1M Tris-HCl, 0.1M NaCl) for 1 minute.

The membrane was transferred to a clean plastic wrap and CSPD (Roche) was added to the membrane. The membrane was placed in a film cassette and was exposed to a sheet of X-ray film (Biomax, Kodak) for 30 minutes at 37°C. The film was developed and the spot intensities of the control and samples were compared in order to estimate the concentration of DIG-labeled probes.

2.2.1.9 Northern blot analysis

Ten micrograms of each total RNA sample was run on a denaturing gel. After recording the ethidium bromide stained image of the RNA samples, the RNA was transferred onto a positively charged nylon membrane by capillary action running in the 10X SSC for 16 hours.

After UV-crosslinking (total 250J), the membrane was first rinsed in DEPC-treated deionized water and then prehybridized in prehybridization solution at 42°C for 2-4 hours and hybridized with 25ng/ml DNA probes in hybridization solution at 42°C for 16 hours. After washing with cold wash solution for 15 minutes twice at room temperature and hot wash solution for 15 minutes twice at 68°C, the membrane was blocked with 1% blocking solution at room temperature for 2-4 hours and incubated with 1: 10,000 anti-DIG antibody at room temperature for 30 minutes. After washing with 1X maleic acid buffer for 15 minutes twice and equilibrating with 1X detection buffer at room temperature, CSPD substrate was added onto the membrane and X-ray film was allowed to expose for 14 hours.

2.2.1.10 PCR techniques

For PCR-aided sequencing, 250ng DNA sample was used as the template. In a 10μl reaction mixture, 0.8pmole primer and 4μl terminator ready reaction mix were

included. The PCR cycle profile was as follows: 94°C for 5 minutes before 25 cycles of 96°C for 10 seconds, 50°C for 5 seconds, 60°C for 4 minutes. For generating DNA fragment for subcloning and PCR screening, the PCR reaction mixture contained 0.5 μM of each primer, 1X PCR buffer with 1.5mM $MgCl_2$, 0.2mM dNTPs and 0.5 Unit Taq DNA polymerase were reacted in a final volume of 25μl. The PCR cycle profile was as follows: 94°C for 5 minutes before 25 cycles of 94°C for 30 seconds, appropriate annealing temperature for 30 seconds, 72°C for 1 minutes and the reaction was terminated after an addition 10-minute extension step after all cycles were completed (the annealing temperature for each primer was listed in Table 9).

**Table 9.** Annealing temperatures of primers used in PCR reactions.

| Primer name | Purposes | Annealing temperature |
|---|---|---|
| 35S promoter sequencing primer | Sequencing | 50.0°C |
| T3 primer | Sequencing | 50.0°C |
| T7 primer | Sequencing | 50.0°C |
| HMOL 1556 & 1557 | Cloning and PCR screening of *GmPAP3* clones | 60.0°C |
| HMOL 1556 & 2050 | Cloning and PCR screening of *GmPAP3-T7* clones | 50.0°C |
| HMOL 2050 | Sequencing | 50.0°C |
| HMOL 6656 & 6658 | Cloning of *GmPAP3* (full length) with HindIII and XbaI site | 52.0°C |
| HMOL 6657 & 6658 | Cloning of *GmPAP3* (truncated) with HindIII and XbaI site | 52.0°C |

2.2.1.11 Sequencing

PCR-aided DNA sequencing was performed by using the ABI prism dRhodamine terminator cycle sequencing ready reaction kit (Applied Biosystems) to make labeled single strand DNA. The PCR reaction product was precipitate by adding 2µl 3M sodium acetate (pH5.2) and 50µl 95% ethanol to the mixture then was kept on ice for 30 minutes and centrifuged at 14000g for 30 minutes. The DNA pellet was washed in 70% ethanol after removal of supernatant. The washed and air-dried pellet

was then resuspended in 10μl Template Suppression Reagent. The sample was then applied to the Genetic Analyzer ABI prism 3100 for analysis

2.1.1.12 Western blot analysis

For western blot analysis in Fig.6, the proteins were electrophoretically separated on a SDS-polyacrylamide gel (4 % stacking; 10 % resolving) as described (Laemmli, 1970) before transferred to an activated PVDF membrane. The transfer, blocking, and detection (solutions provided in the Aurora™ Western Blot Chemiluminescent Detection System, ICN, Solon, OH, USA) steps were performed according to the manufacturer's manual.

For western blot analysis in Fig. 16, Protein on SDS-PAGE was blotted on methanol activated PVDF membrane using mini trans-blot module with Dunn's buffer (Dunn 1986) at 55V for 90min. Membrane was washed with TBST for 2min before incubate in blocking solution (2.5% skim milk blocking solution) overnight at 4℃. Then, the membrane was incubated with 1:5000 primary antibody diluted with blocking solution for at least 1hr with gentle shaking. After washing 4 times with TBST each for 10min, the membrane was incubated with 1:10000 Alkaline phosphatase (AP) conjugated secondary antibody diluted with blocking solution for at least half an hour with gentle shaking. After washing 4 times with TBST each for

10min, the membrane was either detected with *Sigmafast* BCIP/NBT substrate (chromogenic) (Sigma, B5655-25TAB).

### 2.2.2 Plant cell culture and transformation

2.2.2.1 *Arabidopsis thaliana*

**Surface sterilization of seeds**

Seeds of *A thaliana* were surface sterilized in 100% Clorox for 5 minutes with vigorous shaking, before rinsing with autoclaved double distilled water for 3 times to remove Clorox. The surface sterilized seeds were either individually placed and aligned onto MS agar square plates for growth or spread onto MS agar plate with 50mg/L kanamycin for screening of transformants. After keeping in dark at 4°C for 2 days, the seeds were grown in growth chamber at 22°C with 70% relative humidity under the light/ dark cycle of 16 hours light and 8 hours dark.

2.2.2.2 *Nicotiana tabacum* L. cv. Bright Yellow 2 (BY-2) cells

**Transformation of tobacco BY-2 cells**

Agrobacterium-mediated transformation of tobacco BY-2 cells was performed according to standard protocol (An, 1985) with some modifications. Single colony of V7-GmPAP3 (truncated) or V7-GmPAP3 (full length) transformed A. tumefaciens LBA4404 was cultured in 5ml of LB medium supplemented with 50mg/L Kanamycin, 100mg/L Streptomycin and 50mg/L Rifampicin for 16 hours at 28°C with shaking at

250rpm. 200μl of 16-hour Agrobacteria culture was then co-cultivated with 4ml of 3-day-old wild type BY-2 cells in Petri-dish for 2 days at room temperature in tranquility. Then the co-cultivation mixture was washed with 20ml of MS medium in order to remove the Agrobacterium. Finally the washed BY-2 cells were plated onto MS agar plates supplemented with 50mg/L kanamycin and 250mg/L cefotaxime and kept in dark. Individual tiny calluses, which regenerated after 2 to 3 weeks, were selectively transferred to new MS agar plates with 50mg/L kanamycin and 250mg/L cefotaxime. Eventually, transgenic cell lines were continuously sub-cultured in MS agar plates supplemented with 50 mg/L Kanamycin.

2.2.2.3 Making of the constructs with binary vector harbouring GmPAP3*/GmPAP3

The cDNA (spanning 106-1539 bases) of truncated *GmPAP3* (GmPAP3*) was cloned into the pBluescript II KS (+) (see Fig. 13 for sequence of GmPAP3*). To perform *Agrobacterium*-mediated transformation, the *GmPAP3* and *GmPAP3** cDNA was subcloned into the binary vector V7 (Brears *et al.*, 1993). The map of the construct was shown in Fig. 5. The orientation and the correctness of the sequence were confirmed by DNA sequencing in prior to transformation of the constructs into BY-2 cells. *GmPAP3* transgenic cell lines were constructed in parallel to the *GmPAP3** transgenic cell lines for further comparative studies.

**A**

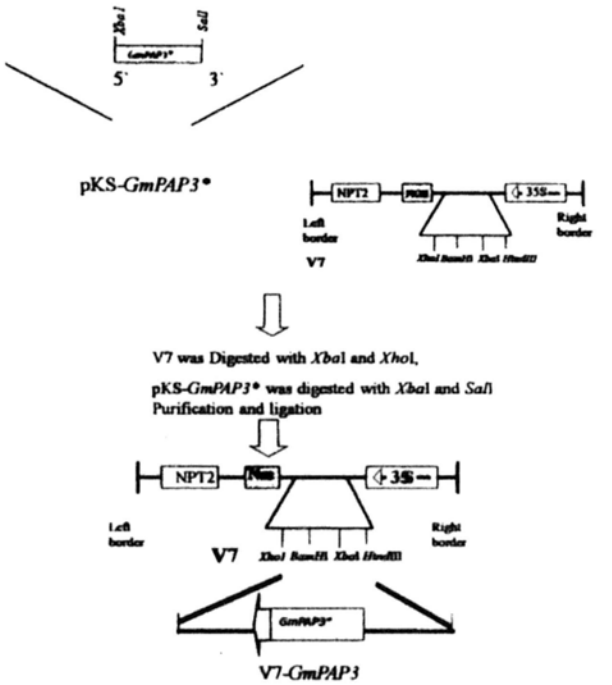


**B**

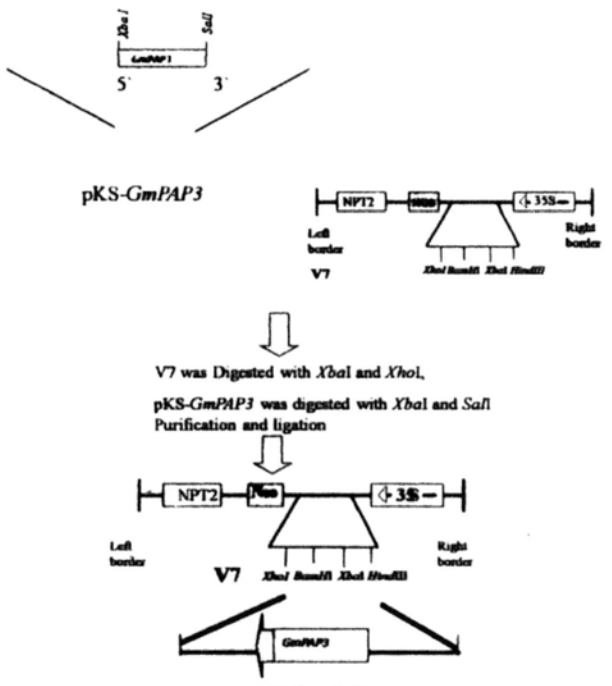


Fig.5. **A:** Constructs of V7-*GmPAP3* and* B:V7-*GmPAP3*. Both the pKS-*GmPAP3** and pKS-*GmPAP3* and the binary vector V7 were digested with *Hind*III and *Xba*I. The fragments were purified and ligated to form the construct V7-*GmPAP3* or V7*-GmPAP3.

### 2.2.3 Growth and treatment conditions for plants

2.2.3.1 Root growth assay of *GmPAP3* transgenic *Arabidopsis thaliana*

Seeds of transgenic lines (*GmPAP3* and the empty vector) and their untransformed parent Columbia-0 (Col-0) were sown on vertical MS plates containing 3 % sucrose and 0.9 % (w/v) agar. Five-day-old (PQ) or 7-day-old (NaCl and PEG) seedlings were transferred onto MS agar plates without other supplements (untreated), with 150 mM NaCl (NaCl), with 15 % PEG 6000, or with 1 μM PQ. The root length of each individual seedling before (by marking on the plates) and 7 d after treatment was recorded and the percentage root elongation was calculated accordingly. Forty-eight seedlings were measured for each treatment. The experiments were repeated twice. For the PEG treatment, the PEG-infused agar plates were prepared as described (Verslues *et al.*, 2006).

### 2.2.4 Detection of Lipid Peroxides in Arabidopsis seedlings

FOX assay was used to determine lipid peroxides as described (Sattler *et al.*, 2004) to indicate the extent of oxidative damage in Arabidopsis seedlings under PQ treatments. Cellular contents of 12 seedlings were extracted with 400 μL of methanol:dichloromethane (1:1 [v/v]) containing 0.05 % (w/v) butylated hydroxytoluene and 50 μL of 150 mM acetic acid. Lipids were partitioned into the

organic phase by adding 300 μL of water, vortexing and centrifugation at 3750 g. The lipid extracts were incubated at room temperature with FOX solution (Pierce, Rockford, IL, USA) for 30 min. Immediately after incubation, the absorbance was measured at 595 nm by a microplate reader. A standard curve was constructed using hydrogen peroxide as suggested in the manufacturer's protocol. The reactivity of 18:2-derived lipid hydroperoxides (LOOHs) with the FOX reagent is nearly identical to hydrogen peroxide (DeLong *et al.*, 2002).

### 2.2.5 Immunolabeling, mitochondria integrity, cell viability, ROS detection and confocal microscopy

2.2.5.1 Immunolabeling of *GmPAP3*/GmPAP3* transgenic cell lines

BY-2 cell fixation and confocal immunofluorescence were carried out according to Jiang & Rogers, 1998 with modifications. 3 days old transgenic BY-2 cell lines were pre-stained with 200nm MitoTracker®-orange CMTMros for 30 minutes before fixed in fixation solution (50mM Na-phosphate buffer pH7.0, 5mM EGTA, 0.02% Sodium azide, 4.5% paraformalydehyde) for at least 24 hours at 4°C. Then the fixed cells were allowed to precipitate and the fixation solution was removed. After washed with Na-phosphate-EGTA buffer, cells walls of the treated cells were partially digested with 1% cellulysin cellulase in Na-phosphate buffer for 20 minutes, followed by wash with Na-phosphate-EGTA buffer. Permeabilization of the cells was done by treatment with 0.2% Triton X-100 for 2.5 minutes. Prior to incubation with primary antibodies, fixed cells were incubated with blocking buffer 1 (1X PBS, 1% BSA) for 30 minutes. Then the cells were incubated with GmPAP3 specific antibody (rabbit) which diluted in Blocking buffer 2 (1X PBS, 0.25% BSA, 0.25% Gelatin, 0.05% NP-40, 0.02% Sodium azide) at 4°C overnight. These stained cells were washed with blocking buffer 2, followed by incubation with anti-rabbit AlexaFluor®

488-conjugated secondary antibody at 1:100 dilutions for one hour at room temperature. Finally the labeled cells were washed twice with blocking buffer 2 and mounted on slides and used for confocal microscope studies.

2.2.5.2 Mitochondria integrity

3 days old *GmPAP3* transgenic BY-2 cell lines were used for assay of mitochondria integrity. The suspension cells were treated with 200mM NaCl for 1 hour or 2% PEG for 30 minutes in prior to staining with 10mg/ml Rhodamine 123 (Rh123) for 1 hour. The signal of Rh123 was observed under a confocal laser scanning microscope. 15-25 cells were counted for each sample to perform statistical analysis. The experiment was repeated three times. Because of its selective accumulation in mitochondria based on the membrane potential, this dye is commonly used for evaluation of variations in activity of mitochondria (Wu, 1987; Petit, 1991).

2.2.5.3 Cell Viability

Cells were treated with 200 mM NaCl or 2 % PEG for 24 h before staining with 0.4 % trypan blue (Sigma, St.Louis, MO, USA). Stained cells were observed under light microscope. Around 200 cells were counted for each sample.

2.2.5.4 Detection of Reactive oxygen species (ROS)

3 days old *GmPAP3* transgenic BY-2 cell lines were used for such experiments. The suspension cells were pre-stained with Dichlorodihydrofluorescein diacetate ($H_2$DCFDA) for 30 minutes in prior to treatment with 200mM NaCl for 1 hour or 2% PEG for 30 minutes. The same level of laser excitation, iris and gain were used for each cell counted. The fluorescence intensity of $H_2$DCFDA were estimated by using the program ImageJ as described in the below section. 10-25 cells were analyzed for each sample to perform statistical analysis. The experiments were repeated three times. The chemical probe $H_2$DCFDA has been used extensively as a non-invasive, in vivo measure of intracellular ROS (LeBel *et al.*, 1992).

For the experiments involving ferric chelator, 1,2-dimethyl-3-hydroxypyrid-4-one that can bind Fe(III) specifically (Hayman & Cox, 1994) was employed. Cells were pretreated with 2.5 mM 1,2-dimethyl-3-hydroxypyrid-4-one for 5 min before staining with $H_2$DCFDA and treatment with NaCl or PEG.

2.2.5.5 Confocal microscopy

All confocal images were collected by either Bio-Rad Radiance 2100 system controlled by LaserSharp2000 software (Bio-Rad) with the following parameters:

60X objective oil lens (Nikon, Tokyo), optimal iris and 512 X 512 box size pixel; or by Olympus Fluoview FV 1000 system controlled by FV10-ASW v 1.7 with the following parameters: 60X objective water lens, optimal iris and 512 X 512 box size pixel. The signal of Rh123 were excited by 543nm Green HeNe laser and HQ590/70 filter set were used for Bio-Rad Radiance 2100 system; or by 543nm HeNe G laser and Rhodamine dye set for Olympus Fluoview FV1000 system. The signal of $H_2$DCFDA were excited by 488nm Argon laser, HQ 515/30 filter set were used for Bio-Rad Radiance 2100 system; or by 488nm Multi-Argon laser and FITC dye set were used for Olympus Fluoview FV1000 system. The signal of MitoTracker® orange CMTMRos was excited by 543nm Green HeNe laser and HQ 590/70 filter set was used for Bio-Rad Radiance 2100 system; or by 543nm HeNe G laser and MitoTracker® orange dye set for Olympus Fluoview FV 1000 system. The signal of Alexa Fluor® 488 was excited by 488nm Multi-Argon laser and Alexa Fluor® 488 dye set was used for Olympus Fluoview FV 1000 system. For double labeling experiments, care was taken to ensure that the laser power and other settings (iris and gain) were set to a condition where no crossover signals between Alexa Fluor® 488 and MitoTracker®orange emissions were detected. The Alexa Fluor® 488 and $H_2$DCFDA images were pseudocolored in green and the MitoTracker® orange and Rh123 images were pseudocolored in red.

2.2.5.6 Images processing and analysis

For quantification of colocalization of Alexa Fluor® 488 and MitoTracker® orange signals, superimposition of green (Alexa Fluo® 488) and red (MitoTracker® orange) images result in yellow where the green and red signal overlap. The pixel area of the image occupied by yellow in the superimposed image, divide by the pixel area of the image occupied by green signal only is therefore a fraction describing how much of the green signal colocalizes with the red signal. To do so, the Alexa Fluor® 488 (green) and MitoTracker® orange (red) images first were converted to Grayscale, 8-bits TIFF files. Then by using the program ImageJ, the pixel area occupied by yellow and the pixel area occupied by green signal can be calculated. Images from at least 10 different cells from double-labeling experiment were analyzed to calculate the colocalization of Alexa Fluor® 488 and MitoTracker® orange signal.

Quantification of $H_2$DCFDA signals in BY-2 cells were performed as describe in (Sukumvanich *et al.*, 2004) with slight modifications. The images collected were converted to Grayscale, 8-bits TIFF files. By using the program ImageJ, the fluorescence intensity of the cell could be estimate. Quantitative analysis was done by tracing the entire cell (by using the selection tools) and the total fluorescence intensity was measured. The fluorescence intensity measurement, measured in pixels, was then divided by the area of the cell, to obtain average pixel fluorescence

intensity. In addition, background fluorescence intensity was measured in the same field and was subtracted.

### 2.2.5 Electron Microscopic Studies

Embedding and electron microscopy were performed as described (Tse *et al.*, 2006)with slight modifications. Samples were fixed in a primary fixative solution contain 0.25 % (v/v) glutaraldehyde and 1.5 % (v/w) paraformaldehyde in 50 mM phosphate buffer, pH 7.4, for 15 min at room temperature before incubating at 4°C for an additional 16 h. After washing with phosphate buffer at room temperature, cells were dehydrated in an ethanol series and then embedded in Lowicryl (HM20) resin. Ultrathin sections were than prepared from these blocks using Ultra Cut S (Leica, Wetzlar, Germany). The GmPAP3 specific antibody was used as the primary antibody followed by detection using the gold-conjugated anti-rabbit secondary antibody. Immuno-labeled sections were then post-stained with 4 % uranyl acetate and examined using a transmission electron microscope (JEM-1200EXII, JEOL, Tokyo, Japan).

### 2.2.6 Statistical analysis

Data were analyzed by appropriate ANOVA tests, in which case significant differences between individual treatments or lines were determined by Tukey's test.

## Chapter 3 Results

### 3.1 A Major Portion of GmPAP3 Proteins in BY-2 Cells is Mitochondrial Localized

Using confocal microscopy, we have previously shown that a major portion of GmPAP3 proteins were localized in mitochondria (See Section 1.6). To further verify the above results, western blot and immunodetection using GmPAP3 specific antibody was performed. As shown in Fig. 6A, signals were detected in mitochondria-enriched protein fraction in both *GmPAP3* transgenic cell lines but not in the wild type. A major band of the right size (about 50 KDa) was observed. This result also provided biochemical evidences to support the mitochondrial localization of the GmPAP3 protein and verified the specificity of the antibody. To further verify the localization of GmPAP3, immunolabeling and transmission electron microscopy was then performed using the GmPAP3 specific antibody used in Fig. 6A. Most gold particles observed were confined to mitochondria (Fig 6B).

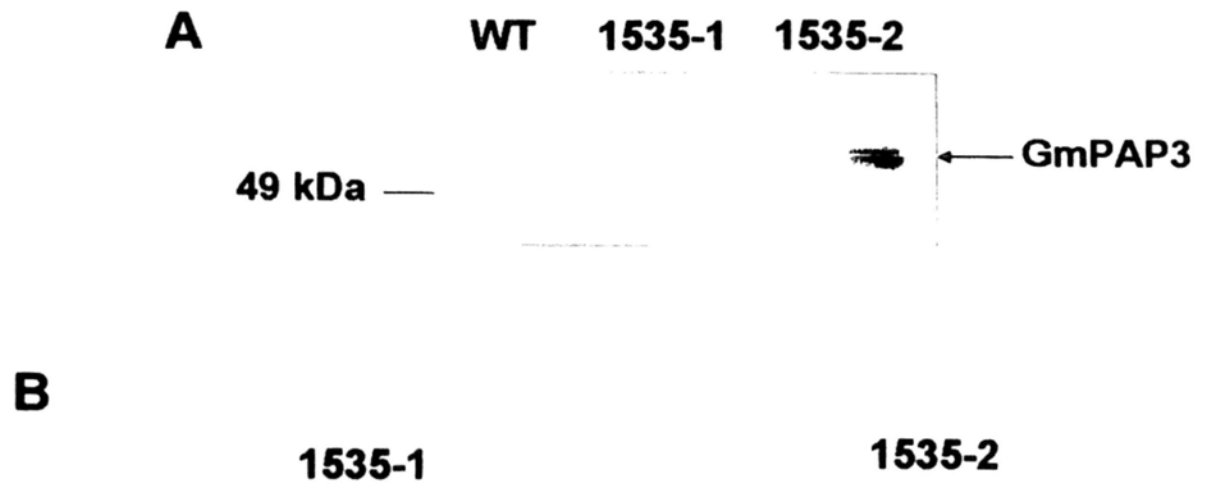





Fig 6. Western blot analysis and electron microscopic studies of GmPAP3. (**A**) Western blot analysis of the mitochondria-enriched protein fraction from different cell lines was performed as described in Materials and Methods. WT: untransformed wild type BY-2 cells; 1535-1 and 1535-2: two independent GmPAP3 transgenic cell lines used in Fig.4 and Table 5, section 1.6. **(B)** Immunodetection of GmPAP3 was conducted using two independent *GmPAP3-T7* transgenic cell lines (1535-1, 1535-2) and the GmPAP3 specific antibody employed in (**A**). Arrow-heads indicated the location of gold particles that were mostly found in mitochondria. Scale bar = 200 nm.

## 3.2 Effect of expressing GmPAP3 in BY-2 cells under NaCl and osmotic treatments.

### 3.2.1 Effect of expressing GmPAP3 on mitochondria integrity of BY-2 cells under NaCl and osmotic treatments.

While salt stress and osmotic stress can induce gene expression of *GmPAP3* in soybean, its function remain unknown. We hypothesize that, with its mitochondria localization, GmPAP3 may involve in scavenging of reactive oxygen species (ROS) in plant cells under salt and osmotic stresses. Salt-induced ROS production was reported in leaf mitochondria of plants (Hernandez *et al.*, 1993; Gomez *et al.*, 1999). On the other hand, it was proved that in plant mitochondria, ROS can cause collapse of mitochondria membrane potential (Pastore *et al.*, 2002). Therefore, mitochondria membrane potential was use as a parameter for ROS-induced mitochondria damage. In this case, the fluorescent dye rhodamine 123 (Rh123), which selectively accumulates in mitochondria based on the transmembrane potential (Petit, 1991), was used to evaluate the integrity of mitochondria of BY-2 cells under salt and osmotic treatment. This dye can only be uptake by active mitochondria while

de-energized or depolarized mitochondria will give weak and diffuse fluorescent signals (Wu, 1987; Petit, 1991).

When untreated BY-2 cells were stained with Rh123, discrete signals were observed (Fig. 7a). However, when the cells were pre-treated with 200mM NaCl or 2% PEG in prior to Rh123 staining, diffuse signal were obtained (Fig.7b and 7c). If the antioxidant ascorbic acid (10mM) was included in the cell medium, such diffusion of signals was prevented (Fig. 7e and 7f). These results suggest that NaCl stress will cause oxidative stress and lead to damage of mitochondrial membranes in BY-2 cells. When subjected to the same treatments as the untransformed BY-2 cells, *GmPAP3* transgenic lines exhibited similar discrete signal pattern without NaCl and PEG treatments (Fig. 7g and 7j). Nonetheless, a clear protection effect was observed in *GmPAP3* transgenic lines under NaCl treatment (Fig. 7h and 7k) as well as under PEG treatment (Fig. 7i and 7l). This experiment was repeated three times and the quantitative results were shown in Table 10.

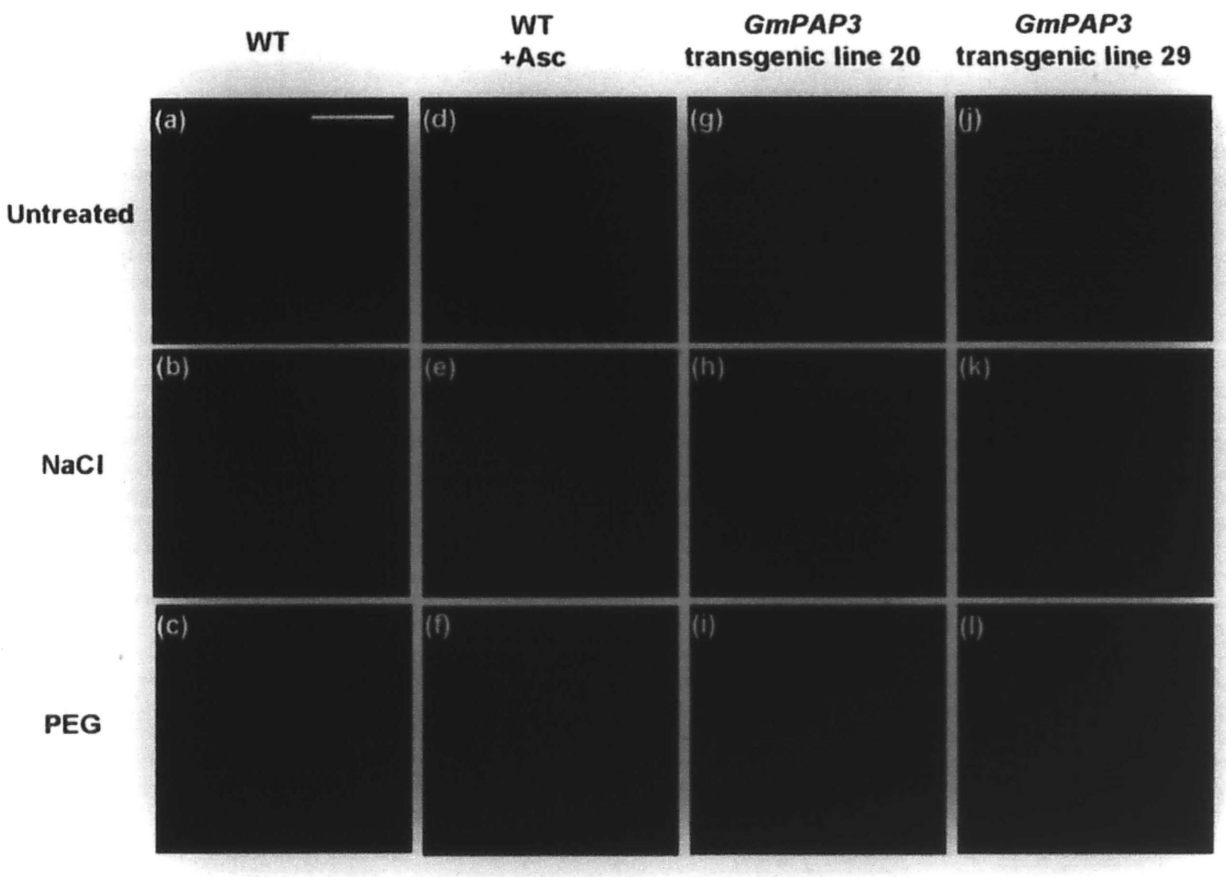


**Fig. 7.** Mitochondrial membrane integrity under salinity and osmotic stresses. Wild type (WT) BY-2 cells (**a-c**) and *GmPAP3* transgenic BY-2 cell lines 20 and 29 (**g-i** & **j-l**, respectively) without ascorbic acid supplements and wild type BY-2 cells with 10 mM ascorbic acid supplements (+Asc) (**d-f**) were pre-treated in a cell culture medium without stress (**a**, **d**, **g**, **j**), with 200 mM NaCl (**b**, **e**, **h**, **k**), or with 2 % PEG for 1 h (**c**, **f**, **i**, **l**) before staining with 10 μg/mL Rh123 for another hour. The signal of Rh123 was observed using the Bio-Rad confocal laser scanning microscope. Ten to 25 cells were counted for each line. Scale bar = 50 μm. Quantitative analysis was shown in Table 10.

**Table 10.** Quantitative analysis on the effects of salinity and osmotic stresses on mitochondria integrity.

| **Cell lines** | **% cells with intact mitochondria** | | |
|---|---|---|---|
| | **Control** | **NaCl** | **PEG** |
| Wild type BY-2 | 100 | 45 ± 6 | 48 ± 3 |
| Wild type BY-2 + 10 mM ascorbic acid | 100 | 86 ± 3** | 82 ± 4** |
| *GmPAP3* transgenic cell line 20 | 100 | 81 ± 4** | 81 ± 6** |
| *GmPAP3* transgenic cell line 29 | 100 | 80 ± 5** | 80 ± 7** |

Experimental details were given in Fig. 7. Quantitation for the percentage of cells with intact mitochondria was estimated by the uptake of the fluorescent dye Rh123. The percentage was presented as the mean value of 3 experiments (10-25 cells for each sample) ± SD. **: statistically different ($p<0.01$) from the wild type BY-2 cells under the same treatment, based on one-way analysis of variance (one-way ANOVA) followed by Tukey test.

### 3.2.2 Effect of expressing GmPAP3 on cell viability under NaCl and osmotic treatments

We have also assess the long term effect of NaCl and osmotic treatments on *GmPAP3* transgenic cell lines using cell death (indicated by Trypan blue staining (Hou & Lin, 1996)) as an indicator. In untreated BY-2 cells, there was no dead cells that could be stained by trypan blue (Fig. 8a). Both salinity and osmotic stresses increased the percentage of dead cells (cells stained blue) (Fig. 8b and 8c). Addition of the antioxidant ascorbic acid to the wild type BY-2 cells under the same stress conditions imposed a significant protective effect (Figs. 8e, 8f), indicating that NaCl and PEG induced oxidative damages were the immediate cause of their detrimental effects in BY-2 cells. Ectopic expression of *GmPAP3* in BY-2 cells mimicked the effect of the antioxidant ascorbic acid and protected the cells from salinity (Figs. 8h, 8k) and osmotic stresses (Figs. 8i, 8l), supporting the notion that GmPAP3 may function to alleviate oxidative damages. This experiment was repeated three times and the quantitative results were shown in Table 11.

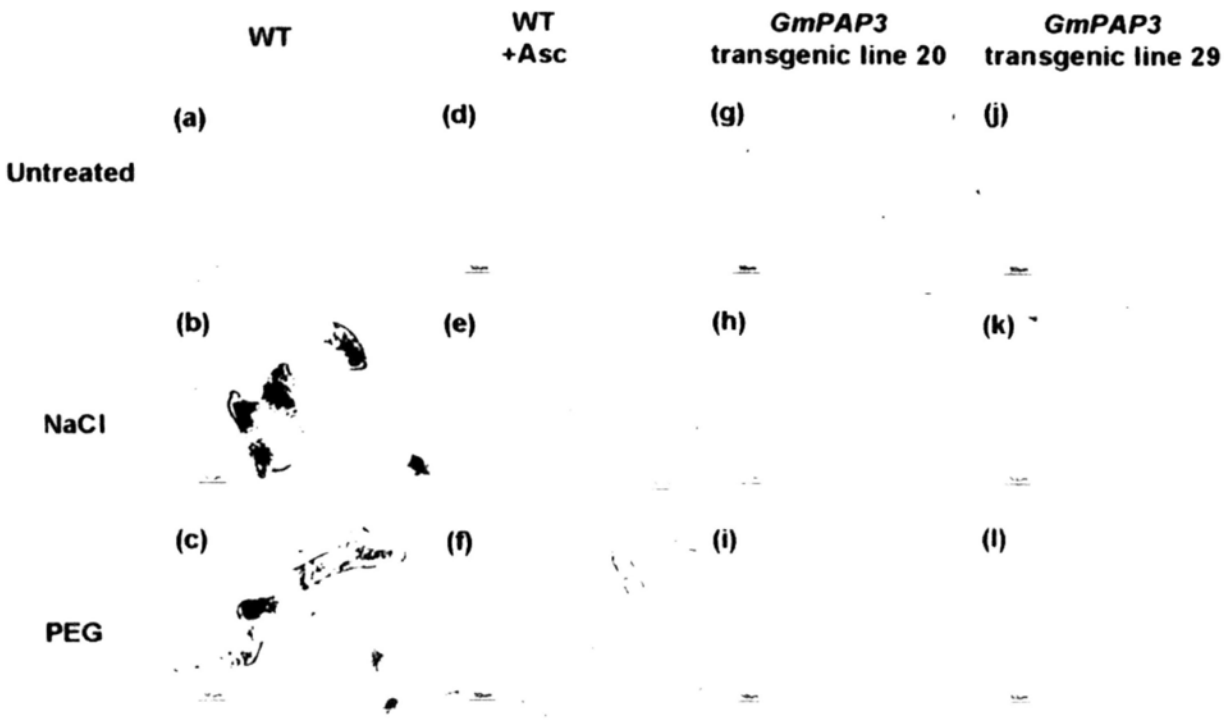


**Fig. 8** Cell viability under salinity and osmotic stresses. Wild type (WT) BY-2 cells (**a-c**) and *GmPAP3* transgenic BY-2 cell lines 20 and 29 (**g-i** & **j-l**, respectively) without ascorbic acid supplements and wild type BY-2 cells with 10 mM ascorbic acid supplements (+Asc) (**d-f**) were pre-treated for 24 h in a cell culture medium without stress (**a**, **d**, **g** and **j**), with 200 mM NaCl (**b**, **e**, **h**, **k**), or with 2 % PEG (**c**, **f**, **i**, **l**). Treated cells were stained with 0.4 % trypan blue. Non-viable cells were stained blue. Around 200 cells were counted for each sample. Scale bar = 50 μm. Quantitative analysis was shown in Table 11.

**Table 11.** Quantitative analysis on the effects of salinity and osmotic stresses on cell survival.

| **Cell lines** | **% of viable cells** | | |
|---|---|---|---|
| | **Untreated** | **200 mM NaCl** | **2 % PEG** |
| Wild type BY-2[a] | 99 ± 3 | 48 ± 9 | 67 ± 8 |
| Wild type BY-2 + 10 mM ascorbic acid[a] | 98 ± 6 | 93 ± 8** | 95 ± 9** |
| Wild type BY-2[b] | 93 ± 11 | 42 ± 7 | 60 ± 13 |
| *GmPAP*3 transgenic cell line 20[b] | 95 ± 6 | 80 ± 17** | 96 ± 6** |
| *GmPAP*3 transgenic cell line 29[b] | 98 ± 3 | 86 ± 18** | 92 ± 13** |

Experimental details were given in Fig. 8. Quantitation for the percentage of dead cells was estimated by trypan blue staining. The percentage was presented as the mean value of around 200 cells ± SD. **: statistically different ($p<0.01$) from the wild type BY-2 cells under the same treatment, based on one-way ANOVA followed by the Tukey test. [a] and [b] indicate two separate sets of experiment.

### 3.2.3 Effect of expressing GmPAP3 on ROS production in BY-2 cells under NaCl and osmotic treatments

Since oxidative damages and tolerance are tightly linked to the formation and scavenging of ROS, we monitored the accumulation of cellular hydrogen peroxide using a fluorescent dye $H_2$DCFDA (see Materials and Methods) under the stress treatments described above (Fig. 9; Table 12). In parallel to the degree of stress-induced cellular damages (see above section 3.2.1 and 3.2.2), hydrogen peroxide was accumulated in the BY-2 cells under both NaCl and PEG treatments (Figs. 9b and 9c), but not in untreated cells (Fig. 9a). The level of hydrogen peroxide under both stress conditions was lowered by the addition of the antioxidant ascorbic acid (Figs. 9e and 9f) or ectopic expression of *GmPAP3* (Figs. 9h, 9i, 9k and 9l).

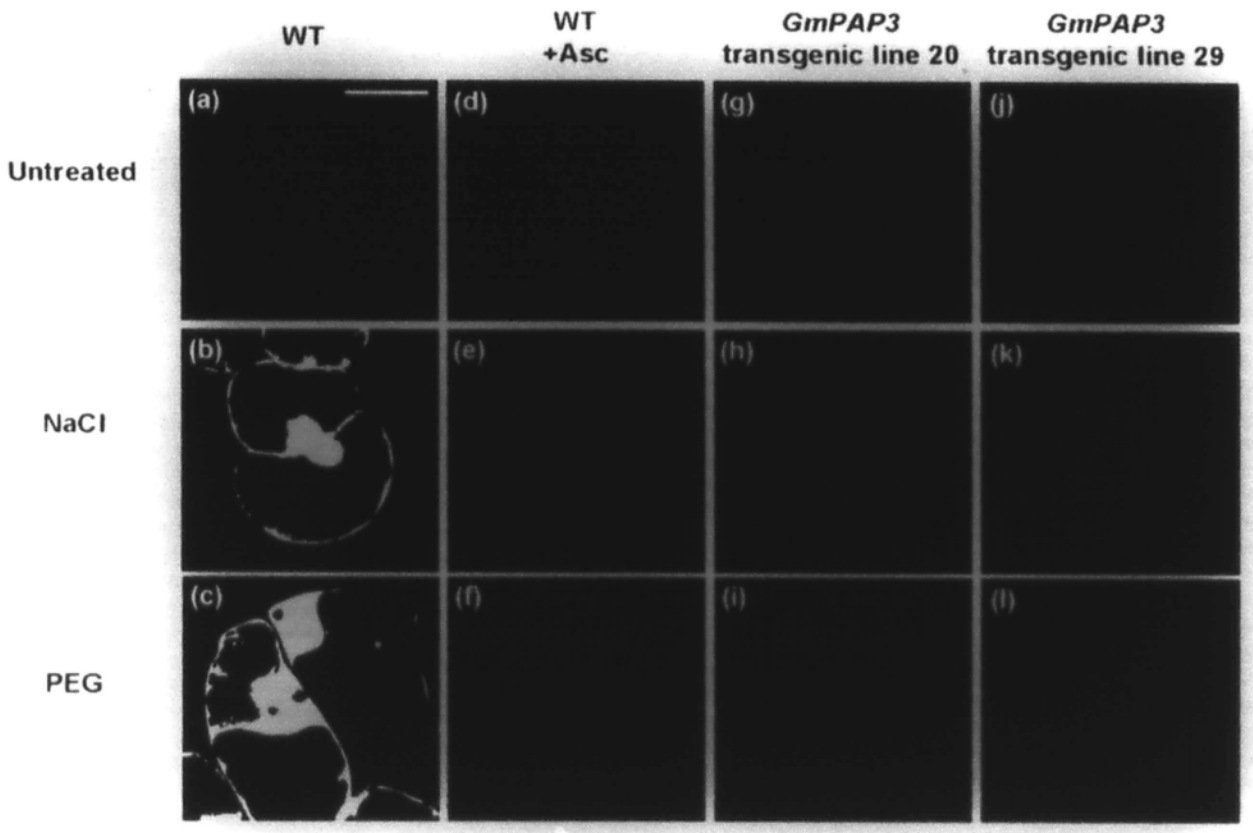


**Fig. 9** Cellular ROS production under salinity and osmotic stresses. Wild type (WT) BY-2 cells (**a-c**) and *GmPAP3* transgenic BY-2 cell lines 20 and 29 (**g-i** & **j-l**, respectively) without ascorbic acid supplements and wild type BY-2 cells with 10 mM ascorbic acid supplements (+Asc) (**d-f**) were pre-stained with $H_2$DCFDA for 30 min before placed in a cell culture medium without stress (**a**, **d**, **g**, **j**), with 200 mM NaCl (**b**, **e**, **h**, **k**), or with 2 % PEG for 1 h (**c**, **f**, **i**, **l**). The signals of $H_2$DCFDA were observed using a confocal laser scanning microscope. Ten to 20 cells were counted for each line. Scale bar = 50 μm. Quantitative analysis was shown in Table 13.

**Table 12.** Quantitative analysis on the effects of salinity and osmotic stresses on ROS accumulation.

| **Cell lines** | **Signal intensity of $H_2$DCFDA (pixel per $cm^2$)** | | |
|---|---|---|---|
| | **Untreated** | **200 mM NaCl** | **2 % PEG** |
| Wild type BY-2[a] | 201 ± 36 | 533 ± 77 | 570 ± 49 |
| Wild type BY-2 + 10 mM ascorbic acid [a] | 197 ± 37 | 199 ± 47** | 190 ± 31** |
| Wild type BY-2[b] | 180 ± 24 | 505 ± 35 | 565 ± 38 |
| *GmPAP*3 transgenic cell line 20 [b] | 194 ± 23 | 234 ± 45** | 210 ± 65** |
| *GmPAP*3 transgenic cell line 29 [b] | 196 ± 32 | 223 ± 38** | 225 ± 58** |

Experimental details were given in Fig. 9. Numerical data represents the mean value of 10-20 cells ± SD. **: statistically different ($p<0.01$) from the wild type BY-2 cells under the same treatment, based on one-way ANOVA followed by the Tukey test. [a] and [b] indicate two separate sets of experiment.

### 3.3 The protective effect of GmPAP3 depended on the presence of Ferric ions

#### 3.3.1 The protective effects of GmPAP3 on mitochondria integrity depended on the presence of Ferric ions

The GmPAP3 protein contains all consensus amino acid residues for metal (Fe(III) and Mn(II)/Zn(II)) binding at the active site (Schenk *et al.*, 1999; Liao *et al.*, 2003). It was believed that the metal binding center is the active site of GmPAP3 and I hypothesized that the ferric center is necessary for removal of ROS. Therefore we tested if the presence of ferric ion is important for protective effect of the *GmPAP3* transgenic BY-2 cell lines under. In the presence of Fe(III) chelators, the perentage of cells with intact mitochondria in all lines (both transgenic and wild type) under NaCl treatment were similar (Fig. 10 and Table 13). This result suggests that the presence of Fe (III) ions, probably for proper formation of binuclear metal center, is necessary for protective effect of GmPAP3 in transgenic BY-2 cells under salt stress.

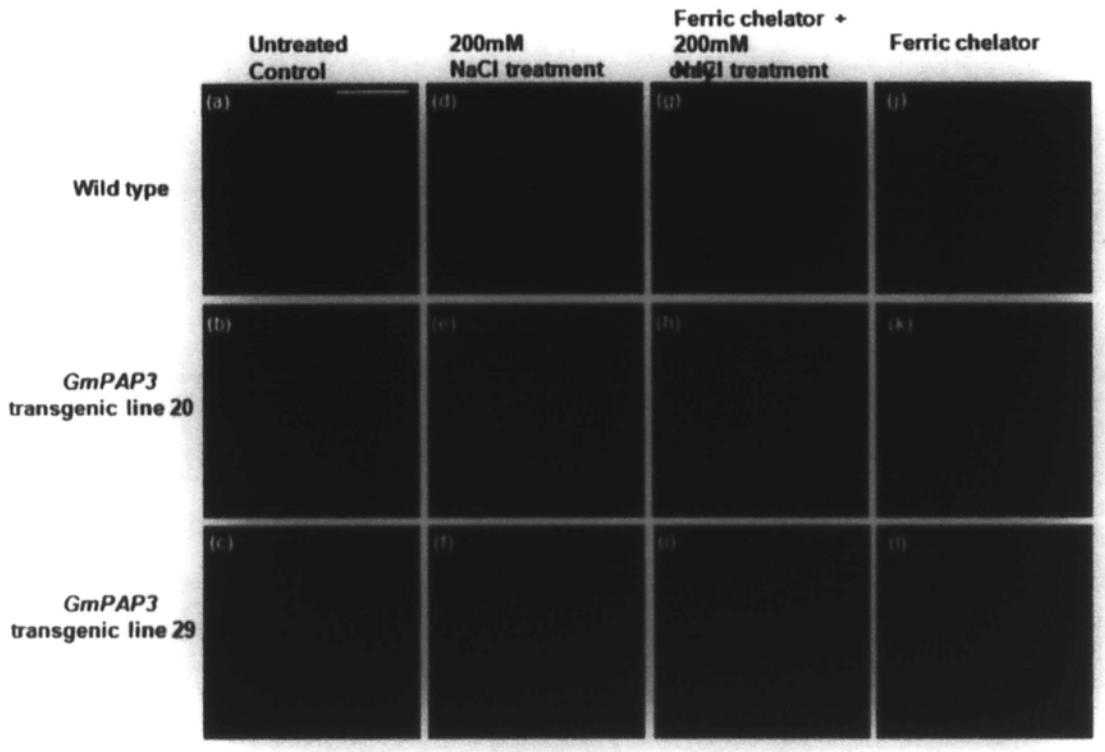


**Fig 10.** Mitochondrial membrane integrity under salt stresses with ferric chelator treatment. Wild type (WT) BY-2 cells (**a, d, g, j**) and *GmPAP3* transgenic BY-2 cell lines 20 and 29 (**b, e, h, k** & **c, f, i, l** respectively) without ferric chelator treatment (**a-f**) and with ferric chelator treatment (**g-l**) were pre-treated in a cell culture medium without stress (**a-c & j-l**), or with 200 mM NaCl (**d-f & g-i**) before staining with 10 μg/mL Rh123 for another hour. The signal of Rh123 was observed using a confocal laser scanning microscope. Ten to 25 cells were counted for each line. Scale bar = 50 μm. Quantitative analysis was shown in Table 13.

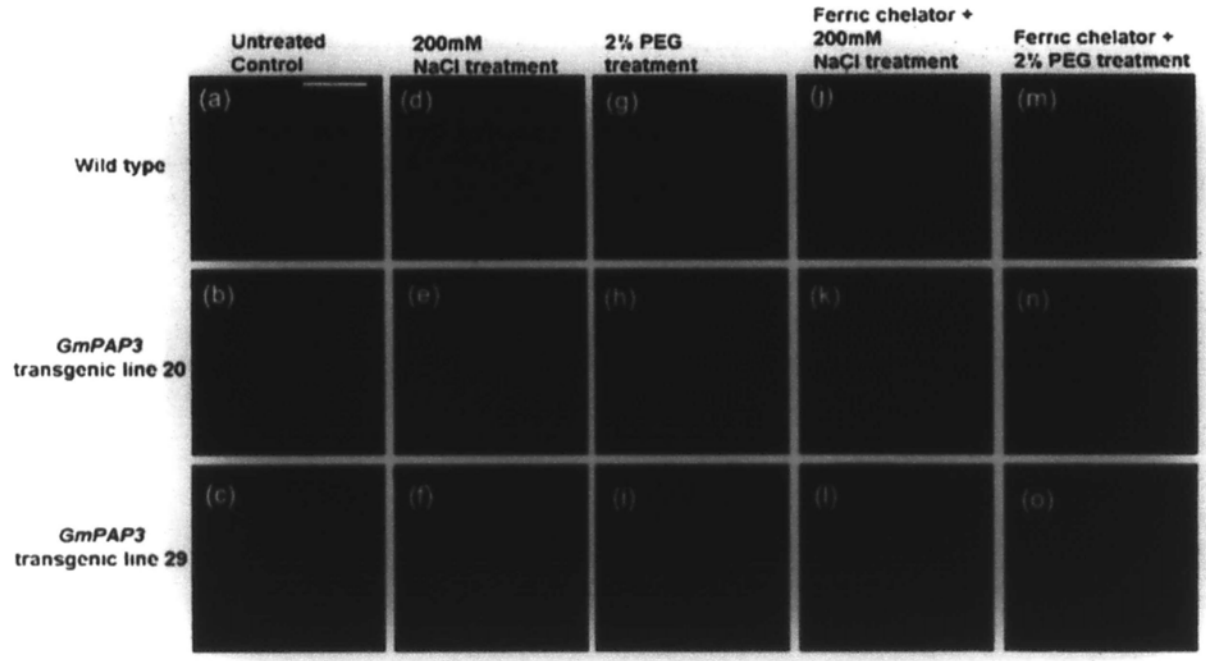


**Fig 11.** Cellular ROS production under salinity and osmotic stresses with chelator treatment. Wild type (WT) BY-2 cells (**a, d, g, j, m**) and *GmPAP3* transgenic BY-2 cell lines 20 and 29 (**b, e, h, k, n** & **c, f, i, l, o** respectively) without ferric chelator treatment (**a-i**) and with ferric chelator treatment (**j-o**) were pre-stained with $H_2$DCFDA for 30 min before placed in a cell culture medium without stress (**a-c**), with 200 mM NaCl (**d-f & j-l**), or with 2 % PEG for 1 h (**g-i & m-o**). The signals of $H_2$DCFDA were observed using a confocal laser scanning microscope. Ten to 20 cells were counted for each line. Scale bar = 50 μm. Quantitative analysis was shown in Table 15.

## 3.4 The mitochindria localization is essential for GmPAP3 to demonstrate its protective effect on plant cells under NaCl and osmotic treatments.

### 3.4.1 Cloning of the GmPAP3 which without a mitochondria transit peptide

Mitochondria are one of the major organelles for ROS accumulation under stress conditions (Bartoli *et al.*, 2004; Noctor *et al.*, 2007). Moreover, GmPAP3 is the only mitochondria localized PAP reported to date (Liao *et al.*, 2003; Li *et al.*, 2008) Therefore, I hypothesized that the mitochondrial localization of GmPAP3 may be essential for its function to alleviate stress response by scavenging of ROS.

To test this hypothesis, a truncated version of GmPAP3 (GmPAP3*) was constructed in which the transit peptide was removed while all other functional parts were retained. As predicted using Mitochondrial transit peptide prediction program MITOPROT and PSORT, the mitochondrial transit peptide of the intact GmPAP3 protein spans from the 1$^{st}$ to 58$^{th}$ amino acid (Fig.12). The nucleotide and amino acid sequences of GmPAP3* were shown in Fig. 13. As shown in Table 15, using all publicly available prediction programs of subcellular localization of proteins, GmPAP3* was not predicted to be located in mitochondria due to the loss of the transit peptide. On the other hand, the full-length GmPAP3 is predicted to be mitochondria localized by all programs used. GmPAP3* is used for the subsequent construction of transgenic cell lines for subcellular localization and functional studies.

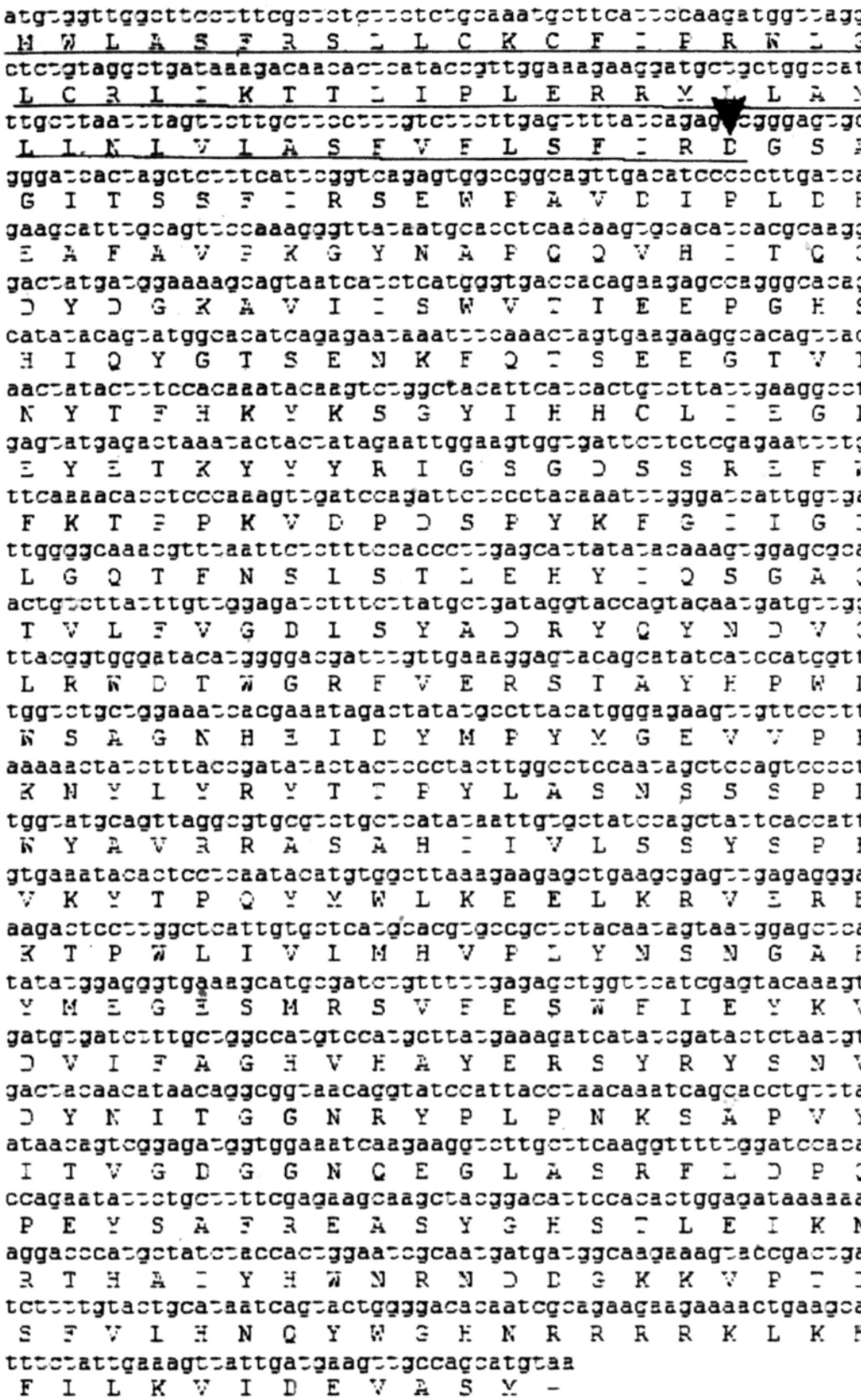

**Fig. 12.** Nucleotide and amino acid sequence of GmPAP3 (full length). The predicted mitochondrial transit peptide was underlined. The predicted cleavage site for the mitochondrial transit peptide is at the 58$^{th}$ amino acid (indicated by an arrow).

```
atgctgctggccatgttgcttaatttagttcttgcttcctttgtcttcttgagttttatc
 M  L  L  A  M  L  L  N  L  V  L  A  S  F  V  F  L  S  F  I
agagacgggagtgcagggatcactagctctttcattcggtcagagtggccggcagttgac
 R  D  G  S  A  G  I  T  S  S  F  I  R  S  E  W  P  A  V  D
atccccttgatcatgaagcatttgcagttccaaagggttataatgcaccttcaacaagtg
 I  P  L  D  H  E  A  F  A  V  P  K  G  Y  N  A  P  Q  Q  V
cacatcacgcaaggtgactatgatggaaaagcagtaatcatctcatgggtgaccacagaa
 H  I  T  Q  G  D  Y  D  G  K  A  V  I  I  S  W  V  T  T  E
gagccagggcacagccatatacagtatggcacatcagagaataaatttcaaactagtgaa
 E  P  G  H  S  H  I  Q  Y  G  T  S  E  N  K  F  Q  T  S  E
gaaggcacagttacaaactatactttccacaaatacaagtctggctacattcatcactgt
 E  G  T  V  T  N  Y  T  F  H  K  Y  K  S  G  Y  I  H  H  C
cttattgaaggccttgagtatgagactaaatactactatagaattggaagtggtgattct
 L  I  E  G  L  E  Y  E  T  K  Y  Y  Y  R  I  G  S  G  D  S
tctcgagaatttggttcaaaacacctcccaaagttgatccagattctccctacaaattt
 S  R  E  F  W  F  K  T  P  P  K  V  D  P  D  S  P  Y  K  F
gggatcattggtgatttggggcaaacgtttaattctcttccaccttgagcattatata
 G  I  I  G  D  L  G  Q  T  F  N  S  L  S  T  L  E  H  Y  I
caaagtggagcgcagactgtcttattgttggagatcttctttatgctgataggtaccag
 Q  S  G  A  Q  T  V  L  F  V  G  D  L  S  Y  A  D  R  Y  Q
tacaatgatgttggtttacggtgggatacatggggacgatttgttgaaaggagtacagca
 Y  N  D  V  G  L  R  W  D  I  W  G  R  F  V  E  R  S  T  A
tatcatccatggttatggtctgctggaaatcacgaaatagactatatgccttacatggga
 Y  E  P  W  L  W  S  A  G  N  E  E  I  D  Y  M  P  Y  M  G
gaagttgttcctttcaaaaactatcttaccgatatactactcccttacttggcctccaat
 E  V  V  P  F  K  N  Y  L  Y  R  Y  T  I  P  Y  L  A  S  N
agctccagtccccctctggtatgcagttaggcgtgcgtctgctcatataattgtgctatcc
 S  S  S  P  L  W  Y  A  V  R  R  A  S  A  E  I  I  V  L  S
agctattcaccatttgtgaaatacactcctcaatacatgtggcttaaagaagagctgaag
 S  Y  S  P  F  V  K  Y  T  P  Q  Y  M  W  L  K  E  E  L  K
cgagttgagagggagaagactccttggctcattgtgctcatgcacgtgccgctctacaat
 R  V  E  R  E  K  T  P  W  L  I  V  L  M  E  V  P  L  Y  N
agtaatggagctcactatatggagggtgaaagcatgcgatctgttttgagagctggttc
 S  N  G  A  H  Y  M  E  G  E  S  M  R  S  V  F  E  S  W  F
atcgagtacaaagttgatgtgatctttgctggccatgtccatgcttatgaaagatcatat
 I  E  Y  K  V  D  V  I  F  A  G  H  V  H  A  Y  E  R  S  Y
cgatactctaatgttgactacaacataacaggcggtaacaggtatccattacctaacaaa
 R  Y  S  N  V  D  Y  N  I  T  G  G  N  R  Y  P  L  P  N  K
tcagcacctgtttacataacagtcggagatggtggaaatcaagaaggtcttgcttcaagg
 S  A  P  V  Y  I  T  V  G  D  G  G  N  Q  E  G  L  A  S  R
ttttttggatccacagccagaatattctgctttttcgagaagcaagctacggacattccaca
 F  I  D  P  Q  P  E  Y  S  A  F  R  E  A  S  Y  G  H  S  I
ctggagataaaaaaataggacccatgctatctaccactggaatcgcaatgatgatggcaag
 L  E  I  K  N  R  T  H  A  I  Y  H  W  N  R  N  D  D  G  K
aaagtaccgactgactctttttgtactgcataatcagtactggggacacaatcgcagaaga
 K  V  P  T  D  S  F  V  L  H  N  Q  Y  W  G  H  N  R  R  R
agaaaactgaagcatttctattgaaagttattgatgaagttgccagcatgtaa
 R  K  L  K  H  F  L  I  K  V  I  D  E  V  A  S  M  -
```

**Fig. 13.** Nucleotide and amino acid sequence of truncated GmPAP3 (GmPAP3*). The predicted mitochondrial transit peptide (span from 1st to 105th bases) is removed.

**Table 15.** Prediction of subcellular localization of full length and truncated GmPAP3.

| Program use | Protein | Prediction |
|---|---|---|
| MITOPROT II ver 1.1 | GmPAP3 | Probability to Mitochondria = 0.9855 |
| | GmPAP3* | Probability to Mitochondria = 0.1961 |
| PSORT | GmPAP3 | Mitochondria inner membrane, probability = 0.886 |
| | GmPAP3* | Outside, probability = 0.820 |
| Target P | GmPAP3 | Prbability of having a mitochondria transit peptide = 0.703 |
| | GmPAP3* | Probability of having a mitochondria transit peptide = 0.088 |

### 3.4.2 Establishment of GmPAP3 (truncated) transgenic BY-2 cell lines

In order to investigate the significance of mitochondria location of *GmPAP3* under salt and osmotic stress, tobacco BY-2 cell lines expressing GmPAP3* were established.

To perform *Agrobacterium*-mediated transformation, the recombinant plasmid V7-*GmPAP3** (truncated) generated (for construct design please see Fig. 5, Section 2.2.3) was transformed into the wild type tobacco BY2 by a co-cultivation method (see the Materials and Methods Section). *GmPAP3* transgenic cell lines were constructed in parallel to the *GmPAP3** transgenic cell lines for further comparative studies. Successful transformation events were screened by PCR using oligonucleotides HMOL 622 and HMOL 1557 (Fig. 14). After obtaining the transformants, PCR screen was performed to confirm the insertion of *transgene* into the genome of BY-2 cells; and Northern blot analysis were performed to confirm expression of the transgene in these transgenic cell lines. For both the *GmPAP3* and *GmPAP3** transgenic cell lines, the presence of recombinant insert was confirmed by PCR in 7 out of 8 independent transformants of each construct. Subsequently, 5 (GmPAP3) and 6 (GmPAP3*) of the transformants were chosen for Northern blot analysis and all candidates showed expression of the transgene (Fig. 15). Transgenic lines with comparable transgene expression were chosen for further study (Fig. 15C).

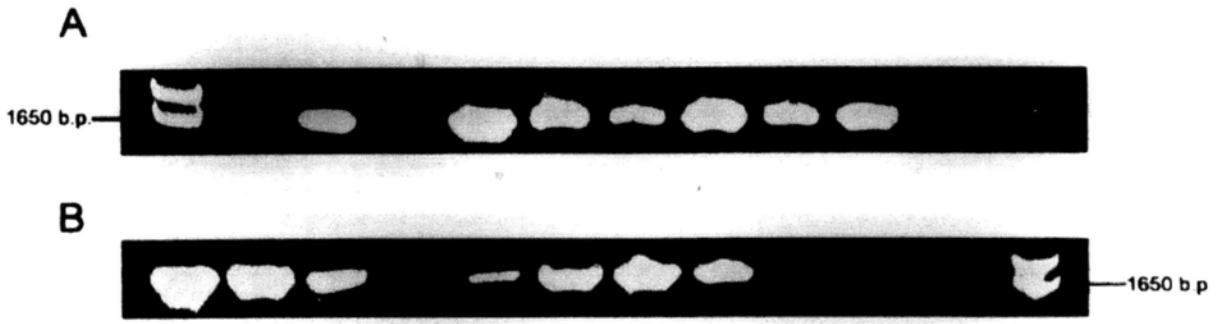


**Fig.14.** PCR screen of *GmPAP3* transgenic BY-2 genomic DNA. PCR condition was as described in the Materials and Methods section. **A**: PCR screen of *GmPAP3** cell lines; Lane 1: 1kb plus ladder, Lane 3: line #43, Lane 4: line #49, Lane 5: line #76, Lane 6: line #50, Lane 7: line #56, Lane 8: line #91, Lane 9: line, #137, Lane 10: line #152, Lane 12: positive control which is the recombinant plasmid V7-*GmPAP3**. **B**: PCR screen of *GmPAP3* cell lines; Lane 1: line #1, Lane 2: line # 5, Lane 3: line # 8, Lane 4: line #9, Lane 5: line #15, Lane 6: line #30, Lane 7: line #49, Lane 8: line #50, Lane 10: positive control, which is the recombinant plasmid V7-*GmPAP3*.

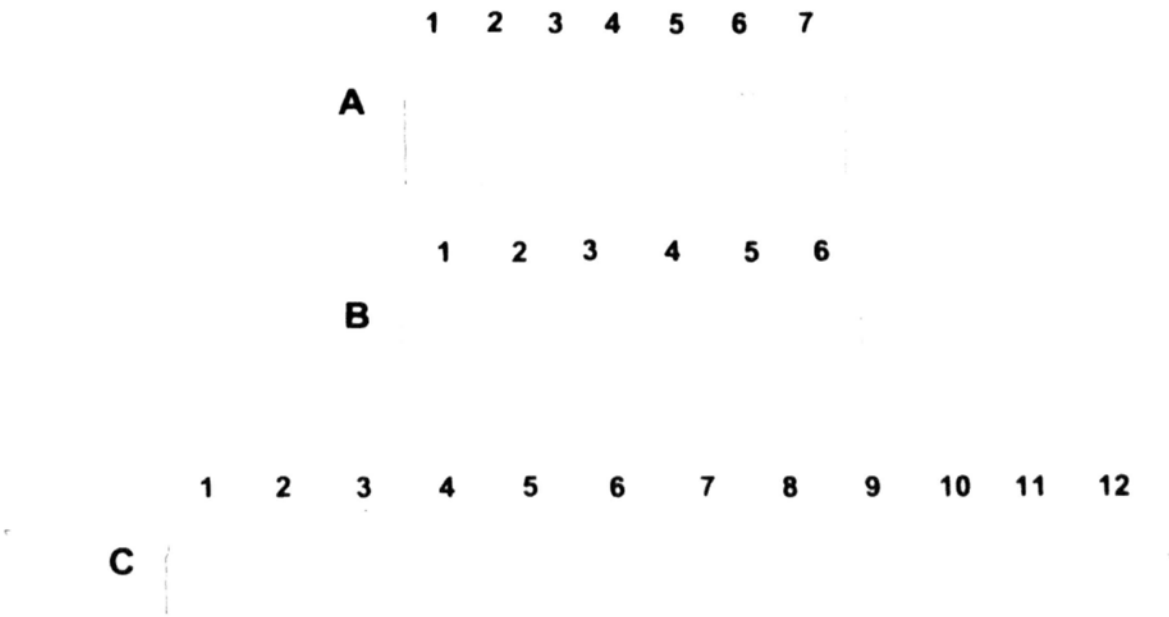


**Fig. 15.** Northern blot analysis of *GmPAP3* transgenic cells lines.

A: Northern blot analysis of *GmPAP3** transgenic BY-2 cell lines. 1: line #43, 2: line #49, 3: line #76, 4: line #56, 5: line # 91, 6: line #137, 7: RNA of untransformed wild type BY-2 cells. Ten μg of total RNA was loaded onto each lane.

B: Northern blot analysis of *GmPAP3* transgenic BY-2 cell lines. 1: line #1, 2: line #5, 3: line #8, 4: line #9, 5: line #29, 6: RNA of untransformed wild type BY-2 cells.

C: Northern blot analysis of *GmPAP3** and *GmPAP3* transgenic BY-2 cell lines. 1- 6: *GmPAP3** transgenic lines; 7-11: *GmPAP3* transgenic lines. 1: #43, 2: line #49, 3: line #76, 4: line #56, 5: line # 91, 6: line #137, 7: line #1, 8: line #5, 9: line #8, 10: line #9, 11: line #29, 12: positive control, i.e. RNA from soybean. Ten μg of total RNA was loaded onto each lane.

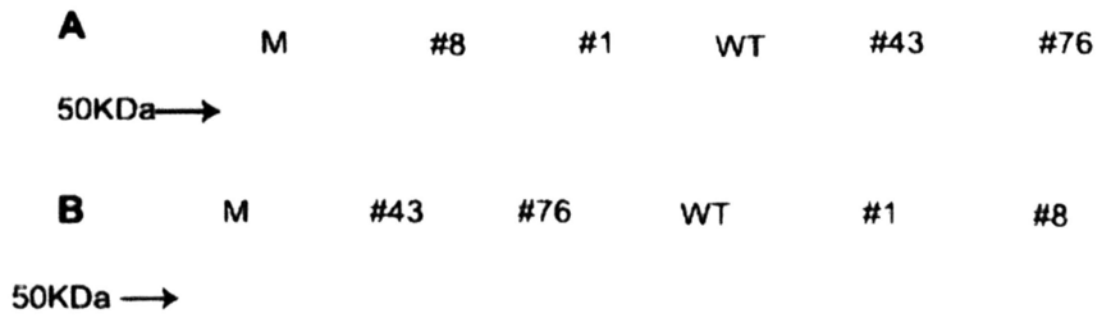


**Fig.16.** Western blot analysis of *GmPAP3** and *GmPAP3* transgenic cell lines. Soluble protein and mitochondrial enriched protein fraction were extracted as described in Materials and methods. **A**: Western blot analysis of soluble protein fraction. WT: untransformed wild type BY-2 cells; #43 and #76: two independent *GmPAP3** transgenic cell lines; #8 and #1: two independent *GmPAP3* transgenic cell lines; M: Precision plus protein standard. B: Western blot analysis of mitochondrial enriched protein fraction. WT: untransformed wild type BY-2 cells; #43 and #76: two independent *GmPAP3** transgenic cell lines; #1 and #8: two independent *GmPAP3* transgenic cell lines; M: Precision plus protein standard.

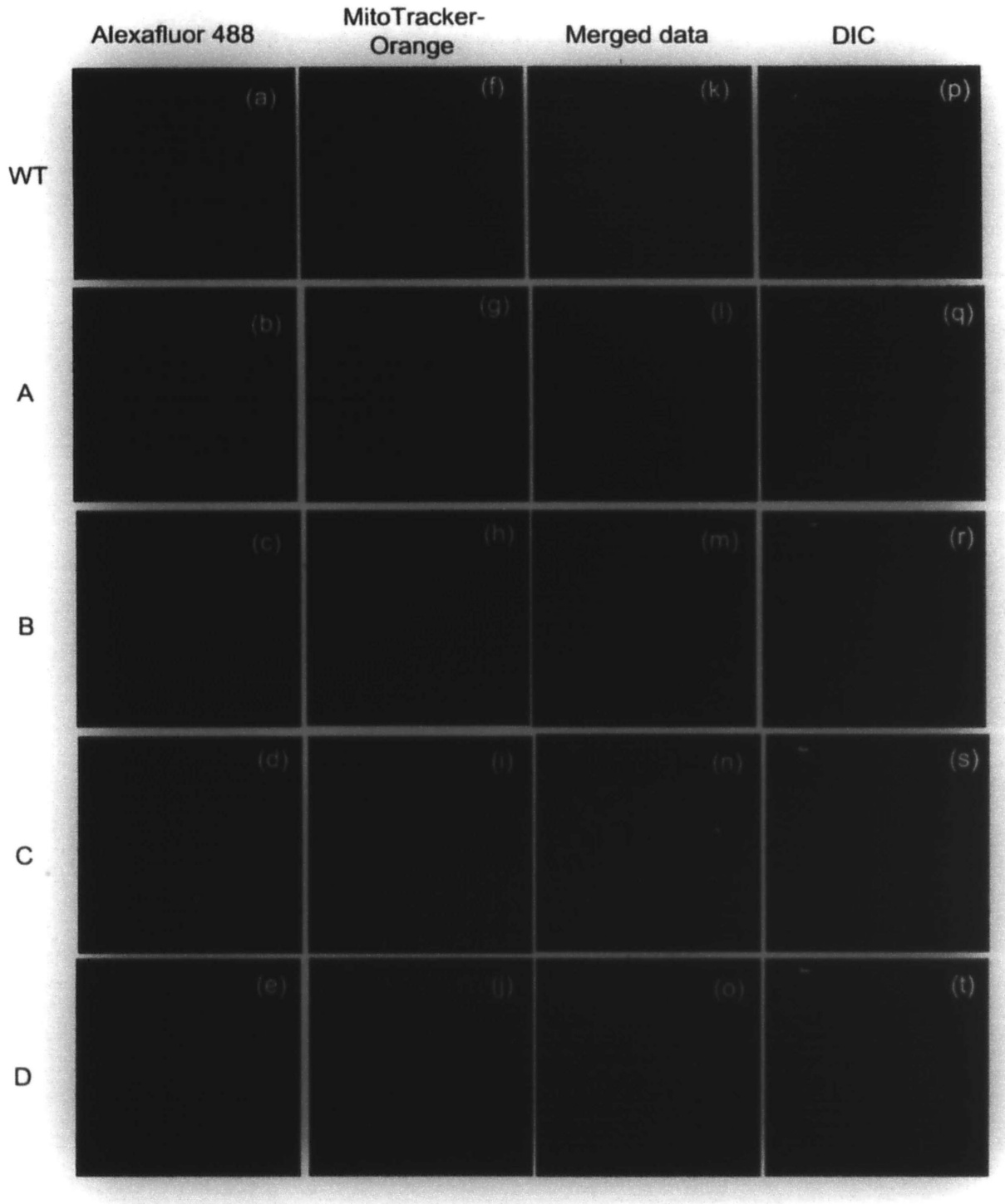


**Fig. 17.** Immunolabeling and confocal microscopy of *GmPAP3** and *GmPAP3* transgenic cell lines. WT: Wild type, A: *GmPAP3** transgenic line 43, B: *GmPAP3** transgenic line 76, C: *GmPAP3* transgenic line 8, D: *GmPAP3* transgenic line 1. The *GmPAP3* protein was labeled with Alexa Fluor® 488-conjugated secondary antibody (pseudocolored in green). MitoTracker® orange (pseudocolored in red) was used as a marker for mitochondria. Scale bar= 20 microns

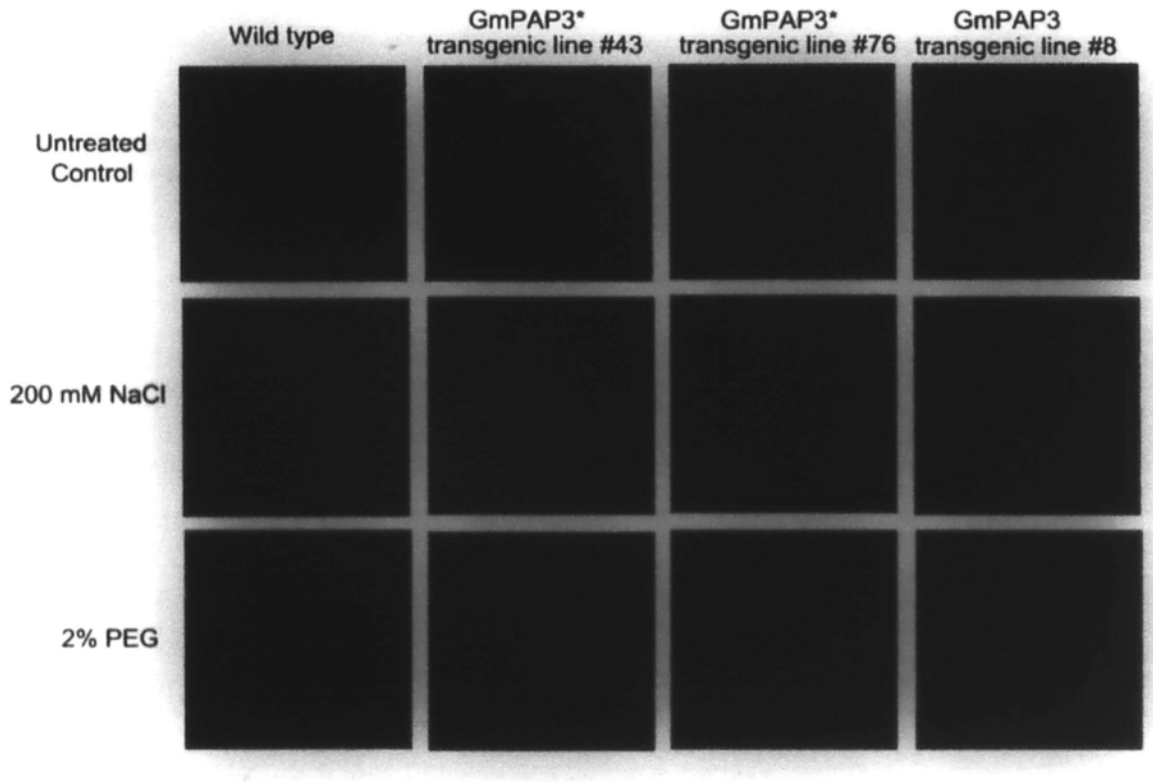


**Fig. 18**. Mitochondrial integrity under salinity and osmotic stresses of *GmPAP3** and *GmPAP3* transgenic cell lines. Wild type (WT) BY-2 cells (**a-c**) and *GmPAP3* (truncated and full length) transgenic BY-2 cell lines (**d-f**, **g-i** & **j-l**, respectively) were pre-treated in a cell culture medium without stress (**a**, **d**, **g**, **j**), with 200 mM NaCl (**b**, **e**, **h**, **k**), or with 2 % PEG for 1 h (**c**, **f**, **i**, **l**) before staining with 10 μg/mL Rh123 for another hour. The signal of Rh123 was observed using a confocal laser scanning microscope. Ten to 25 cells were counted for each line. Scale bar = 20 μm. Quantitative analysis was shown in Table 18.

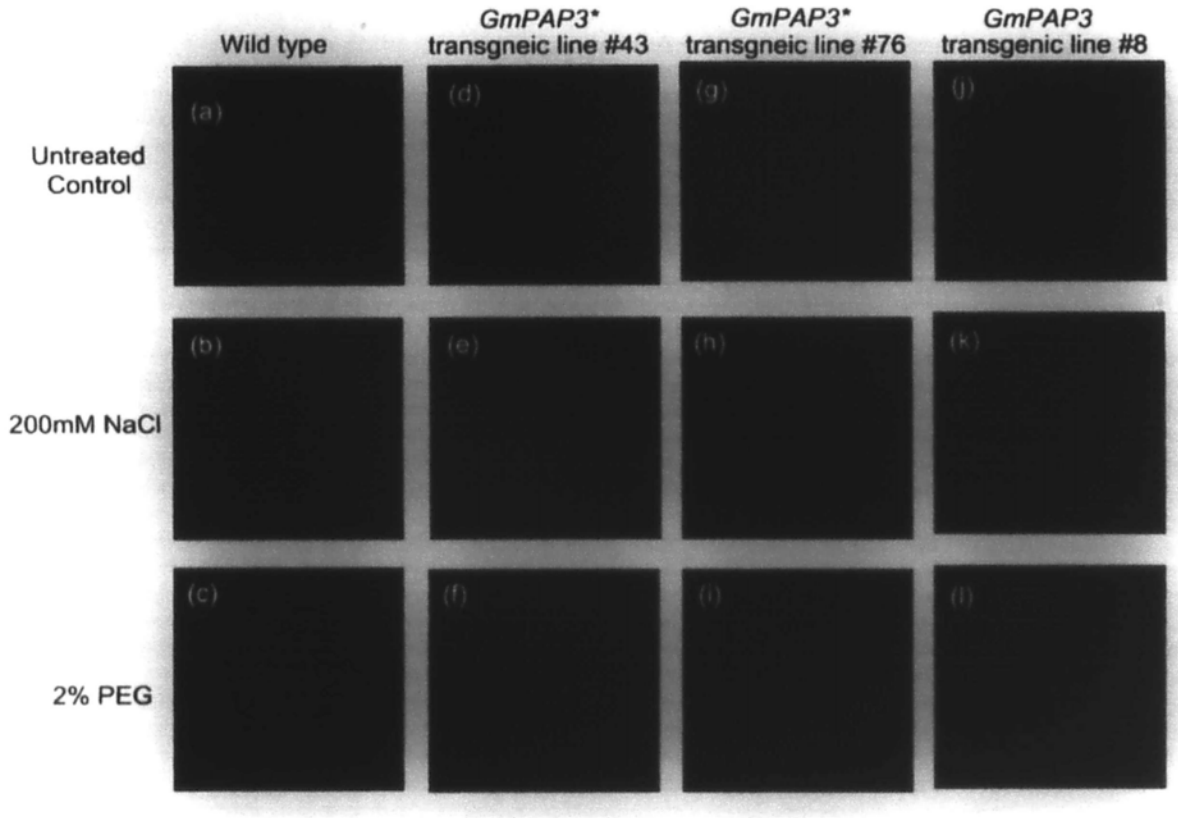


**Fig. 19.** Cellular ROS production under salinity and osmotic stresses in *GmPAP3** and *GmPAP3* transgenic cell lines. Wild type BY-2 cells (**a-c**) and *GmPAP3* (truncated and full length) transgenic BY-2 cell lines (**d-f, f-I** & **j-l**) were pre-stained with $H_2$DCFDA for 30 min before placed in a cell culture medium without stress (**a,d, g, j**), with 200 mM NaCl (**b, e, h, k**), or with 2 % PEG for 1 h (**c, f, i, l**). The signals of $H_2$DCFDA were observed using a confocal laser scanning microscope. Ten to 20 cells were counted for each line. Scale bar = 20 μm. Quantitative analysis was shown in Table 18.

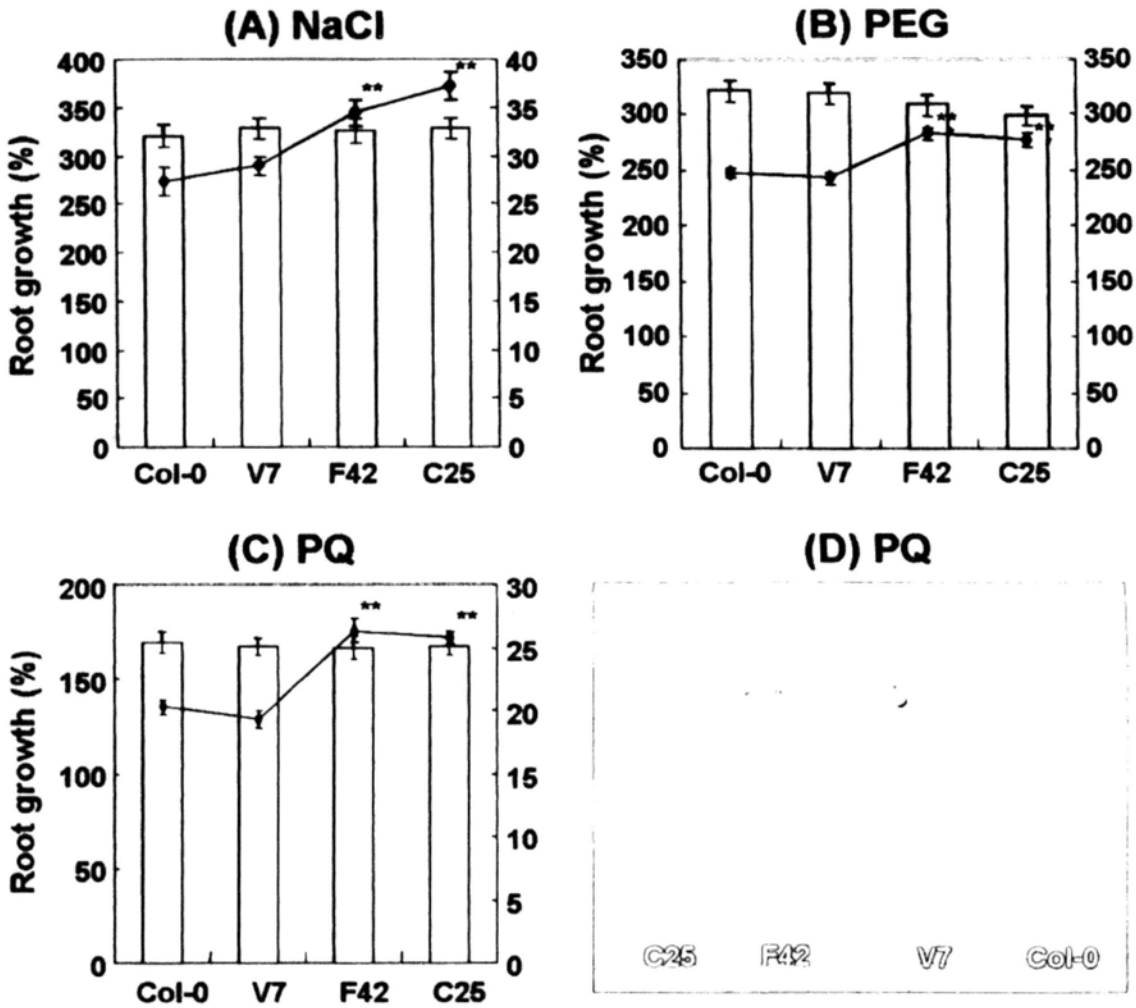


**Fig. 20.** Effects of salinity, osmotic, and oxidative stresses on root elongation. The percentage of root elongation after treated with 150 mM NaCl (**a**), 15 % PEG (**b**), and lc) was compared among the wild type Col-0, the empty vector transgenic control (V7) and two independent *GmPAP3* transgenic lines (F42 and C25). Y-axis on the left and right of each graph indicated the percentage root elongation of untreated (bar) and stressed (line) seedlings, respectively. The percentage root elongation was calculated as follow: the root length after treatment minus root length before treatment divided by root length before treatment. Error bar: standard error. N=48. Data obtained were analyzed by one-way analysis of variance (one-way ANOVA) followed by the Tukey test. ** indicates that the mean difference (compared to wild type) is significant at $p<0.01$ level.

**Table 16.** Quantification of colocalization of Alexa Fluor® 488 and MitoTracker® orange in confocal immunofluorescence.

| Transgenic cell lines | Percentage colocalization (mean ± SD) | No. of cells analyzed |
|---|---|---|
| *GmPAP3** transgenic line # 43 | 23± 7% | 22 |
| *GmPAP3** transgenic line # 76 | 24 ± 10% | 15 |
| *GmPAP3* transgenic line #1 | 70 ± 5 % | 10 |
| *GmPAP3* transgenic line #8 | 74 ± 10% | 11 |

Subcellular localization of GmPAP3 was studied by confocal immunofluorescence localization. Alexa Fluor® 488 conjugated secondary antibody was used to labeled the GmPAP3 protein. MitoTracker® orange is a fluorescence dye which specifically labels mitochondria in cells. Quantification of the extent of colocalization for the signal of Alexa Fluor® 488 and MitoTracker® orange was performed from one direction only (i.e. it ask how much of the signal of Alexa Fluor® 488 colocalize with the signal of MitoTracker® orange, not the other way round.) as described in the Materials and Methods section. Percent colocalization is expressed as the mean ± standard deviation (SD) for the number of cells analyzed.

### 3.4.4 Effect of expressing the truncated *GmPAP3* on mitochondria integrity in BY-2 cells under NaCl and osmotic treatments

To test the effect of expressing the truncated *GmPAP3* in BY-2 cells under NaCl and osmotic stress, the *GmPAP3** and *GmPAP3* transgenic lines were subjected to NaCl and osmotic stresses and the percentage of cells with intact mitochondria (indicate by Rh123) was used as a parameter for ROS-induced mitochondria damage. As shown in Fig. 18 and Table 18, Under NaCl and PEG treatment, both *GmPAP3** cell lines used in this experiment showed diffuse Rh123 signals (e, h and f, i), similar to the wild type cells (b, c); while the *GmPAP3* (full length) cell lines exhibited a clear protective effect (with discrete Rh123 signals). This result suggests that the mitochondrial location is necessary for the protective function of *GmPAP3* under NaCl and osmotic stress. This experiment was repeated three times and the quantitative results were shown in Table 17.

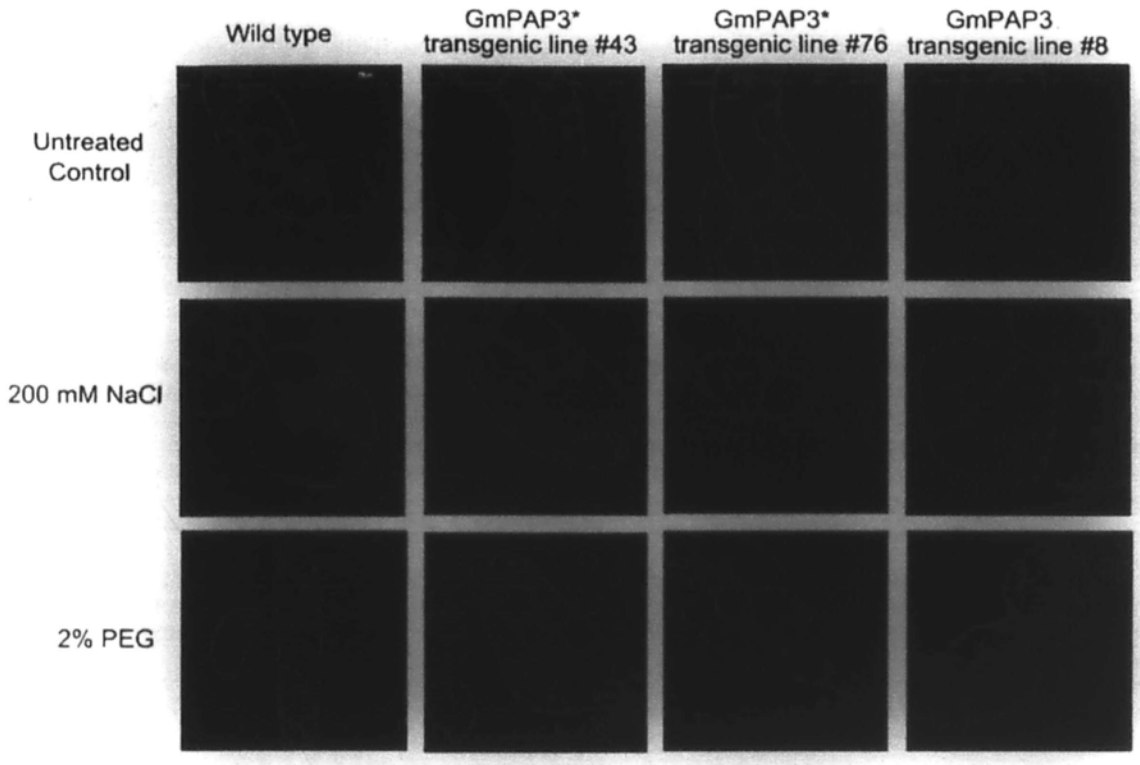


**Fig. 18**. Mitochondrial integrity under salinity and osmotic stresses of *GmPAP3** and *GmPAP3* transgenic cell lines. Wild type (WT) BY-2 cells (**a-c**) and *GmPAP3* (truncated and full length) transgenic BY-2 cell lines (**d-f**, **g-i** & **j-l**, respectively) were pre-treated in a cell culture medium without stress (**a**, **d**, **g**, **j**), with 200 mM NaCl (**b**, **e**, **h**, **k**), or with 2 % PEG for 1 h (**c**, **f**, **i**, **l**) before staining with 10 μg/mL Rh123 for another hour. The signal of Rh123 was observed using a confocal laser scanning microscope. Ten to 25 cells were counted for each line. Scale bar = 20 μm. Quantitative analysis was shown in Table 18.

**Table 17.** Quantitative analysis on the effects of salinity and osmotic stresses on mitochondria integrity.

| **Cell lines** | **% cells with intact mitochondria** | | |
|---|---|---|---|
| | **Control** | **NaCl** | **PEG** |
| Wild type BY-2 | $94 \pm 10^{a}$ | $31 \pm 3^{b}$ | $34 \pm 5^{b}$ |
| *GmPAP3** transgenic cell line #43 | $94 \pm 5^{a}$ | $38 \pm 3^{b}$ | $38 \pm 6^{b}$ |
| *GmPAP3** transgenic cell line #76 | $91 \pm 4^{a}$ | $38 \pm 3^{b}$ | $45 \pm 7^{b}$ |
| *GmPAP3* transgenic line #8 | $98 \pm 4^{a}$ | $76 \pm 5^{c}$ | $73 \pm 4^{c}$ |

Experimental details were given in Fig. 18. Quantitation for the percentage of cells with intact mitochondria was estimated by the uptake of the fluorescent dye Rh123. The percentage was presented as the mean value of 3 experiments (10-25 cells for each sample) ± SD. $^{a}$, $^{b}$, and $^{c}$ represent groups that exhibited statistically different ($p<0.01$) mean values based on one-way ANOVA followed by the Tukey posthoc test.

### 3.4.5 Effect of expressing of truncated *GmPAP3* on ROS production in BY-2 cells under NaCl and osmotic treatments

Since the *GmPAP3** cell lines show a loss of protective effect under NaCl and osmotic stresses and such protection are tightly linked to the formation and scavenging of ROS, we monitored the accumulation of cellular hydrogen peroxide (using $H_2$DCFDA as an indicator) in both *GmPAP3** and *GmPAP3* cell lines under NaCl and osmotic stress treatments. The level of hydrogen peroxide under both stress conditions was lowered in the *GmPAP3* transgenic cell lines (Figs. 19k and 19l) but not in the G*mPAP3** transgenic cell lines (Figs. 19e and 19f; and 19h and 19i). Statistical analysis of the signal intensity of $H_2$DCFDA indicated that the fluorescence intensity of $H_2$DCFDA in *GmPAP3** transgenic cell lines showed no difference when compare to the wild type cells under both stress treatment. This result showed that when the GmPAP3 protein is not localized in mitochondria, it failed to lower the ROS content in plant cells under NaCl and osmotic stresses, leading to the loss of protective effect (Fig. 19 and Table 18). This experiment was repeated 3 times and the quantitative result was shown in Table 18.

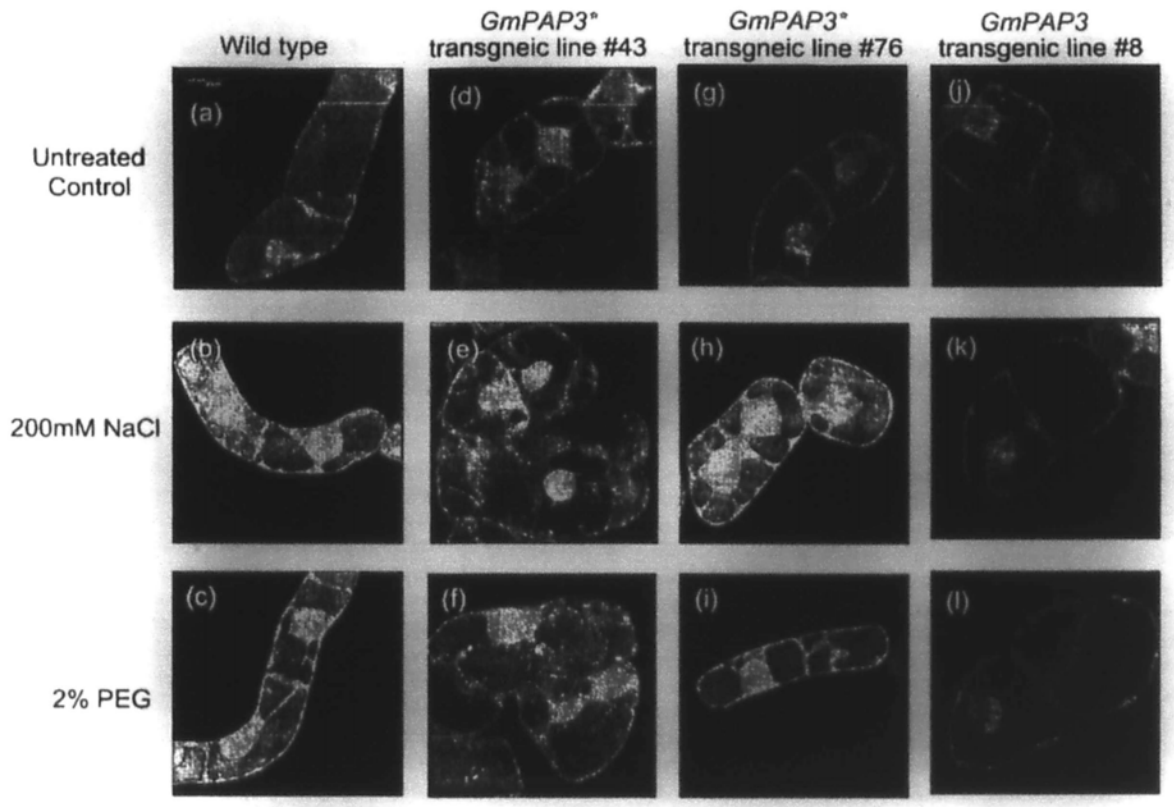


**Fig. 19.** Cellular ROS production under salinity and osmotic stresses in *GmPAP3** and *GmPAP3* transgenic cell lines. Wild type BY-2 cells (**a-c**) and *GmPAP3* (truncated and full length) transgenic BY-2 cell lines (**d-f, f-I** & **j-l**) were pre-stained with $H_2$DCFDA for 30 min before placed in a cell culture medium without stress (**a,d, g, j**), with 200 mM NaCl (**b, e, h, k**), or with 2 % PEG for 1 h (**c, f, i, l**). The signals of $H_2$DCFDA were observed using a confocal laser scanning microscope. Ten to 20 cells were counted for each line. Scale bar = 20 μm. Quantitative analysis was shown in Table 18.

**Table 18.** Quantitative analysis on the effects of salinity and osmotic stresses on ROS accumulation

| **Cell lines** | **Signal intensity of $H_2$DCFDA (pixel per $cm^2$)** | | |
|---|---|---|---|
| | **Untreated** | **200 mM NaCl** | **2 % PEG** |
| Wild type BY-2 | 212 ± 87 [a] | 769 ± 31 [b] | 789 ± 14 [b] |
| *GmPAP3** transgenic cell line 43 | 241± 83 [a] | 795 ± 6 [b] | 788 ± 22 [b] |
| *GmPAP3** transgenic cell line 76 | 272 ± 74 [a] | 794 ± 17 [b] | 785 ± 32 [b] |
| *GmPAP3* transgenic cell line 8 | 180 ± 79 [a] | 253 ± 78 [c] | 226 ± 72 [c] |

Experimental details were given in Fig. 19. Numerical data represents the mean value of 10-20 cells ± SD. [a], [b], and [c] represent groups that exhibited statistically different ($p<0.01$) mean values based on one-way ANOVA followed by the Tukey posthoc test.

### 3.5 Ecotopic Expression of *GmPAP3* in Transgenic *Arabidopsis thaliana* Alleviated Salinity, Osmotic, and Oxidative Stresses *In Planta*

The above studies demonstrated the function of GmPAP3 at the cellular level. Subsequently, we examined if ectopic expression of *GmPAP3* can also alleviate salinity, osmotic, and oxidative stresses *in planta*. *GmPAP3* was transformed into *A. thaliana* and expressed constitutively (see Materials and Methods). The fresh weight and the percentage of root elongation after treatment with NaCl, PEG, or PQ was used as a physiological parameter to measure stress-induced growth inhibition. The fresh weight of the *GmPAP3* transgenic seedlings is significantly higher under NaCl, PEG and PQ treatments than that of the wild type and vector only seedlings (Table 19). The percentage root elongation of the *GmPAP3* transgenic seedlings is also significantly higher under all stress conditions, compared to the untransformed wild type Col-0 and the transgenic seedlings containing an empty vector (Figs. 20a, 20b, and 20c). The percentage root elongation of *GmPAP3* transgenic seedlings was significantly higher.

Furthermore, the degree of lipid peroxidation induced by PQ was also measured as a biochemical parameter to indicate the extent of oxidative damage (Shalata & Neumann, 2001). The enhancement of oxidative tolerance in *A. thaliana* by ectopic expression of *GmPAP3* was demonstrated by a reduction of PQ-induced lipid peroxidation in young seedlings (Fig. 21).

**Table 19.** Effects of salinity, osmotic, and oxidative stresses on fresh weight of transgenic *A. thaliana* expressing *GmPAP3*.

| **Treatment** | **Fresh weight (mg)** | | | |
|---|---|---|---|---|
| | **Col-0** | **Empty vector control** | **F42** | **C25** |
| Untreated | 6.2 ± 0.36 | 6.1 ± 0.056 | 6.6 ± 0.37 | 6.5 ± 0.48 |
| NaCl treatment | 3.4 ± 0.027 | 3.5 ± 0.13 | 3.8 ± 0.064* | 3.9 ± 0.19* |
| | **Col-0** | **Empty vector control** | **F42** | **C25** |
| Untreated | 6.8 ± 0.13 | 6.7 ± 0.72 | 6.9 ± 0.58 | 6.7 ± 0.49 |
| PEG treatment | 3.8 ± 0.086 | 3.9 ± 0.41 | 4.4 ± 0.22* | 4.2 ± 0.074* |
| | **Col-0** | **Empty vector control** | **F42** | **C25** |
| Untreated | 6.1 ± 0.44 | 6.2 ± 0.098 | 6.7 ± 0.42 | 6.2 ± 0.30 |
| PQ treatment | 4.3 ± 0.079 | 3.4 ± 0.19 | 5.0 ± 0.21* | 5.0 ± 0.109* |

The seedlings samples described in Fig. 20 were collected. Since the fresh weight of individual seedlings was too small for accurate measurement, mean fresh weight of 12 randomly pooled seedlings was used. Each numerical data in the table represents the mean value from four sets of pooled samples ± standard deviation. *: statistically different ($p<0.05$) from the wild type Col-0 under the same treatment, based on one-way ANOVA followed by the Tukey posthoc test.

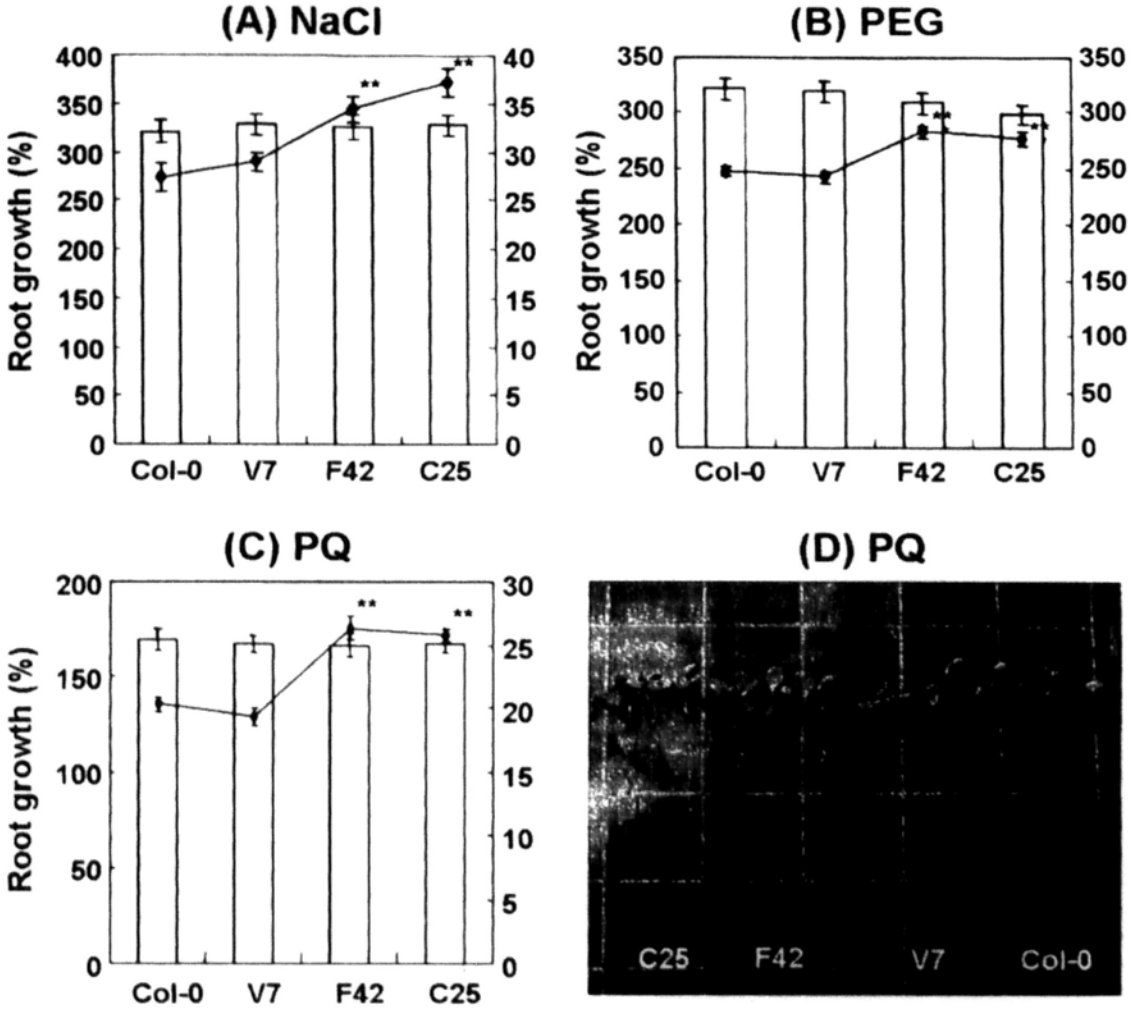


**Fig. 20.** Effects of salinity, osmotic, and oxidative stresses on root elongation. The percentage of root elongation after treated with 150 mM NaCl (**a**), 15 % PEG (**b**), and 1 M PQ (**c**) was compared among the wild type Col-0, the empty vector transgenic control (V7) and two independent *GmPAP3* transgenic lines (F42 and C25). Y-axis on the left and right of each graph indicated the percentage root elongation of untreated (bar) and stressed (line) seedlings, respectively. The percentage root elongation was calculated as follow: the root length after treatment minus root length before treatment divided by root length before treatment. Error bar: standard error. N=48. Data obtained were analyzed by one-way analysis of variance (one-way ANOVA) followed by the Tukey test. ** indicates that the mean difference (compared to wild type) is significant at $p<0.01$ level.

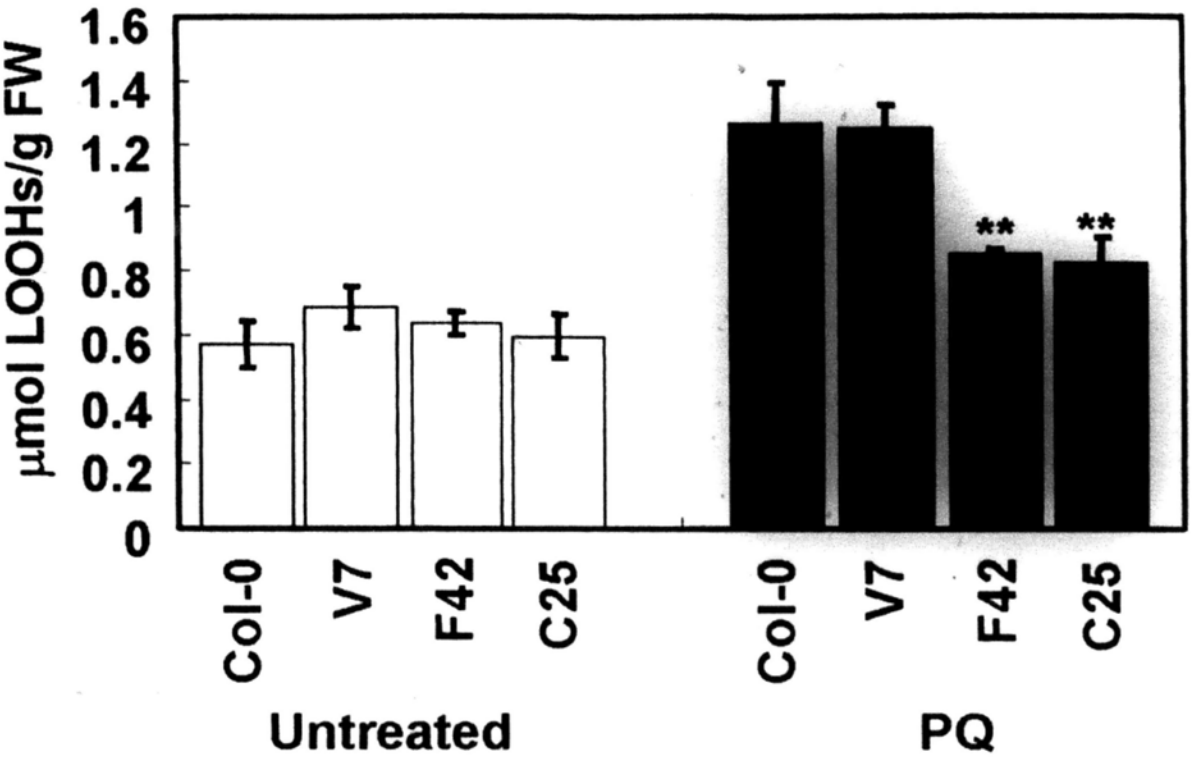


**Fig. 21.** Lipid peroxidation in Arabidopsis seedlings under oxidative stress. Seedlings were grown and treated with PQ as described in Fig. 20. The reactivity of 18:2-derived lipid hydroperoxides (LOOHs) levels were expressed in µmole LOOHs per g fresh weight (FW). Error bar: standard error. N=4 (four sets of 12 seedlings for each data point). Data obtained was analyzed by one-way ANOVA test followed by the Tukey test. ** indicates that the mean difference (compared to wild type) is significant at $p<0.01$ level. Open and close bars indicate untreated control and treated samples, respectively.

## Chapter 4 Discussion

### 4.1 Subcellular localization of GmPAP3

Previous Confocal microscopic studies showed that 60-70 % of the proteins were localized in mitochondria (Fig.4 and table 4, Section 1.6). In this study, the subcelllular localization of GmPAP3 is verified by both western blot analysis of mitochondrial enriched protein fraction as well as ImmunoGold electromicroscopy. Both results show that GmPAP3 is localized in the mitochondria (Fig. 6). In confocal microscopy studies, permeabilization is required to expose the epitope for immunolabeling but this step will lead to loss of structural integrity. A compromised condition may result in some inefficiency during permeabilization. The reported percentage of co-localization will be reduced in case not all the cells can effectively uptake either the fluorophore-conjugated secondary antibody or the dye MitoTracker®.

In plants, both salinity and osmotic challenges are able to induce ROS production in cellular compartments (Smirnoff, 1998; Bartels, 2001; Apel & Hirt, 2004). To prevent further damages to essential cellular components, the excessively produced ROS molecules should scavenged at the site of production such as mitochondria (Sweetlove *et al.*, 2002; Noctor *et al.*, 2007). The mitochondrial

localization of GmPAP3 suggested that it may take a role in ROS scavenging during abiotic stress, whilst excessive ROS accumulation occurred in mitochondria (Bartoli *et al.*, 2004; Noctor *et al.*, 2007).

The activities and gene expression of most plant PAPs were frequently found to be phosphorus (P) regulated (induced under P starvation) (Cashikar *et al.*, 1997; del Pozo *et al.*, 1999; Li *et al.*, 2002), consistent with their roles in P metabolism. However, a systematic study of the *PAP* gene family in *Arabidopsis thaliana* showed that some of the gene members are irresponsive to P status (Li *et al.*, 2002), suggesting that some members may be involved in other physiological functions. To the best of our literature search, we are not aware of any other mitochondrial localized plant PAPs. For instance, Arabidopsis PAPs were encoded by a gene family (29 members). However, none of them has a predicted mitochondrial transit peptide. However, we cannot rule out the possible existence of mitochondrial located PAPs in *A. thaliana* without experimental verification. Some PAPs do possess signal peptides but they do not share significant homology to the putative mitochondrial transit peptide of GmPAP3. Thus GmPAP3 is a novel purple acid phosphatase which possesses a mitochondrial transit peptide and this is a first report of a mitochondrial localized purple acid phosphatase.

**4.2 Ectopic expression of *GmPAP3* in tobacco BY-2 cells can alleviates NaCl and osmotic stress**

In plants, mitochondria are the major sites for ROS production (Moller, 2001) as well as main targets of ROS attack under abiotic stress (Bartoli *et al.*, 2004; Taylor *et al.*, 2004). Since we have show that the majority of GmPAP3 were located in mitochondria (Fig.6), and the expression level of *GmPAP3* is elevated when under salt, osmotic and oxidative stress (Fig.3), it is very likely that the function of GmPAP3 might related to plant adaptation to salt and osmotic stresses, most probably by involve in ROS scavenging or forming in the mitochondria.

ROS can cause the collapse of mitochondrial membrane potential (Pastore *et al.*, 2002) and this explains the dramatic and rapid (within 1 h after treatment) decrease in the uptake of Rh123 by mitochondria when the BY-2 cells were subjected to salinity and osmotic stresses (Figs. 7b and 7c; Table 10). Under prolonged (24 h) stress treatments, a significant portion of the BY-2 cells did not survive (Figs. 8b and 8c; Table 11). The loss of mitochondrial activity and cell death occurred in parallel to an accumulation of cellular ROS (Fig. 9; Table 12).

Under stress conditions, treatment with the antioxidant ascorbic acid led to an unambiguous effect on maintaining both mitochondrial activities and cell viability (Figs. 7e & 7f and 8e & 8f; Tables 10 and 11) and caused a reduction in ROS

accumulation (Figs. 9e & 9f; Table 12). These results strongly support the notion that the detrimental effects of salinity and osmotic stresses can be alleviated by ROS scavenging activities. Expression of *GmPAP3* (which encodes a PAP protein) mimicked all the protective effects (Figs. 7, 8 and 9; Tables 10, 11 and 12) exhibited by ascorbic acid, suggesting that the GmPAP3 protein may play a significant physiological role in ROS scavenging.

### 4.3 The Ferric center is essential for the function of GmPAP3

All Purple acid phosphatases contain a binuclear metal center. The binuclear metal center is believed to be involved in hydrophilic attack of phosphate group during hydrolysis of phosphomonoesters (Klabunde *et al.*, 1996; Olczak *et al.*, 2003). In mammalian PAPs, the presence of a Fe(III)-Fe(II) di-iron binuclear center has been shown to endow theses proteins ROS scavenging as well as ROS-producing activities through Fenton's type reaction (Hayman & Cox, 1994; Kaija *et al.*, 2002). In plant PAPs, the binuclear metal center is essential for their redox activities (Klabunde *et al.*, 1995; Klabunde *et al.*, 1996). One metal ion involved is Fe(III) (Klabunde *et al.*, 1995; Schenk *et al.*, 1999). In the presence of ferric chelator, the ROS scavenging effects due to the expression of *GmPAP3* were diminished (Table 14), indicating that redox reactions of GmPAP3 may be involved in the ROS scavenging activities. At this point, we cannot conclude whether GmPAP3 acts directly on ROS or via other Redox intermediates. The question whether GmPAP3 proteins can directly react with ROS through the Fenton's type reaction should be addressed in future studies.

## 4.4 The mitochondria localization is essential for the protective function of GmPAP3

Mitochondria, as one of the main targets of ROS attack under abiotic stress are also the front line of defense for excessive ROS accumulation (Mittova *et al.*, 2003; Taylor *et al.*, 2004; Noctor *et al.*, 2007). To prevent damages to essential cellular components, which will eventually lead to cell death, most ROS molecules are scavenged at the site of production such as mitochondria (Sweetlove *et al.*, 2002; Noctor *et al.*, 2007; Schwarzländer *et al.*, 2009). By immunodetection, confocal microscopy and electromicroscopy we have proved that a major portion of GmPAP3 is localized in the mitochondria (Fig. 4, table 4; and Fig. 6). In this work, we also show that ectopic expression of this mitochondrial localized GmPAP3 can alleviate salt and osmotic stress (Fig. 7, table 10 and Fig. 8, table 11) by lower excessive accumulation of ROS (Fig. 9, table 12). These evidences suggest that the mitochondria localization is necessary for the protective function of GmPAP3. Therefore we further tested if the protective effect exerts by GmPAP3 under NaCl and osmotic stress will loss if it is not targeted to mitochondria. Transgenic cell lines expressing *GmPAP3* with the mitochondrial transit peptide removed (GmPAP3*) were successfully established (Fig. 14 and 15). By using western blot analysis, immunolabeling and confocal microscopy, the GmPAP3* were not

targeted to the mitochondria (Fig. 16 and Fig. 17). The *GmPAP3** transgenic cell lines behave as wild type cell lines when under NaCl and osmotic stress (Fig. 18 and Fig. 19). For both mitochondria integrity and ROS accumulation level, the GmPAP3* transgenic cell lines show no significant different when compare to the wild type cell lines under NaCl and osmotic stress (Table 17 and Table 18). These experimental evidences suggested that the mitochondria location is essential for the protective effect of GmPAP3 under NaCl and osmotic stress. As mitochondria is the front line of defense for ROS accumulation when under stress (Noctor *et al.*, 2007; Schwarzländer *et al.*, 2009), GmPAP3 may be required to targeted to the mitochondria to deal with the excessively accumulated ROS at first hand.

### 4.5 Ectopic expression of *GmPAP3* can alleviate NaCl, osmotic, and oxidative stress in *in planta* system as well

The protection effects of GmPAP3 were also demonstrated *in planta*. Using fresh weight and percentage root elongation as a measuring parameter, transgenic *A. thaliana* expressing *GmPAP3* exhibited an overall better growth performance towards NaCl, PEG, and PQ treatments (Table 19 and Fig. 20). The protective effects conferred by *GmPAP3* are probably related to alleviation of oxidative damage since PQ-induced lipid peroxidation was significantly reduced in transgenic lines (Fig. 21).

Salinity and osmotic stresses are two major environmental constrains to plant growth. However, it should be noted that salinity stress and osmotic stress are sometimes difficult to distinguish. While experiments using PEG treatment can uncouple osmotic stress from salinity stress, NaCl treatment may lead to both salinity and/or osmotic stress. Nonetheless, GmPAP3 transgenic lines show an overall better growth performance (Fig. 7, 8 & 20), and a lower ROS accumulation (Fig. 9), or less oxidative damage under both NaCl treatment and PEG treatment (Fig. 21). These results indicate that GmPAP3 can protect the cells indiscriminantly from both NaCl and osmotic stress.

### 4.6 Future perspectives

In this studies, using cellular model and *in planta* model, we have provide evidences which demonstrate the identification of a mitochondrial located PAP that can alleviate salinity and osmotic stresses by reducing the accumulation of ROS; and the mitochondrial localization is essential for the protective function of this GmPAP3. By means of chemical blocker, we have also provided evidences that redox reactions may be involved in the ROS scavenging activities. Yet at this point, we cannot prematurely concluded that GmPAP3 acts directly on ROS. The question whether GmPAP3 proteins can directly react with ROS through the Fenton's type reaction remains to be addressed biochemically in future studies.

On the other hand, as every purple acid phosphatase contain a binuclear metal center (Olczak *et al.*, 2003). And if the Ferric center is the active center responsible for Fenton reactions for ROS scavenging, it will be interesting to see will there be any protective effect occurred if any other purple acid phosphatases are being targeted to the mitochondria. Such evidences will be phenomenal for demonstrating the importance of subcellular localization to the physiological function of a ROS scavenger.

## Chapter 5 Conclusion

Abiotic stresses, by upsetting cellular homeostasis of ROS formation and scavenging, will cause oxidative stress. To survive, plants have evolves several mechanisms to scavenge the excessively accumulated ROS at the site of production. (Smirnoff, 1998; Bartels & Sunkar, 2005.; Miller *et al.*, 2008)

By using Suppression subtractive hybridization techniques, GmPAP3 was identified as a salt-inducible gene candidates from soybean. The inducibility of the *GmPAP3* gene expression by salinity, osmotic, and oxidative stresses; and the predicted mitochondrial localization of GmPAP3 prompt us to further investigate the possible physiological roles of *GmPAP3* under oxidative stress.

In this work, in order to understand the cellular functions of the GmPAP3 protein, we used gain-of-function approach in transgenic BY-2 cells to show that ectopic expression of *GmPAP3* can partially alleviate oxidative damages caused by salinity and osmotic stresses, probably via ROS scavenging. *In planta* experiments using transgenic *A. thaliana* provided further supportive evidences. We have also provide evidences which suggest that redox reactions of GmPAP3 may be involved in the ROS scavenging activities. In addition, we have successfully established transgenic cell lines which ectopically express a truncated GmPAP3 which have its

mitochondrial peptide removed. The truncated GmPAP3 are not targeted to mitochondria and shown no protective effect towards both NaCl and osmotic stress. These evidences suggest that the mitochondrial localization is essential for the protective function of GmPAP3.

In summary, this work provides evidence to demonstrate the identification of a mitochondrial located PAP that can alleviate salinity and osmotic stresses by reducing the accumulation of ROS, and the mitochondrial location is essential for the protective function.

## References


**An G. 1985.** High efficiency transformation of cultured tobacco cells. *Plant Physiology* **79**: 568-570.

**Ananyev G, Renger G, WackerU., Klimov V. 1994.** The photoproduction of superoxide radicals and the superoxide dismutase activity of Photosystem II. The possible involvement of cytochrome b559 *Photosynthesis Research* **41**: 327-338.

**Apel K, Hirt H. 2004.** Reactive oxygen species: Metabolism, oxidative stress and signal transduction. . *Annual Review of Plant Biology* **55**: 373-399.

**Asada K. 1994.** *Production and action of active oxygen species in photosynthetic tissues.* . Fla.: CRC: Boca Raton.

**Asada K. 2006.** Production and scavenging of reactive oxygen species in chloroplasts and their functions. *Plant Physiology* **141**: 391-396.

**Attia H, Arnaud N, Karray N, Lachaal M. 2008.** Long-term effects of mild salt stress on growth, ion accumulation and superoxide dismutase expression of Arabidopsis rosette leaves. *Physiologia Plantarum* **132**: 293-305.

**Ausubel FM, Brent R, Kingston RE, Moore DD, Seidman JG, Smith JA, Struhl K. 1995.** *Phenol/SDS method for plant RNA preparation.* New York: John Wiley & Sons, Inc.

**Badawi GH, Kawano N, Yamauchi Y, Shimada E, Sasaki R, Kubo A, Tanaka K. 2004.** Over-expression of ascorbate peroxidase in tobacco chloroplasts enhances the tolerance to salt stress and water deficit. *Physiologia Plantarum* **121**: 231-238.

**Bannister JV, Bannister WH, Rotilio G. 1987.** Aspects of the structure, function and applications of superoxide dismutase. *CRC Crit. Rev. Biochem.* **22**: 111-180.

**Banu MNA, Hoque MA, Watanabe-Sugimoto M, Matsuoka K, Nakamura Y, Shimoishi Y, Murata Y. 2008.** Proline and glycine betaine induce antioxidant defense gene expression and suppress cell death in cultured tobacco cells under salt stress. *Journal of Plant Physiology* **166**: 146-156.

**Bartels D. 2001.** Targeting detoxification pathways: An efficient approach to obtain plants with multiple stress tolerance? *Trends in Plant Sciences* **6**: 284-286.

**Bartels D, Sunkar R. 2005.** Drought and salt tolerance in plants. *Critical Review in Plant Sciences* **24**: 23-58.

**Bartoli CG, Gomez F, Martinez DE, Guiamet JJ. 2004.** Mitochondria are the main target for oxidative damage in leaves of wheat (Triticum aestivum L.). *Journal of Experimental Botany* **55**: 1663-1669.

**Bhattacharjee S. 2005.** Reactive oxygen species and oxidative burst: Roles in stress, senescence and signal transduction in plants. *Current Science* **89**: 1113-1121.

**Bozzo GG, Raghothama KG, Plaxton WC. 2002.** Purification and characterization of two secreted purple acid phosphatase isozymes from phosphate-starved tomato (*Lycopersicon esculentum*) cell cultures. *Eur. J. Biochem.* **269**: 6278-6286.

**Bozzo GG, Raghothama KG, Plaxton WC. 2004.** Structural and kinetic properties of a novel purple acid phosphatase from phosphate-starved tomato (Lycopersicon esculentum) cell cultures. *Biochemical Journal* **377**: 419-428.

**Brears T, Liu C, Knight TJ, Coruzzi GM. 1993a.** Ectopic overexpression of asparagine synthetase in transgenic tobacco. *Plant Physiology* **103**: 1285-1290.

**Brears T, Liu C, Knight TJ, Coruzzi GM. 1993b.** Ectopic overexpression of asparagines synthetase in transgenic tobacco. *Plant Physiology* **103**: 1285-1290.

**Buchanan BB, Gruissem W, Jones RL. 2000.** *Biochemistry and molecular biology of plants*. Rockville, Maryland: American society of plant physiologists.

**Buhi WC, Ducsay CA, Bazer FW, Roberts RM. 1982.** Iron transfer between the purple phosphatase uteroferrin and transferrin and its possible role in iron metabolism of the fetal pig. *J Biol Chem.* **257**: 1712-1713.

**Burton GWJ, A. , Ingold KU. 1982.** First proof that vitamin E is major lipid-soluble, chain-breaking antioxidant in human blood plasma. *Lancet* **2**: 327.

**Cashikar AG, Kumaresan R, Rao NM. 1997.** Biochemical characterization and subcellular localization of the red kidney bean purple acid phosphatase. . *Plant Physiology* **114**: 907-915.

**Chaves MM, Oliveira MM. 2004.** Mechanisms underlying plant resilience to water deficit: Prospects for water-saving agriculture. *Journal of Experimental Botany* **55**: 2365-2384.

**Chew O, Whelan J, Millar AH. 2003.** Molecular definition of the ascorbate-glutathione cycle in Arabidopsis mitochondria reveals dual targeting of antioxidant defenses of plants. *J. Biol. Chem.* **278**: 46869-46877.

**del Pozo JC, Allona I, Rubio V, Leyva A, Pena ADL, Aragoncillo C, Paz-Ares J. 1999.** A type 5 acid phosphatase gene from Arabidopsis thaliana is induced by phosphate starvation and by some other types of phosphate mobilising/oxidative stress conditions. *The Plant Journal* **19**: 579-589.

**DeLong JM, Prange RK, Hodges DM, Forney CF, Bishop MC, Quilliam M. 2002.** Using a modified ferrous oxidation xylenol orange (FOX) assay for detection of lipid hydroperoxides in plant tissue. *Journal of Agriculture and Food Chemistry* **50**: 248-254.

**Douce R, Bourguignon J, Brouquisse R, Neuburger M. 1987.** Isolation of plant mitochondria: General principles and criteria of integrity. *Methods in*

*Enzymology* **148**: 403-415.

**Dower WJ, Chassy BM, Trevors JT, Blaschek HP. 1992.** *Protocols for the transformation of bacteria by electroporation. Guide to electroporation and electrofusion*. San Diego: Academic Press.

**Doyle JJ, Doyle JL. 1987.** A rapid DNA isolation procedure for small quantities of fresh leaf tissue. *Phytochem. Bull.* **19**: 11-15.

**Duff SMG, Sarath Ga, Plaxton WC. 1994.** The role of acid phosphatase in plant phosphorus metabolism. *Physiologia Plantarum* **90**: 791-800.

**Elthon TE, McIntosh L. 1987.** Identification of the alternative terminal oxidase of higher plant mitochondria. *Proc. Natl. Acad. Sci. USA* **84**: 8399-8403.

**Fath A, Bethke PC, Belligni MV, Spiegel YNa, Jones RL. 2001.** Signalling in the cereal aleurone: hormones, reactive oxygen and cell death. *New Phytologist* **151**: 99-107.

**Fedoroff N. 2006.** Redox Regulatory Mechanisms in Cellular Stress Responses *Annals of Botany* **98**: 289-300.

**Foyer CH, Halliwell B. 1976.** The presence of glutathione and glutathione reductase in chloroplasts: a proposed role in ascorbic acid metabolism. *Planta* **133**: 21-25.

**Foyer CH, Harbinson JC, eds. CH Foyer, PM Mullineaux. 1-42. Boca Raton, Fla.: CRC. 1994.** *Oxygen metabolism and the regulation of photosynthetic electron transport.* Fla.: CRC: Boca Raton.

**Foyer CH, Lelandais M, Kunert KJ. 1994.** Photooxidative stress in plants. *Physiologia Plantarum* **92**: 696-717.

**Gomez J, Hernandez J, Jimenza A, del Rio L, Sevilla F. 1999.** Differential response of antioxidative enzymes of chloroplasts and mitochondria to long-term NaCl stress of pea plants. *Free Radical Research* **31**: S11-18.

**Gossett DR, Banks SW, Millhollon EP, Lucas MC. 1996.** Antioxidant response to NaCl stress in a control and an NaCl-tolerant cotton cell line grown in the presence of paraquat, buthionine sulfoximine, and exogenous glutathione. . *Plant Physiology* **112**: 803-809.

**Hayman AR, Bune AJ, Bradley JR, Rashbass J, Cox TM. 2000.** Osteoclastic tartrate-resistant acid phosphatase (Acp 5): its localizationto dendritic cells and diverse murine tissues. *J. Histochem Cytochem.* **48**: 219-228.

**Hayman AR, Cox TM. 1994.** Purple acid phosphatase of the human macrophage and osteoclast. *Journal of Biological Chemistry* **269**: 1294-1300.

**Hayman AR, Jones SJ, Boyde A, Foster D, Colledge WH, Carlton MB, Evans MJ, Cox TM. 1996.** Mice lacking tartate-resistant acid phosphatase (Acp5) have disrupted endohondral ossification and mild osteoporosis. *Development* **122**: 3151-3162.

**Hernandez JA, Corpas FJ, Gomez M, del Rio LA, Sevilla F. 1993.** Salt-induced oxidative stress mediated by activated oxygen species in pea leaf mitochondria. . *Physiologia Plantarum* **89**: 103-110.

**Hernandez JA, Olmos E, Corpas FJ, Sevilla F, del-Rio LA. 1995.** Salt-induced oxidative stress in chloroplasts of pea plants. *Plant Sciences* **105**: 151-167.

**Hoekema A, Hirsch PR, Hooykaas PJJ, Schilperoort RA. 1983.** A binary plant vector strategy based on separation of vir- and T-region of the Agrobacterium tumefaciens Ti-plasmid. *Nature* **303**: 179-180.

**Hou BH, Lin CG. 1996.** Rapid optimization of electroporation conditions for soybean and tomato suspension cultured cells. *Plant Physiology* **111**: 166.

**Jiang L, Rogers JC. 1998.** Integral membrane protein sorting to vacuoles in plant cells: Evidence for two pathways. *Journal of Cell Biology* **143**: 1183-1199.

**Jimenez A, Hernandez JA, del Rio LA, Sevilla F. 1997.** Evidence for the presence

of the ascorbate-glutathione cycle in mitochondria and peroxisomes of pea leaves. *Plant Physiology* **114**: 275-284.

**Kaija H, Alatalo SL, Halleen JM, Lindqvist Y, Schneider G, Vaananen HK, Vihko P. 2002.** Phosphatase and oxygen radical-generating activities of mammalian purple acid phosphatase are functionally independent. *Biochemical and Biophysical Research Communications* **292**: 128-132.

**Kanematsu S, Asada KPCP-. 1990.** Characteristic amino acid sequences of chloroplast and cytosol isozymes of Cu, Zn superoxide dismutase in spinach, rice and horsetail. *Plant and Cell Physiology* **31**: 99-112.

**Kasai H, Crain PF, Kuchino Y, Nishimura S, Ootsuyama A, Tanooka H. 1986.** Formation of 8-hydroxyguanine moiety in cellular DNA by agents producing oxygen radicals and evidence for its repair. *Carcinogenesis* 7: 1849-1851.

**Klabunde T, Strater N, Krebs B, Witzel H. 1995.** Structural relationship between the mammalian Fe(III)-Fe(II) and Fe(III)-Zn(II) plant purple acid phosphatases. *FEBS Letters* **367**: 56-60.

**Klabunde T, Strater N, Witzel H, Frohlich R, Krebs B. 1996.** Mechanism of Fe(III)-Zn(II) purple acid phosphatases based on crystal structures. *Journal of Molecular Biology* **259**: 737-748.

**Kranner I, Beckett RP, Wornik S, Zorn M, Pfeifhofer HW. 2002.** Revival of a resurrection plant correlates with its antioxidant status. *The Plant Journal* **31**: 13-24.

**Kwiatowski J, Safianowska A, Kaniuga Z. 1985.** Isolation and characterization of an iron-containing superoxide dismutase from tomato leaves, Lycopersicon esculentum. *Eur. J. Biochem.* **146**: 459-466.

**Laemmli UK. 1970.** Cleavage of structural proteins during the assembly of the head of bacteriophage T4. *Nature* **227**: 680-685.

**Law MY, Charles SA, Halliwell B. 1983.** Glutathione and ascorbic acid in spinach (Spinacea oleracea) chloroplasts. *Biochem. J.* **210**: 899-903.

**LeBel CP, Ischiropoupos H, Bondy SCCRT-. 1992.** Evaluation of the probe 2',7'-dichlorofluorescein as an indicator of reactive oxygen species formation and oxidative stress. *Chem. Res. Toxic.* **5**: 227-231.

**Li D, Zhu H, Liu K, Liu X, Leggewie G, Udvardi M, Wang D. 2002.** Purple acid phosphatases of Arabidopsis thaliana. *Journal of Biological Chemistry* **277**: 27772-27781.

**Li W-YF, Shao G, Lam H-M. 2008.** Ectopic expression of GmPAP3 alleviates oxidative damage caused by salinity and osmotic stresses. *New Phytologist* **178**: 80-91.

**Liao H, Wong F-L, Phang T-H, Cheung M-Y, Li W-YF, Shao G-H, Yan X-L, Lam H-M. 2003.** GmPAP3, a novel purple acid phosphatase-like gene in soybean induced by NaCl stress but not phosphorus deficiency. *Gene* **318**: 103-111.

**Mahalingam R, Fedoroff N. 2003.** Stress response, cell death and signalling: the many faces of reactive

oxygen species. *Physiologia Plantarum* **119**: 56-68.

**Maxwell DP, Wang Y, McIntosh L. 1999.** The alternative oxidase lowers mitochondrial reactive oxygen production in plant cells. *Proceedings of the National Academy of Sciences, USA* **96**: 8271-8276.

**Miller G, Shulaevb V, Mittler R. 2008.** Reactive oxygen signaling and abiotic stress. *Physiologia Plantarum* **133**: 481-489.

**Mittler R. 2002.** Oxidative stress, antioxidants and stress tolerance. *Trends in Plant Sciences* **7**: 405-410.

**Mittler R, Vanderauwera S, Gollery M, Van Breusegem F. 2004.** The reactive oxygen gene network of plants. *Trends in Plant Sciences* **9**: 490-498.

**Mittova V, Guy M, Tal M, Volokita M-. 2004.** Salinity up-regulates the antioxidative system in root mitochondria and peroxisomes of the wild salt-tolerant tomato species Lycopersicon pennellii. *Journal of Experimental Botany* **55**: 1105-1113.

**Mittova V, Tal M, Volokita M, Guy M. 2003.** Up-regulation of the leaf mitochondrial and peroxisomal antioxidative systems in response to salt-induced oxidative stress in the wild salt-tolerant tomato species Lycopersicon pennellii. *Plant, Cell & Environment* **26**: 845-856.

**Moller IM. 1997.** The oxidation of cytosolic NAD(P)H by external NAD(P)H dehydrogenases in the respiratory chain of plant mitochondria. *Physiologia Plantarum* **100**: 85-90.

**Moller IM. 2001.** Plant mitochondria and oxidative stress: electron transport, NADPH turnover, and metabolism of reactive oxygen species. *Annu.Rev. Plant Physiol.* **52**: 561-591.

**Moller IM, Rasmusson AG. 1998.** The role of NADP in the mitochondrial matrix. *Trends in Plant Sciences* **3**: 21-27.

**Moran JF, M. B, Iturbe-Ormaetxe I, Frechilla S, Klucas RV, Aparicio-Trejo P. 1994.** Drought induces oxidative stress in pea plants. *Planta* **194**: 346-352.

**Nijs D, Kelley PM. 1991.** Vitamins C and E donate single hydrogen atoms *in vivo*. *FEBS Lett.* **284**: 147-151.

**Noctor G, De Paepe R, Foyer CH. 2007.** Mitochondrial redox biology and homeostasis in plants. *Trends in Plant Sciences* **12**: 125-134.

**Noctor G, Foyer GH. 1998.** Ascorbate and glutathione: keeping active oxygen under control. *Annu. Rev. Plant Physiol. Plant Mol. Biol.* **49**: 249-279.

**Olczak M, Morawiecka B, Watorek W. 2003.** Plant purple acid phosphatases - genes, structures and biological function. *Acta Biochimica Polonica* **50**:

**Mittova V, Guy M, Tal M, Volokita M-. 2004.** Salinity up-regulates the antioxidative system in root mitochondria and peroxisomes of the wild salt-tolerant tomato species Lycopersicon pennellii. *Journal of Experimental Botany* **55**: 1105-1113.

**Mittova V, Tal M, Volokita M, Guy M. 2003.** Up-regulation of the leaf mitochondrial and peroxisomal antioxidative systems in response to salt-induced oxidative stress in the wild salt-tolerant tomato species Lycopersicon pennellii. *Plant, Cell & Environment* **26**: 845-856.

**Moller IM. 1997.** The oxidation of cytosolic NAD(P)H by external NAD(P)H dehydrogenases in the respiratory chain of plant mitochondria. *Physiologia Plantarum* **100**: 85-90.

**Moller IM. 2001.** Plant mitochondria and oxidative stress: electron transport, NADPH turnover, and metabolism of reactive oxygen species. *Annu.Rev. Plant Physiol.* **52**: 561-591.

**Moller IM, Rasmusson AG. 1998.** The role of NADP in the mitochondrial matrix. *Trends in Plant Sciences* **3**: 21-27.

**Moran JF, M. B, Iturbe-Ormaetxe I, Frechilla S, Klucas RV, Aparicio-Trejo P. 1994.** Drought induces oxidative stress in pea plants. *Planta* **194**: 346-352.

**Nijs D, Kelley PM. 1991.** Vitamins C and E donate single hydrogen atoms *in vivo*. *FEBS Lett.* **284**: 147-151.

**Noctor G, De Paepe R, Foyer CH. 2007.** Mitochondrial redox biology and homeostasis in plants. *Trends in Plant Sciences* **12**: 125-134.

**Noctor G, Foyer GH. 1998.** Ascorbate and glutathione: keeping active oxygen under control. *Annu. Rev. Plant Physiol. Plant Mol. Biol.* **49**: 249-279.

**Olczak M, Morawiecka B, Watorek W. 2003.** Plant purple acid phosphatases - genes, structures and biological function. *Acta Biochimica Polonica* **50**:

1245-1256.

**Orva BL, Ellis BE. 1997.** Transgenic tobacco plants expressing antisense RNA for cytosolic ascorbate peroxidase show increase susceptibility to ozone injury. *The Plant Journal* **11**: 1297-1305.

**Padh H. 1990.** Cellular functions of ascorbic acid. *Biochem. Cell Biol.* **68**: 1166-1173.

**Palma JM, Sandalio LMa, del Rio LA-. 1986.** Manganese superoxide dismutase in higher plant chloroplasts: a reappraisal of a controverted cellular localization. *Journal of Plant Physiology* **125**: 427-439.

**Pastore D, Laus MN, Fonzo ND, Passarella S. 2002.** Reactive oxygen species inhibit the succinate oxidation-supported generation of membrane potential in wheat mitochondria. *FEBS Letters* **516**: 15-19.

**Perl-Treves R, Perl A. 2002.** *Oxidative stress: An introduction.* New York: Taylor and Francis.

**Petit PX. 1991.** Flow cytometric analysis of rhodamine 123 fluorescence during modulation of the membrane potential in plant mitochondria. *Plant Physiology* **98**: 279-286.

**Rubio MC, Bustos-Sanmamed P, Clemente MR, Becana M. 2009.** Effects of salt stress on the expression of antioxidant genes and proteins in the model legume *Lotus japonicus*. *New Phytologist* **181**: 851-859.

**Sambrook J, Russell DW. 2001.** *Molecular Cloning: A Laboratory Manual.* New York: Cold Spring Harbor Laboratory Press.

**Sattler SE, Gilliland LU, Magallanes-Lundback M, Pollard M, DellaPenna D. 2004.** Vitamin E is essential for seed longevity and for preventing lipid peroxidation during germination. *The Plant Cell* **16**: 1419-1432.

**Scandalios JG, Tong W-F, Roupakias DG. 1980.** Cat 3, a third gene locus coding for

a tissue specific catalase in maize: genetics, intracellular location, and some biochemical properties. *Mol. Gen. Genet.* **179**: 33-41.

**Schenk G, Ge YB, Carrington LE, Wynne CJ, Searle IR, Carroll BJ, Hamilton S, de Jersey J. 1999.** Binuclear metal centers in plant purple acid phosphatases: Fe-Mn in sweet potato and Fe-Zn in soybean. *Archives of Biochemistry and Biophysics* **370**: 183-189.

**Schenk G, Korsinczky MLJ, Hume DA, Hamilton S, Dejersey J. 2000.** Purple acid phosphatases from bacteria: Similarities to mammalian and plant enzymes. *Gene* **255**: 419-424.

**Schwarzländer M, Fricker MD, Sweetlove LJ. 2009.** Monitoring the in vivo redox state of plant mitochondria: Effect of respiratory inhibitors, abiotic stress and assessment of recovery from oxidative challenge. *Biochimica et Biophysica Acta* **1787**: 468-475.

**Shalata A, Neumann PM. 2001.** Exogenous ascorbic acid (Vitamin C) increases resistance to salt stress and reduce lipid peroxidation. *Journal of Experimental Botany* **52**: 2207-2211.

**Siedow JN, Umbach AL. 1995.** Plant Mitochondrial Electron Transfer and Molecular Biology. *The Plant Cell* **7**: 821-831.

**Smirnoff N. 1998.** Plant resistance to environmental stress. *Current Opinion in Biotechnology* **9**: 214-219.

**Sukumvanich P, DesMarais V, Sarmiento CV, Wang Y, Ichetovkin I, Mouneimne G, Almo S, Condeelis J-. 2004.** Cellular localization of activated N-WASP using a conformation-sensitive antibody. *Cell Motility and the Cytoskeleton* **59**: 141-152.

**Suzuki N, Mittler R. 2006.** Reactive oxygen species and temperature stresses: A delicate balance between signaling and destruction. *Physiologia Plantarum*

**126**: 45-51.

**Sweetlove LJ, Heazlewood JL, Herald V, Holtzapffel R, Day DA, Leaver CJ, Millar AH. 2002.** The impact of oxidative stress on Arabidopsis mitochondria. *The Plant Journal* **32**: 891-904.

**Tambussi EA, Bartoli CG, Beltrano J, Guiamet JJ, Araus JL. 2000.** Oxidative damage to thylakoid proteins in water stressed leaves of wheat (Triticum aestivum). *Physiologia Plantarum* **108**: 398-404.

**Taylor NL, Day DA, Millar AH. 2004.** Targets of stress-induced oxidative damage in plant mitochondria and their impact on cell carbon/nitrogen metabolism. *Journal of Experimental Botany* **55**: 1-10.

**Tse YC, Lo SW, Hillmer S, Dupree P, Jiang L. 2006.** Dynamic response of prevacuolar compartments to brefeldin a in plant cells. *Plant Physiology* **142**: 1442-1459.

**Vanlerberghe GC, Vanlerberghe AE, McIntosh L. 1997.** Molecular genetic evidence of the ability of alternative oxidase to support respiratory carbon metabolism. *Plant Physiology* **113**: 657-661.

**Veljanovski V, Vanderbeld B, Knowles VL, Snedden WA, Plaxton WC. 2006.** Biochemical and molecular characterization of AtPAP26, a vacuolar purple acid phosphatase up-regulated in phosphate-deprived Arabidopsis suspension cells and seedlings. *Plant Physiology* **142**: 1282-1293.

**Verslues PE, Argarwal M, Katiyar-Argarwal S, Zhu J, Zhu JK. 2006.** Methods and concepts in quantifying resistance to drought, salt and freezing, abiotic stresses that affect plant water status. . *The Plant Journal* **45**: 523-539.

**Vogel A, Spener F, Krebs B. 2001.** *Purple acid phosphatase.* Chichester: John Wiley & Sons.

**Wu WS. 1987.** Localization of mitochondria in plant cells by vital staining with

rhodamine 123. *Planta* **171**: 346.

**Yu BP. 1994.** Cellular defenses against damage from reactive oxygen species. *Physiol. Rev.* **74**: 139-162.

**Appendix I – Restriction and modifying enzymes**

| Enzymes | Company and catalog number |
|---|---|
| Go*Taq* Flexi DNA polymerase | Promega M8295 |
| Taq DNA polymerase | Roche 1647679 |
| Taq DNA polymerase | Invitrogen 10342-053 |
| Tag DNA polymerase | Promega M1665 |
| Advant II Taq DNA polymerase | Clontech 639201 |
| Pfu | Promega M7741 |
| T4 DNA ligase | NEB M0202L |
| *Hind*III | Promega R6041 |
| *Xba*I | Promega R6181 |

**Appendix II – Chemicals:**

1. Alexa Fluor® 488 conjugated anti-rabbit antibodies — Invitrogen A11008
2. Ammonium acetate — Ajax 27
3. Ampicillin — Sigma A9518
4. Agarose — GibcoBRL 15510-027
5. Bacto-peptone — Difco 0118-01-8
6. Bacto™ Agar — Difco 214010
7. Benzyl-aminopurine — Sigma B5898
8. Blocking reagent — Boehringer 1096176
9. Boric acid — Ajax 101
10. Bovine serum albumin — Sigma A7906
11. Bromophenol blue — Merck 8122
12. Calcium chloride — Merck 2380
13. Calcium nitrate — Ajax 135
14. Cefotaxime, sodium salt — Amresco E868
15. Cetyldimethylethylammonium bromide (CTAB) — Sigma C5335
16. Chloroform — Merck 3445
17. Disodium 3-14-methoxyspiro{1,2-dioxetane-3,2'-(5'-chloro) tricyclo[3.3.1.$1^{3,7}$] decan}-4yl) phenyl phosphate — Boehringer 1 655 884
18. Copper sulfate, anhydrate — Sigma C1297
19. Cupric chloride, dihydrate — Sigma C6641
20. dATP — Boehringer 1277049
21. Dichlorophenoxyacetic acid (2,4-D) — Sigma D2128

| | |
|---|---|
| 22. 2'-7'-dichlorodihydrofluorescein diacetate | Molecular probe D399 |
| 23. Disodium hydrogen phosphate | Sigma S0876 |
| 24. Dithiothreitol, DDT (100mM) | Promega P1171 |
| 25. EDTA, disodium salt | Sigma E5143 |
| 26. EDTA, ferrous-sodium salt | Sigma EDFS |
| 27. EGTA, sodium salt | Sigma E3889 |
| 28. Ethanol (absolute) | Merck 100986 |
| 29. Ethidium bromide | Sigma E7637 |
| 30. Formaldehyde (37%) | Sigma F8775 |
| 31. Formamide | Boehringer 1814320 |
| 32. Gelrite gellan gum | Sigma G1910 |
| 33. Gelatin | Sigma G7765 |
| 34. Genetamicin sulfate | Sigma G3632 |
| 35. Glacial acetic acid | Sigma A4508 |
| 36. Glycine | Sigma G7403 |
| 37. Hydrochloric acid (36%) | Ajax 1364 |
| 38. Iso-amylalcohol | Merck 100979 |
| 39. Isopropanol | Labscan C2519 |
| 40. Isopropyl b-D-thiogalactopyanside (IPTG) | Boehringer 1411446 |
| 41. Kanamycin, monosulfate | Sigma K4000 |
| 42. Luria Bertani broth, Miller | Difco 0446-17-3 |
| 43. Maleic acid | Sigma M0375 |
| 44. Magnesium chloride | Sigma M9272 |
| 45. Magnesium sulphate | Ajax 302 |
| 46. Mannitol | Ajax 530 |
| 47. β-mercaptoethanol | Sigma M6250 |

| | |
|---|---|
| 48. MES | Sigma 3023 |
| 49. Methanol | Merck 6007 |
| 50. Metro-mix soil | Hummert 10-0325 |
| 51. MitoTracker® Orange | Molecular Probes M7510 |
| 52. 4-Morpholineethanesulfonic acid | Boehringer 223794 |
| 53. MOPS | Sigma M8899 |
| 54. Murashige & Skoog salt mixture | GibcoBRL 11117-017 |
| 55. Murashige & Skoog Basal salt mixture (MS) powder, plant cell culture tested | Sigma M5524 |
| 56. Myoinositol | Sigma I5125 |
| 57. Sigmafast BCIP/NBT substrate (chromogenic) | Sigma, B5655-25TAB |
| 58. N-lauroylsarcosine | Sigma L5125 |
| 59. Phenol-chloroform-isoamylalcohol (25:24:1) | Amersco 883 |
| 60. PIPES | B/M 239496 |
| 61. Polyvinylpyrrolidone | Sigma PVP-40T |
| 62. Potassium dihydrogen orthophosphate | Ajax 391 |
| 63. Potassium acetate | Sigma P1147 |
| 64. Potassium hydroxide | Merck 5033 |
| 65. Potassium nitrate | Sigma P8394 |
| 66. Potassium phosphate, monobasic | Sigma P5379 |
| 67. Pyridoxine-HCl | Sigma P9755 |
| 68. Rifampicin | Sigma R3501 |
| 69. SDS | Bio-Rad 161-0302 |
| 70. Silwet-77 | Lehle seeds |
| 71. Sodium acetate, anhydrous | Sigma S2889 |
| 72. Sodium chloride | RDH 31434 |

| | |
|---|---|
| 73. Sodium citrate, trisodium salt | Sigma S4641 |
| 74. Sodium dihydrogen phosphate | RDH 10245 |
| 75. Sodium dodecyl sulfate | B/M 1028693 |
| 76. di-Sodium hydrogen phosphate-2-hydrate | RdH 30435 |
| 77. Sodium hydroxide | Merck 6498 |
| 78. Sodium molybdate | RDH 31439 |
| 79. Sucrose | Sigma S1888 |
| 80. Tris/ HCl | Amresco 0826 |
| 81. Tween 20 | Bio-Rad 170-6531 |
| 82. Triton X-100 | Sigma T6878 |
| 83. Urea | Sigma U1250 |
| 84. Zinc sulfate, heptahydrate | Sigma Z4750 |

**Appendix III – Commercial Kits:**

| Kits | Company | Cat.no. |
|---|---|---|
| ABI prism dRhodamine terminator cycle sequencing ready reaction kit | Peckin-Elmer | 402078 |
| ABI prism BigDye v.3.1 terminator cycle sequencing ready reaction kit | Applied Biosystems | 4337455 |
| Advantage® II cDNA PCR kit | Clontech | K1905-1 |
| Aurora™ Western Blot Chemiluminescent Detection | ICN | 004821539 |
| DIG DNA labeling kit | Roche Diagnostic limited | 11175033910 |
| DIG detection system (CSPD, ready-to-use and Anti digoxigenin-AP, Fab fragments) | Roche Diagnostic limited | 11755633001 |
| Lowicry HM20 Embedding kit | Electron microscopy sciences | RT 14340 |
| PeroXOquant Quantitative peroxide assay kit | PIERCE | 23280 |
| Wizard plus minipreps DNA purification kit | Promega Biosciences | A7510 |

**Appendix IV – Equipments and facilities used:**

| Equipments and facilities | Company and Cat. no. |
|---|---|
| 1. The ABI PRISM® 3100 Genetic Analyzer | Applied Biosystems 3100-01 |
| 2. Automatic Freeze Substitution | Leica EM AFS |
| 3. Biological Safety Cabinet | Baker SG600E 59419 |
| 4. Centrifuge J2-MI | Beckman T373 with JA-14 rotor |
| 5. Confocal laser scanning microscope | Bio-Rad (Zeiss) Radiance 2100™ |
| 6. Confocal laser scanning microscope | Olympus FluoView FV 1000 |
| 7. Cyrofixation & Cryopreparation system | Leica EM CPC |
| 8. Gene Pulser Apparatus | Bio-Rad 165-2076 |
| 9. Growth chamber | Percival AR-32L 3859-05-971 |
| 10. GS Gene Linker UV Chamber | Bio-Rad 0392-92-0336 |
| 11. Microcooler II | Bockel Scientific 260010 |
| 12. Mini trans-blot module | Bio-Rad 170-3935 |
| 13. Orbital shaker | Lab line 4628-1 |
| 14. Power supply MIDI MP-250 | Life technologies 4801311 |
| 15. Programmable Thermal Controller | MJ Research PTC100 96VHB 200003879 |
| 16. Refrigerated Centrifuge 5810R | Eppendorf 03463 |
| 17. Reichert-Jung Ultra-cut S | Leica Ultra-cut 701701 |
| 18. Solvent System Centrivap Unit | Labconco 79840-01 |
| 19. TELCO incubator | Cole-Parmer 39352-02 |
| 20. Transmission electron microscope | JEM-1200EXII, JEOL |

**Appendix V – Buffer, solution, gel and medium formulation**

| | |
|---|---|
| Agarose gel (0.8%) | 0.8% agarose, 1μg/ ml ethidium bromide in 1X TAE buffer |
| Arabidopsis fertilizer (10X) | 50mM $KNO_3$, 25mM 1M $KPO_4$ (pH 5.5), 20mM $MgSO_4$, 20mM $Ca(NO_3)_2$, 0.5mM FeNaEDTA and 1% micronutrients. Fill up to 1 litre with $H_2O$ |
| Arabidopsis micronutrients | 70mM boric acid, 14mM $MnCl_2$, 5mM $CuSO_4$, 0.2mM $NaMoO_4$, 10mM NaCl, and 0.01mM $CuCl_2$. Fill up to 500ml with $H_2O$. |
| B5 vitamine (1000X) | 1000mg myo-inositol, 100mg thiamine-HCl, 10mg nicotine acid, 10mg pyridoxine-HCl. Fill up to 10ml with $H_2O$ |
| Bacterial cell lysis solution | 20mM Tris-HCl, 100mM NaCl, 8M urea |
| Blocking buffer (for northern blot) | Dilute blocking reagent stock solution 1:10 with maleic acid buffer |
| Blocking buffer (for western blot) | 2.5% skimmed milk powder in TBST |
| Blocking reagent stock solution (10%) (for northern blot) | Add 10g blocking reagent to 100ml maleic acid buffer with several 30s heat pulses in the microwave |
| Bromophenol blue loading dye (6X) | 0.25% bromophenol blue in 30% glycerol |
| Calcium chloride solution | 60mM $CaCl_2$, 15% glycerol and 10mM PIPES, pH 7.0, sterilized by autoclave |
| Cold washing solution | 2x SSC, 0.1% SDS |
| CTAB extraction buffer | 0.1M Tris-HCl (pH8), 1.4M NaCl, 0.1M EDTA (pH8), 2% (w/v) CTAB, 1% (w/v) Polyvenylpyrolidone and 0.2% β-mercaptoethanol |
| CTAB washing buffer | 76% EtOH with 0.01M $NH_4Oac$ |
| DEPC-treated $H_2O$ | Dissolve DEPC to 1% in ultrapure $H_2O$ and keep overnight<br>Autoclave to remove residual DEPC. |
| Detection buffer | 100mM Tris-HCl, pH 9.5 and 100mM NaCl |
| 10X Dunn's buffer | 8.4g $NaHCO_3$, 3.2g $Na_2CO_3$ in 1L $H_2O$ |

| | |
|---|---|
| Hot washing solution | 0.5x SSC, 0.1% SDS |
| Infiltration medium | 2.2g MS salts, 1x B5 vitamins, 50g sucrose, 0.5g MES and 200µl Silwet$_{TM}$ L-77, 0.044µM benzylaminopurine. Adjust pH to 5.7 with KOH and fill up to 1 litre solution. Autoclave. |
| LB broth | 25g/ L LB powder, autoclave |
| LB agar plate | 25g/ L LB powder and 15g/ L bacto-agar, autoclave |
| Maleic acid buffer | 0.1M maleic acid, 0.15M NaCl, pH 7.5. Adjust pH with concentrated NaOH; autoclave. |
| MOPS (10X) | 200mM MOPS, 50mM sodium acetate, 10mM EDTA, pH 7.0. Make up in sterile $H_2O$. After autoclaving, the solution will turn yellow |
| MS plate for *Arabidopsis thaliana* | 4.3g/ L Murashige & Shoog salt mixture (GibcoBRL), 3% sucrose, 0.05% MES, pH 5.7, 0.9% bacto-agar |
| MS plate for BY-2 cells | 4.3g/L Murashige & Skoog Basal salt mixture (Sigma), 3% sucrose, 1.8mM $KH_2PO_4$, 3% gelrite gellan gum, pH 5.8 |
| MS for BY-2 cells (suspension culture) | 4.3g/L Murashige & Skoog Basal salt mixture (Sigma), 3% sucrose, 1.8mM $KH_2PO_4$, pH 5.0 |
| Neutralization solution | 0.5M Tris-HCl, 0.5M Tris-HCl, pH 7.5 |
| N-lauroylsarcosine | 10% (w/v) in sterile $H_2O$ filtered through a 0.2µm membrane |
| Phosphate buffer saline (PBS) (10X) | 0.58M $Na_2HPO_4$, 0.17M $NaH_2PO_4$, 0,68M NaCl, pH7.2 |
| Phosphate buffer saline (PBS) (1X) | Dilute 10X PBS ten fold with milli-Q $H_2O$, pH7.2 |
| RNA extraction buffer | 200mM Tris base, 400mM KCl, 200mM Sucrose, 35mM $MgCl_2 \cdot 6H_2O$, 25mM EGTA, pH 9 |
| RNA loading buffer | 250µl formamide, 83µl formaldehyde 37% (w/v), 50µl 10x MOPS buffer, 0.01% (w/v) bromophenol blue, 50µl |

| | |
|---|---|
| | glycerol. Fill up to 500µl with DEPC-treated $H_2O$. |
| 10% SDS | 10% (w/v) in sterile $H_2O$ filtered through a 0.2µm membrane |
| SDS sample loading buffer (5X) | 0.5M Tris pH6.8, 50% glycerol, 0.5% bromophenol blue, 10% SDS<br>Mix β-mercaptoethanol with sample dye in 1:3 ratio before use |
| SOC | 2% bacto-tryptone, 0.5% bacto-yeast extract, 10mM NaCl, 2.5mM KCl, 10mM $MgCl_2$, 10mM $MgSO_4$, 20mM glucose |
| Sodium acetate | 3M NaOAc, pH 5.2<br>3M NaOAc, pH 5.6 |
| Sodium phosphate | 1M $NaH_2PO_4$, 1M $Na_2HPO_4$, pH7 |
| SSC (20X) | 3M NaCl, 300mM sodium citrate, pH 7.0 |
| TAE buffer (1X) | 4.84g/ L Tris base, 0.1142% acetic acid, 0.744g/ L EDTA disodium salt |
| TBS | 20mM Tris-HCl (pH 7.5) and 150mM NaCl |
| TBST | TBS with 0.1% Tween-20 |
| YEP meidum | 10g tryptone, 10g yeast extract and 5g NaCl. Fill up with 1 litre with $H_2O$ |